Doctoral Dissertation

Influence of host association and biogeography on Pacific marine gregarine speciation

（宿主との関連性と生物地理学が太平洋産グレガリナの種分化に与える影響）

Eric Odle

Graduate School of Science, Hokkaido University

Department of Natural History Sciences

2025 September

CONTENTS

ABSTRACT

Marine gregarines, a diverse group of single-celled parasitic protists within Apicomplexa, are widespread in marine invertebrates yet remain poorly understood at the molecular level. This project investigates patterns of speciation among marine gregarines using an integrative approach that synthesizes morphological traits (via light and electron microscopy), molecular phylogenetics (18S and ITS rRNA), host association (COI), and biogeographical data. Collectively, these results show that both host phylogeny and biogeography shape gregarine evolution, with host identity often playing the dominant role.

Chapter 2 explores the biodiversity and host associations of archigregarines from polychaete hosts in Japan, revealing novel clades within *Lunidium*, *Metzidium*, and *Devanium*. Chapter 3 investigates biogeographic and cryptic diversity in paralecudinid gregarines from Pacific polychaetes, uncovering new *Ferraria* and *Paralecudina* clades. Chapter 4 focuses on early-branching lecudinids, describing one novel *Difficilina* clade and three novel Lecudinidae clades—including likely the first known gregarine from an ostracod host. Chapter 5 reconstructs the phylogeny of *Lankesteria* gregarines from ascidian hosts and finds a strong link between gregarine biodiversity and the evolution of tunicates. Chapter 6 examines *Lecudina* gregarines from lumbrinerid polychaetes, demonstrating cryptic speciation and morphological diversity in *Lecudina* Clade B. Finally, Chapter 7 analyzes *Lecudina* parasites from nereidid polychaetes, identifying multiple novel clades as well as a *Lecudina tuzetae* species complex.

TAXONOMIC PROPOSALS AND OTHER WORK

Parts of this dissertation were published in the following article:

Odle, E., Riewluang, S., Ageishi, K., Kajihara, H. and Wakeman, K.C., 2024. Pacific marine gregarines (Apicomplexa) shed light on biogeographic speciation patterns and novel diversity among early apicomplexans. *European Journal of Protistology*, *94*, p.126080.

Specifically, some clades were published as the following taxa in Odle et al. (2024):

Lecudinidae sp. Clade B = *Undularius* Odle and Wakeman, 2024 (n. gen.)

Lecudinidae sp. Clade B = *Undularius glycerae* Odle and Wakeman, 2024 (n. sp.)

Difficilina sp. Clade A = *Difficilina fasoliformis* Odle and Wakeman, 2024 (n. sp.)

Lecudina sp. Clade B = *Lecudina* cf. *longissima*

Lecudina sp. Clade C = *Lecudina* cf. *tuzetae*

Lecudina sp. Clade D = *Lecudina kitase* Odle and Wakeman, 2024 (n. sp.)

These published names are provided alongside their corresponding clade names within figures and tables for clarity. Other taxonomic revisions suggested during this dissertation are not formal proposals.

The following articles were also published during this Ph.D. course:

Odle, E., Kahng, S., Riewluang, S., Kurihara, K. and Wakeman, K.C., 2024. GINSA: an accumulator for paired locality and next-generation small ribosomal subunit sequence data. *Bioinformatics*, *40*(4), p.btae152.

Kahng, S.E., Odle, E. and Wakeman, K.C., 2024. Coral geometry and why it matters. *PeerJ*, *12*, p.e17037.

ACKNOWLEDGMENTS

I want to thank Dr. Kevin C. Wakeman for his guidance as my research advisor, Dr. Kazuhiro Kogame for his administrative supervision, and Dr. Hiroshi Kajihara for his advice and collaboration. I also appreciate their roles as committee members. Funding from the Hokkaido University DX Doctoral Fellowship supported this research. I am grateful to Dr. Samuel Kahng for allowing me to be a part of his coral geometry project. Special thanks is owed to Dr. Hiroko Yamamoto for her repeated assistance with using and maintaining the shared research equipment, especially the 48-sample sequencer and the electron microscopes. Finally, thanks to my labmates Siratee and Shaun for their helpful feedback.

PREFACE. Objectives of biodiversity research

I begin with a basic question: what is *biodiversity*? At first, I thought biodiversity just meant “a lot of species”. After spending some time studying marine gregarines, I began to think that biodiversity was a special word with a complicated definition to be memorized so people think you are smart. Now I see that biodiversity just means a lot of species… and it is very important to know a lot of species!

Why is biodiversity important? Biodiversity is important because we need many species to live. We need bees to pollinate plants. We need those plants to eat. We even need bacteria to help digest those plants. But biodiversity is also about understanding how those species relate to each other. Are all mushrooms safe to eat? If not, how can we identify which mushrooms are dangerous? Furthermore, what if we find a new type of mushroom? Can the close relatives of that mushroom give us clues about its safety? Clearly, understanding biodiversity can be a matter of life and death.

Now that we appreciate the importance of biodiversity, we need a way to study it. Over 200 years ago, people started making lists of plants and animals. Eventually, they noticed patterns where certain groups all shared similar traits. For example, all fish have scales, all birds have feathers, and all mammals have body hair. However, fish, birds, and mammals all have bones, whereas worms and crabs do not. Researchers could then use those traits to map evolution. We still use such traits to define species and understand biodiversity, but we also have more modern tools. With DNA sequences and some clever math, we can make far more reliable evolutionary trees than people could make in the late 1800s. We also have powerful tools such as electron microscopes that allow us to look at details inside individual cells.

What, then, is the main goal of biodiversity research? The goal is simply to know more species. If we can know more species, we can also know more about how they evolved. If we

know more about how species evolved, we can make more food, make better medicine (e.g., for malaria), make a safer environment, and maybe even make a better world.

CHAPTER 1. General introduction

1.2. Apicomplexa Levine, 1970

Apicomplexans are a diverse group of unicellular eukaryotes known for their obligate parasitic lifestyle, infecting a wide range of hosts while significantly impacting global health, economies, and ecosystems. At the cellular level, apicomplexans are defined by the presence of a specialized structure called an apical complex located at the anterior of the cell (Hu et al., 2006; Boisard and Florent, 2020; Valigurová and Florent, 2021). This unique trait of apicomplexans is likely a modified flagellar apparatus (Okamoto and Keeling, 2014). Another unique feature of apicomplexans is the presence of an apicoplast. The debated chromalveolate hypothesis (Cavalier-Smith, 1999; Keeling, 2009; Green, 2011; Pietluch et al., 2024), which builds on endosymbiotic theory (Sagan, 1967; Gray, 2017), posits that apicomplexans acquired their biosynthetically active (Maréchal and Cesbron-Delauw, 2001; Lim and McFadden, 2010) apicoplast from a red algal endosymbiont (Pietluch et al., 2024).

Evolutionarily, apicomplexans are a lineage of alveolate parasites closely related to ciliates and dinoflagellates (Fig. 1.1 A), and are conventionally classified into four key groups—haemosporidians (e.g., *Plasmodium*), piroplasmids (e.g., *Babesia*), coccidians (e.g., *Toxoplasma*), and Gregarinasina Dufour, 1828 (e.g., *Gregarina* and *Lecudina*) (Fig. 1.1 B–C). Phylogenetic relationships among these apicomplexan subgroups are an active area of research (Leander et al., 2003; Nishimoto et al., 2008; Rueckert et al., 2010; Rueckert et al., 2015; Schrével et al., 2016; Simdyanov et al., 2017; Wakeman et al., 2018; Iritani et al., 2021; Lax et al., 2024). Estimates suggest that less than 1% of apicomplexan diversity has been formally described (Morrison, 2009), and groups such as the gregarines remain particularly under-explored due to a lack of immediate risk to humans.

1.3. Marine gregarine apicomplexans and their host associations

Gregarines are a highly diverse and abundant group of apicomplexans (Perkins et al., 2000) found in hosts inhabiting freshwater (McKinley et al., 2024) and terrestrial environments (Miroliubova et al., 2025) as well as a range of invertebrates (e.g., polychaetes, echinoderms, sipunculids, crustaceans, mollusks, nemerteans, hemichordates, and ascidians) from the ocean (Table 1.1). One notable trait of gregarines is their multi-stage life cycle. Gregarines typically infect host intestines via ingested spores, develop into trophozoites, undergo sexual reproduction (gamogony) typically after pairing (syzygy), and produce spores that release infective sporozoites (Desportes and Schrével, 2013). While this is generally true, some gregarines inhabit other tissue types. For example, *Ascogregarina taiwanensis* infects the excretory organs of mosquitoes (Chen et al., 1997), while *Monocystis* targets the sexual organs of earthworms (Field and Michiels, 2006).

1.3.1 The concept for archigregarines

Marine gregarines encompass two main subgroups: archigregarines (Archigregarinorida Grassé, 1953) and eugregarines (Eugregarinorida Léger, 1900). Archigregarines are morphologically characterized by a worm-like shape as well as both longitudinal and transverse epicytic folds (often appearing as striations under light microscopy) supported by a sub-membrane network of microtubules (Fig. 1.2). Archigregarines also tend to retain an apical complex and the ability to feed via myzocytosis (Simdyanov and Kuvardina, 2007): traits shared with their alveolate relatives, the perkinsids (Leander et al., 2003). Moreover, archigregarines tend to display a pendular/bending motility (Mellor and Stebbings, 1980; Simdyanov and Kuvardina, 2007; Rueckert and Leander, 2009; Kováčiková et al., 2019) rather than the gliding motility often seen among eugregarines (Desportes and Schrével, 2013; Valigurová et al., 2013; Kováčiková et al., 2017) or the peristaltic motility seen among some early branching lecudinids (Leander et al., 2006; Rueckert and Leander, 2009; Odle et al., 2024). However, this pattern does not always hold. Until recently, archigregarines were grouped under the genus *Selenidium* Giard, 1884, which included more than 60 species from a range of marine invertebrate hosts (Wakeman

and Leander, 2013a; Schrével et al., 2016; Paskerova et al., 2018; Wakeman, 2020). Notably, there was a recent reclassification of *Selenidium* into several distinct genera, including *Lunidium*, *Devanium*, and *Metzidium* based on a combination of host preference, morphology, and molecular phylogenetic evidence (Lax et al., 2024).

1.3.2 The concept for eugregarines

Eugregarines, the most biodiverse group of gregarines (Levine, 1976), exhibit a range of morphologies. Trophozoites can range from oblong or lemon-shaped, to bifurcated with rounded appendages (Fig. 1.3 A–B, E–F). Cell surfaces are typically covered in dense longitudinal folds, but these surface features may instead be sparse, short, or even take a crenulated shape (Fig. 1.3 C–D). Eugregarine mucrons can also have a diverse range of configurations (Fig. 1.3 E–G). For movement, eugregarines primarily rely on gliding motility driven by actin and myosin (Valigurová et al., 2013). Although traditionally identified by gliding motility and the presence of an epimerite/mucron (Desportes and Schrével, 2013), there is growing evidence that these traits may have arisen through convergent evolution rather than shared ancestry (Wakeman and Leander, 2012; Wakeman et al., 2014). Eugregarines are mainly intestinal but can also inhabit other host compartments such as the coelom (Leander, 2008). Overall, the diverse morphology among eugregarines likely reflects their adaptation to a diverse range of hosts.

1.4. Molecular phylogenetics in the study of gregarine evolution

Recent trends in the study of gregarine evolution have moved from a purely morphology- and host-based concept towards a phylogenetic species concept (Ridley, 1989; de Queiroz, 2007) based principally on small ribosomal subunit (SSU) molecular data (Rueckert et al., 2011a). Gregarines were first described nearly two centuries ago (Dufour, 1828), well before the adoption of sequencing technology and electron microscopy. During this era, qualities observable by light microscopy were used to conceptualize the gregarines: namely, position of syzygy (e.g., fronto-frontal, caudo-caudal, latero-lateral, and various combinations thereof), the cell anterior (presence of an apical complex), epicytic folds, cell shape (e.g., worm-like or

lemon-shaped), type of motility (e.g., bending, peristaltic, or gliding) and host association (e.g., tunicates or polychaetes) (Desportes and Schrével, 2013).

The modern concept of gregarines relies heavily on phylogenetic inference (Field et al., 1988; Meyer et al., 2010) while also retaining morphological and host association data to help define species boundaries. Efforts to phylogenetically map the evolution of species date back to the Age of Enlightenment (Haeckel, 1866). Key developments followed: the proposal of the DNA double helix structure (Watson and Crick, 1953), the formalization of cladistics (Huxley, 1957), and the commercial availability of Sanger sequencers in 1987 (Chait et al., 1988). By the early 1990s, researchers began publishing molecular phylogenies of apicomplexans using ribosomal RNA (rRNA) sequences (Wolters, 1991; Escalante and Alaya, 1995). Genes commonly used for molecular phylogenetic analysis include the rRNA small ribosomal subunit gene (18S), mitochondrial cytochrome *c* oxidase I (COI) gene, as well as chloroplast genes such as ribulose-1,5-bisphosphate carboxylase/oxygenase large subunit (rbcL) and maturase (matK) (Patwardhan et al., 2014). In particular, the 18S rRNA gene is widely used in biodiversity studies for its high conservation among, for example, ticks (Mangold et al., 1997), copepods (Wu et al., 2015), and soil-dwelling eukaryotic microbes called dictyostelids (Chittavichai et al., 2025). The 18S gene is widely used to study specific apicomplexan groups such as *Plasmodium* (Nishimoto et al., 2008), coccidians, and pyroplasmids (Morrison and Ellis, 1997), as well as apicomplexans in general (Leander et al., 2003a; Morrison, 2009). Moreover, 18S-based phylogenies are regarded as the current “gold standard” for delineating species boundaries among marine gregarines.

Over the past decade and a half, molecular phylogenetic evidence has reshaped marine gregarine genera such as *Lecudina* (Rueckert et al., 2011b; Odle et al., 2024; Park and Leander, 2024), *Lankesteria* (Iritani et al., 2021), and *Selenidium* (Wakeman and Leander, 2012; Lax et al., 2024; Park and Leander, 2024b), and introduced novel genera such as *Amplectina* (Park and Leander, 2024a), *Caliculium* (Wakeman et al., 2014b), *Cuspisella* (Iritani et al., 2018a),

Devanium (Lax et al., 2024), *Difficilina* (Simdyanov, 2009), *Lunidium* and *Metzidium* (Lax et al., 2024), *Sphinctocystis* (Park and Leander, 2024a), *Trollidium* (Wakeman, 2020), *Undularius* (Odle et al., 2024), and *Veloxidium* (Wakeman and Leander, 2012). Still, there is much biodiversity among the marine gregarines that remains to be explored.

1.5. Goals of this project

Informed by the work summarized above, this project aims to investigate novel biodiversity and speciation patterns among marine gregarines through an integrative framework that combines morphology, molecular phylogenetics, host association, and biogeography. Marine gregarines remain under-sampled at the molecular level, with relatively few SSU rRNA sequences available. Consequently, fundamental questions about their evolutionary relationships, species boundaries, and diversification patterns remain unanswered. Specifically, this project aims to address our gaps in marine gregarine knowledge through the following two objectives:

1. I aim to delimit species boundaries and describe novel gregarine biodiversity.
2. I aim to investigate how host phylogeny and biogeography influence speciation patterns among marine gregarines.

To achieve these objectives, I will use an integrative approach that incorporates high-resolution microscopy (light and electron microscopy), host identity, geographic origin, and rRNA as well as COI sequence data obtained through polymerase chain reactions (PCR) and Sanger sequencing.

Figure 1.4 presents a maximum likelihood phylogenetic tree of 18S sequences from across apicomplexa. This tree also includes 130 marine gregarine sequences generated during the present project and serves as a road map for the content herein. Novel marine gregarine data are organized into six distinct groups: archigregarines, paralecudinids, early branching lecudinids, *Lankesteria*, *Lecudina* Clade B, and *Lecudina* Clade A. Each of these groups are explored in greater detail within their respective chapters.

CHAPTER 2. Novel biodiversity and host associations among archigregarines (Apicomplexa) from polychaete hosts around Japan

SUMMARY

Archigregarines are a diverse group of marine apicomplexans characterized by traits such as a worm-like morphology and broad epicytic folds supported by an underlying network of microtubules. This study integrates light and electron microscopy with molecular phylogenetics to investigate the diversity, morphology, and host associations of novel archigregarine lineages from marine annelid hosts in northern Japan. I identified five distinct clades: *Lunidium* sp. Clade A from an orbiniid host, *Metzidium* sp. Clade A from a chaetopterid, and *Devanium* spp. Clades A–C from cirratulid hosts. These lineages exhibited unique combinations of morphological traits including variable epicytic fold densities, transverse folds, and intracellular symbionts, and formed phylogenetic groups that extend current genus-level classifications. Notably, *Lunidium* and *Metzidium* were found in host families previously unrecognized for these genera, suggesting broader host specificity than previously understood. Together, these findings highlight previously uncharacterized archigregarine biodiversity and reveal a strong correlation between parasite clades and host phylogeny.

2.1. INTRODUCTION

Archigregarines represent a subgroup of marine gregarines with characteristics such as myzocytosis-mediated feeding (Leander, 2007; Simdyanov and Kuvardina, 2007; Simdyanov et al., 2018), oocysts that generate four sporozoites (Levine, 1971), and early branching from the *Lecudina* lineage as recovered through phylogenetic analysis (Lax et al., 2024; Odle et al., 2024).

Since these traits are similar to those of related flagellate-possessing parasites known as colopdellids, it is suggested that archigregarines occupy an early-evolving position among marine gregarines (Cox, 1994). This ancestral phylogenetic branching allows archigregarines to serve as an informative group in the study of early apicomplexan evolution (Kuvardina et al., 2002; Leander and Keeling, 2003; Leander, 2008; Rueckert and Horák, 2017).

Host associations among archigregarines have been found with sipunculids (Ormières, 1979; Leander et al., 2006; Rueckert and Leander, 2009), echinoderms (Wakeman and Leander, 2012), and hemichordates (Léger and Duboscq, 1917; Théodorides and Desportes, 1968; Wakeman et al., 2014b). In particular, archigregarines are known to parasitize sedentaria polychaetes in the families Terebellidae (Schrével et al., 2016; Wakeman et al., 2014), Sabellidae (Park and Leander, 2024b), and Cirratulidae (cirratulids) (Wakeman, 2020; Lax et al., 2024). Cirratulids are of particular interest in this study because they are commonly found around the intertidal zones of Hokkaido, Japan (Jimi et al., 2024), where the current study was largely conducted.

Morphologically, archigregarines possess several unique traits, including a generally worm-like (vermiform) cellular shape. Whereas eugregarines are distinguished by their narrow epicytic folds accompanied by apical filaments and rippled dense structures (Schrével et al., 1983; Valigurová et al., 2013; Odle et al., 2024), archigregarines feature broad, longitudinal folds that can appear as striations upon light microscopy (Desportes and Schrével, 2013; Lax et al., 2024). These folds are supported by an underlying layer of microtubules situated beneath a three-layered inner membrane complex (Stebbings et al., 1974; Mellor and Stebbings, 1980). Another characteristic morphological trait of archigregarines is the presence of transverse epicytic folds. This feature is observed in multiple species (Leander et al., 2003b; Leander, 2006; Wakeman and Leander, 2012), although they can be absent in others, such as *Selenidium orientale* and *S. pisinnus* (Rueckert and Leander, 2009). Yet another trait that can distinguish these groups is motility, with archigregarines exhibiting a bending action (Mellor and Stebbings,

1980; Simdyanov and Kuvardina, 2007; Rueckert and Leander, 2009; Kováčiková et al, 2019) as opposed to the gliding motility of eugregarines.

Until recently, the genus *Selenidium* Giard, 1884 served as a broad classification for archigregarines, encompassing over 60 species found in various marine invertebrate hosts (Wakeman and Leander, 2013b; Schrével et al., 2016; Paskerova et al., 2018; Wakeman, 2020). However, a recent taxonomic revision based on host specificity, morphological features, and molecular phylogenetic data has led to the division of *Selenidium* into several distinct genera, including *Lunidium, Devanium*, and *Metzidium* (Lax et al., 2024). In this study, I integrate light and electron microscopy with host cytochrome *c* oxidase I (COI) and isolate rRNA gene (18S and ITS) phylogenetics to characterize the biodiversity, morphology, and evolutionary placement of novel archigregarine clades from northern Japan. These findings shed new light on the early evolution of apicomplexans and their complex symbiotic interactions.

2.2. MATERIALS AND METHODS

2.2.1. Host collection and sample processing

Hosts were collected opportunistically in the intertidal zones near Akkeshi Bay (43°1′9″N 144°50′4″E) and Oshoro Marine Station (43°12′37″N 140°51′25″E) in Hokkaido, Japan, and Kabira Bay (24°26′46″N 124°8′25″E) on Ishigaki Island, Japan between September 2022 and September 2023 (Table 2.1) from under intertidal rocks and inside tufts of seagrass. Individual hosts were then separated, photographed, and dissected. Host digestive tracts were removed and shredded with forceps in a Petri dish to separate gregarine parasites from host tissue. Gregarine trophozoites (feeding stages) were isolated using hand-drawn glass pipettes under an inverted microscope (Olympus CKX53, Tokyo, Japan or Nikon Eclipse Ts2 Tokyo, Japan). Isolates were then washed 2–3 times in well slides containing filter-sterilized seawater until clean. Single cell isolates taken for DNA were photographed using a Kiss X8i DSLR camera (Canon, Tokyo, Japan) mounted to the inverted microscope prior to transfer into 0.2 ml PCR microcentrifuge

tubes. Remaining isolates were placed in 2.5% glutaraldehyde for electron microscopy. Remaining host tissue was preserved in 100% ethanol for molecular (barcode) identification.

2.2.2. Electron microscopy

Trophozoites used for electron microscopy were fixed in baskets containing 2.5% glutaraldehyde (diluted in seawater) on ice for 30 min. These baskets were constructed using Isopore 5.0 µm PC Membrane filters (Merck Millipore Ltd., Ireland, UK) attached to trimmed 1000 µl pipette tips with silicone adhesive. Cells were next washed three times in filter-sterilized seawater, then post-fixed in 1% osmium tetroxide (diluted in seawater) for 30 min in the dark. Following post-fixation, cells were washed in filter-sterilized seawater (three times, 3 min each), desalted in deionized water (three times, 3 min each), then dehydrated using an ethanol series (70%, 80%, 90%, 100%, 100%) for 3 min at each concentration. Samples used for scanning electron microscopy (SEM) were dried using an HCP-2 815B critical point dryer (Hitachi, Tokyo, Japan) and sputter coated with gold for 400 sec at 15 µA. Imaging of SEM samples was performed on an S-3000N scanning electron microscope (Hitachi, Tokyo, Japan). Images of larger isolates were taken in sections, stitched together, then cropped from the background using Affinity Photo 2 (Serif Ltd., Nottingham, United Kingdom).

Samples used for transmission electron microscopy (TEM) were fixed in 2.5% glutaraldehyde (diluted in seawater) on ice for 30 min, washed with filter-sterilized seawater (three times, 3 min each), then post-fixed with 1% osmium tetroxide for 1.5 h in the dark. Following another wash in filter-sterilized seawater (three times, 3 min each), samples were desalted in deionized water (three times, 3 min each) and then dehydrated using an ethanol series (70%, 80%, 90%, 100%, 100%) for 3 min at each concentration. Fixed cells were next permeabilized in 1:1 ethanol:acetone for 5 min, 100% acetone (two times, 5 min each), 1:1 acetone:resin (Agar Scientific Ltd., Essex, United Kingdom) for 30 min, then 100% resin (two times, 5 h each). Finally, resin-embedded samples were polymerized at 68°C for 48 h and shaped using an EM UC6 ultramicrotome (Leica, Wetzlar, Germany). Sections 50–65 nm in thickness

were cut using a diamond knife then placed atop formvar-coated TEM grids and imaged on an H-7650 transmission electron microscope (Hitachi, Tokyo, Japan).

2.2.3. Amplification and sequencing of 18S and ITS rRNA regions

Gregarine trophozoites were transferred individually to 0.2 ml PCR microcentrifuge tubes and stored at –20°C for 1–5 days. Genomic DNA was then extracted from these samples using a QuickExtract FFPE DNA Extraction Kit (Lucigen, Middlesex, United Kingdom) in line with manufacturer protocol. General and specific primers (Table 2.2) with KOD One® PCR Master Mix (Toyobo, Osaka, Japan) were used in initial amplification of genetic material. Thermal cycling during initial amplification was run with the following parameters: denaturation at 94°C for 1 min, followed by 35 cycles of denaturation at 98°C for 10 sec, annealing at 52°C for 5 sec, and extension at 68°C for 15 sec, then ending in a final extension at 68°C for 1 min. Initial amplification products were then diluted 1:100 with ultrapure water (UltraPure™ DNase/RNase-Free Distilled Water, Thermo Fisher Scientific Inc., Massachusetts, USA) and used as template for a nested reaction with internal primers (Table 2.2). Nested amplification was run with the following parameters: denaturation at 94°C for 1 min, followed by 30 cycles of denaturation at 98°C for 10 sec, annealing at 54°C for 5 sec, and extension at 68°C for 10 sec, then ending in a final extension at 68°C for 1 min. Amplicons were confirmed by gel electrophoresis and ranged from 600–1000 bp in size. Samples with single, sharp bands were purified with polyethylene glycol (PEG) in preparation for sequencing. Sequencing was performed using the SupreDye™ v1.1 Cycle Sequencing Kit (AdvancedSeq LLC, California, USA) with a 3730 DNA Analyzer (Applied Biosystems, Massachusetts, USA).

2.2.4. Molecular phylogenetic analyses

All sequence reads were imported into Geneious Prime 2024.0.5 (https://www.geneious.com) for assembly and alignment. Within Geneious, reads were initially screened against the National Center for Biotechnology Information (NCBI) GenBank database using the Basic Local Alignment Search Tool (BLAST). Contigs were generated using the

Geneious de novo assembler with built-in trimming feature. A second NCBI BLAST screen was then performed on contigs followed by primer site visualization to mitigate chimeric sequence generation.

Partial 18S and ITS sequences obtained from single-cell isolates were aligned along with sequences of related taxa using MAFFT (Katoh et al., 2002) multiple sequence alignment (E-INS-i model, 100PAM/k = 2 scoring matrix, gap penalty = 1.53). Alignments were masked in regions containing 70% or greater gaps. Optimal substitution models were determined using the Akaike Information Criterion with Correction (AICc) via IQTREE ModelFinder (Kalyaanamoorthy et al., 2017), and a GTR substitution model with gamma rate variation was used during Bayesian analysis. Maximum-Likelihood (ML) analysis and Bayesian Inference (BI) were both used to infer isolate phylogeny. Maximum-Likelihood analysis was performed using IQTREE (Nguyen et al., 2015) with 1000 bootstrap pseudoreplicates, while Bayesian posterior probabilities (PP) were calculated using MrBayes Ver. 3.2.6 (Huelsenbeck and Ronquist, 2001) via the Geneious plug-in. Markov Chain Monte Carlo was set for ten million generations, and other BI settings were kept as plug-in defaults.

2.2.5. Host identification

Fragments of host tissue remaining after gregarine isolation were preserved in 100% ethanol for barcoding. Host DNA was extracted from samples using the MasterPure Complete DNA & RNA Purification Kit (LGC Biosearch Technologies, Hoddesdon, United Kingdom). The COI gene was amplified using primers polyLCO and polyHCO (Table 2.2) with KOD One® PCR Master Mix (Toyobo, Osaka, Japan). Thermal cycling during COI amplification was run under the following parameters: initial denaturation at 94°C for 1 min, 5 cycles of denaturation at 94°C for 20 sec, annealing at 45°C for 20 sec, and extension at 68°C for 30 sec, 35 cycles of denaturation at 94°C for 20 sec, annealing at 51°C for 20 sec, and extension at 68°C for 30 sec, and a final extension at 68°C for 1 min. Amplicons were approximately 650 bp. Host COI sequencing and read processing were performed similarly to the rRNA protocol. Obtained COI

data were then analyzed using the above phylogenetic analysis protocol.

2.3. RESULTS

2.3.1. Morphology of *Lunidium* sp. Clade A

Lunidium sp. Clade A trophozoites were elongate, ribbon-like in shape, possessed a pointed mucron (Fig. 2.1), and moved by bending and coiling (Fig. 2.1 A–B). Longitudinal epicytic folds (Fig. 2.1 A, C–D) ran along the cells with a density of 0.15 folds/µm, and transverse folds were also observed (Fig. 2.1 C). Isolates measured 100–228 µm in length ($\bar{x}$ = 163.2 µm; n = 4) and 10–20 µm in width ($\bar{x}$ = 15.8 µm; n = 7). Spherical nuclei were in the cell center and measured 6–7 µm in diameter ($\bar{x}$ = 6.5 µm; n = 2).

2.3.2. Morphology of *Metzidium* sp. Clade A

Metzidium sp. Clade A trophozoites were elongate with a rounded posterior and anterior (Fig. 2.2 A, C), and moved by worm-like bending. Longitudinal epicytic folds ran along the cells with a density of 1.2 folds/µm, and transverse folds were also observed (Fig. 2.2 B–C). Isolates measured 120–140 µm in length ($\bar{x}$ =130 µm; n = 3) and 15–20 µm in width ($\bar{x}$ = 16.6 µm; n = 3). Spherical nuclei were located centrally and measured 9–11 µm in diameter ($\bar{x}$ = 10 µm; n = 2).

2.3.3. Morphology of *Devanium* sp. Clade A

Devanium sp. Clade A trophozoites had a whale-like morphology with a bulbous anterior and a pointed, tail-like posterior (Fig. 2.3 A–C, E). Longitudinal epicytic folds ran along the cells with a density of 1.1 folds/µm (Fig. 2.3 D), and no transverse folds were observed. Cells had an elliptical cross-section surrounded by short, knob-like epicytic folds and contained many large amylopectin granules (Fig. 2.3 F). Isolates measured 70–90 µm in length ($\bar{x}$ =81.2 µm; n = 4) and 15–25 µm in width ($\bar{x}$ = 22.5 µm; n = 4). Spherical nuclei were found in the anterior third of cells and measured 5–7 µm in diameter ($\bar{x}$ = 5.6 µm; n = 2).

2.3.4. Morphology of *Devanium* sp. Clade B

Devanium sp. Clade B trophozoites were elongate with a tapered posterior and rounded anterior (Fig. 2.4 A–B). Longitudinal epicytic folds ran along the cells with a density of 1.4 folds/µm (Fig. 2.4 B–E) and had a visible inner membrane complex (Fig. 2.4 D). Transverse epicytic folds were also observed (Fig. 2.4 C). Cells had a circular cross-section surrounded by short, knob-like epicytic folds and contained numerous amylopectin granules (Fig. 2.4 D–E) as well as infection with metchnikovellid parasites (Fig. 2.4 E). Isolates measured 140–220 µm in length ($\bar{x}$ =171.6 µm; n = 6) and 10–30 µm in width ($\bar{x}$ = 19.2 µm; n = 4). Nuclei were found in the anterior third of cells and measured 5 µm in diameter ($\bar{x}$ = 5 µm; n = 1).

2.3.5. Morphology of *Devanium* sp. Clade C

Devanium sp. Clade C trophozoites were elongate with a pointed posterior and rounded anterior (Fig. 2.5 A, C) often concealed by a sustained coiled state. Longitudinal epicytic folds ran along the cells with a density of 1.4 folds/µm (Fig. 2.5 B–C), and no transverse folds were observed. A large nucleus (Fig. 2.5 A) was also visible. Isolates measured 125–400 µm in length ($\bar{x}$ =221.6 µm; n = 3) and 10–20 µm in width ($\bar{x}$ = 15 µm; n = 3). Spherical nuclei were found in the anterior of cells and measured 5 µm in diameter ($\bar{x}$ = 5 µm; n = 1).

2.3.6. Molecular phylogeny of gregarine apicomplexans

Phylogenetic analysis of a 91-sequence 18S (and concatenated 18S+ITS sequences for *Lunidium* sp. Clade A) alignment (Fig. 2.6) included archigregarines, lecudinids, *Polyplicarium*, *Chromera*, *Vitrella*, and distantly related marine gregarines (*Cephaloidophora*) as outgroup. *Devanium* spp. Clades A, B, and C (Oshoro Bay, Hokkaido) formed distinct, strongly supported clades sister to other *Devanium* lineages, all nested within a moderately supported (ML:89/PP:0.99) *Devanium* clade. *Lunidium* sp. Clade A (Akkeshi Bay, Hokkaido) formed a strongly supported clade sister to the remaining *Lunidium* sequences; together, all *Lunidium* sequences formed a strongly supported clade sister to chromerids (*Chromera velia* and *Vitrella brassicaformis*). *Metzidium* sp. Clade A was recovered as a distinct, strongly supported clade sister to *Metzidium perlucensae*, nested within a strongly supported clade of all *Metzidium*

sequences.

2.3.7. Molecular phylogeny of host material

Phylogenetic analysis of a 71-sequence COI alignment (Fig. 2.7) included representatives from polychaete families Arenicolidae, Capitellidae, Chaetopteridae, Cirratulidae, Eunicidae, Glossoscolecidae, Glyceridae, Lumbrineridae, Maldanidae, Nereididae, Orbiniidae, Sabellidae, Siboglinidae, Sipunculidae, and Terebellidae. Hosts of *Metzidium* sp. Clade A were placed within a strongly supported clade composed exclusively of *Phyllochaetopterus* sequences. *Lunidium* sp. Clade A host material was nested within a strongly supported clade of *Nainereis* and *Scoloplos* (Orbiniidae). Hosts of *Devanium* spp. Clades A–C were recovered within two strongly supported Cirratulidae sister clades which together formed a clade of cirratulid sequences under moderate support (ML:76/PP:--). Mollusk sequences served as the outgroup.

2.4. DISCUSSION

2.4.1. Morphological and phylogenetic insights into *Lunidium* sp. Clade A

This study uncovered novel biodiversity among multiple archigregarine lineages from marine hosts across Japan. *Lunidium* sp. Clade A trophozoites, isolated from an orbiniid host in Akkeshi Bay, were characterized by an elongate, ribbon-like shape and a pointed mucron (Fig. 2.1). Isolates displayed sparse longitudinal epicytic folds (0.15 folds/µm) and some transverse folds were apparent as well. Low fold density and elongate morphology coincide with descriptions of other *Lunidium* species (Wakeman et al., 2014; Rueckert and Horák, 2017; Lax et al., 2024). Phylogenetically, *Lunidium* sp. Clade A formed a well-supported lineage sister to other *Lunidium* sequences (Fig. 2.6).

Notably, the current description of *Lunidium* (Lax et al., 2024) diagnoses members as inhabiting terebellid hosts. Known Terebellidae host genera associated with *Lunidium* include *Amphitritides, Eupolymnia,* and *Thelepus* (Table 2.3). *Lunidium* sp. Clade A was isolated from a

polychaete in the family Orbiniidae, which is of uncertain taxonomic placement (Zhadan et al., 2015; Meca et al., 2021) and was recovered as a monophyletic group under strong statistical support (Fig. 2.7). Taken together, these findings justify the inclusion of this novel clade within *Lunidium* based on its distinct morphological traits and robust phylogenetic placement. Moreover, these results suggest that host affiliation within the genus *Lunidium* are broader than previously recognized.

2.4.2. Novel lineage of *Metzidium* from chaetopterid hosts

Metzidium sp. Clade A, recovered from *Phyllochaetopterus* (Chaetopteridae Audouin and Milne Edwards, 1833), also formed a morphologically and genetically distinct lineage. These trophozoites were broadly elongate with rounded ends and exhibited denser longitudinal epicytic folds (1.2 folds/μm) as well as distinct transverse folds. With worm-like motility, *Metzidium* Clade A is morphologically consistent with other *Metzidium* species (Table 2.3) but distinct phylogenetically (Fig. 2.6) and in host type (Fig. 2.7, Table 2.3).

A recently published (Lax et al., 2024) description of the genus *Metzidium* mentions sipunculid hosts as a defining trait of these archigregarines. Although *Metzidium* sp. Clade A isolates were collected from a chaetopterid worm, phylogenetic analysis (Fig. 2.7) recovered sipunculids and chaetopterids as well-supported monophyletic groups that both branch comparatively early along the Cirratulidae lineage. For these reasons, *Metzidium* sp. Clade A was identified as a novel archigregarine clade.

2.4.3. *Devanium* spp. Clades A, B, and C highlight a trend of cirratulid specialization among *Devanium* archigregarines

Genus *Devanium* exhibited the highest biodiversity among these novel data, with three novel clades (*Devanium* spp. Clades A–C) isolated from cirratulid (Cirratulidae Carus, 1863) hosts. *Devanium* sp. Clade A trophozoites had a unique whale-like morphology, with a bulbous anterior and tail-like posterior, as well as an elliptical cross-section with knob-like epicytic folds. These isolates also had a relatively short length and were rich in amylopectin granules while

lacking transverse folds. Meanwhile, *Devanium* sp. Clade B was larger and displayed a more classic elongate gregarine form, with both longitudinal (1.4 folds/µm) and transverse folds, and notable features such as an inner membrane complex and metchnikovellid (Metchnikovellidae Caullery and Mesnil, 1914) infection. For reference, metchnikovellids are microsporidian hyperparasites known to infect gregarines (Sokolova et al., 2014; Rotari et al., 2015; Frolova et al., 2021; Frolova et al., 2022; Frolova et al., 2023). *Devanium* sp. Clade C was the longest and thinnest of the three, often observed in a coiled state. Like Clade B, these isolates had a relatively high epicytic fold density (1.4 folds/µm) but lacked visible transverse folds. All three *Devanium* clades formed discrete, strongly supported phylogenetic lineages (Fig. 2.6).

Overall, these results reveal a clear mirroring pattern between archigregarine clades and the phylogenetic identities of their hosts. Each of the five clades—*Lunidium* sp. Clade A, *Metzidium* sp. Clade A, and *Devanium* spp. Clades A–C—were associated with a distinct group of annelid hosts. *Metzidium* sp. Clade A was found in *Phyllochaetopterus* (Chaetopteridae), while *Lunidium* sp. Clade A was associated with an orbiniid host (*Nainereis*). Similarly, the three *Devanium* clades were all found in cirratulid hosts. This study reveals previously unknown archigregarine biodiversity and host associations, providing a foundation for future research on their biodiversity, host associations, and patterns of speciation.

CHAPTER 3. Biogeographic patterns and cryptic biodiversity in marine paralecudinid gregarines (Apicomplexa) from Pacific polychaetes

SUMMARY

Marine gregarines are an understudied group of apicomplexans that inhabit invertebrates. This study examines the biodiversity, host specificity, and biogeography of marine gregarines associated with polychaetes from the northern Pacific Ocean, focusing on eunicid, nereid, and lumbrinerid host families. By combining morphological, molecular (host COI, isolate rRNA), and biogeographic data, I uncover novel biodiversity and delineate speciation patterns among lecudinid and paralecudinid gregarines. Herein, I describe a new clade of *Ferraria* and revise the taxonomy of *F. cornucephala iwamusi.* I also highlight cryptic diversity in *Paralecudina*, with newly identified clades (*P*. spp. Clades B and C) from northern Japan, demonstrating biogeographic differentiation and supporting allopatric speciation as a driver of paralecudinid biodiversity. These findings offer new insights into the evolutionary mechanisms shaping marine gregarine speciation and their complex interactions with polychaete hosts.

3.1. INTRODUCTION

Marine gregarines, single-cell parasites found globally within invertebrate hosts, represent a largely unexplored component of the approximately 350 extant apicomplexan genera (Adl et al., 2019). These early branching apicomplexans are noteworthy for their presence across a broad spectrum of habitats, ranging from marine and freshwater environments to terrestrial ecosystems (Desportes and Schrével, 2013). Despite their evolutionary importance, research has traditionally focused on apicomplexans that parasitize vertebrates due to their impact on public

health and agriculture (Rueckert et al., 2015; Wakeman et al., 2021; Park and Leander, 2024a). In contrast, marine gregarines remain understudied (Morrison, 2009), leaving significant gaps in our understanding of their biodiversity and host interactions.

Polychaetes, particularly members of the families Eunicidae Berthold, 1827 (Bhatia and Setna, 1938; Rueckert et al., 2013), Nereididae Blainville, 1818 (Rueckert et al., 2011; Schrével et al., 2016; Odle et al., 2024), and Lumbrineridae Schmarda, 1861 (Rueckert et al., 2010; Iritani et al., 2018b), often serve as hosts for marine gregarines. Gregarines associated with these polychaete families include the genera *Ferraria* (Setna, 1931; Hoshide, 1957; Hoshide, 1973; Elbarhoumi and Zghal, 2010), *Lecudina* (Rueckert et al., 2010, Rueckert et al., 2011b), and *Paralecudina* (Schrével, 1969; Leander et al., 2003; Rueckert et al., 2010; Rueckert et al., 2013; Iritani et al., 2018b), respectively, and are known to exhibit a variety of morphologies (Leander et al., 2006; Rueckert et al., 2013, Iritani et al., 2018b). These gregarines are characterized by traits such as highly folded epicytic membranes, gliding motility, and distinct mucrons, which likely reflect their adaptations to specific host types.

The Pacific Ocean harbors a rich diversity of polychaetes (Canales-Aguirre et al., 2011; Saeedi et al., 2022), a group of organisms known for their cosmopolitan distribution across the globe (Pamungkas et al., 2021). However, most studies of marine gregarines in this region have relied heavily on morphological observations, with molecular data available for fewer than 100 species (Wakeman et al., 2021). This lack of molecular information has limited our understanding of their speciation processes, host preferences, and biogeographical patterns. Recent efforts to integrate morphological data with molecular evidence have begun to shed light on these morphologically similar yet phylogenetically distinct (cryptic) organisms (Rueckert et al., 2011). Still, significant gaps remain in reconciling historical descriptions with modern phylogenetic frameworks.

This study explores the biodiversity and host specificity of marine gregarines from eunicid, nereid, and lumbrinerid polychaetes across the northern Pacific Ocean. By combining

morphological, molecular (rRNA), and ecological data, I aim to uncover cryptic diversity and clarify patterns of host preference among lecudinid and paralecudinid gregarines. These findings provide crucial insights into the evolutionary mechanisms driving speciation in marine gregarines and their adaptation to polychaete hosts in diverse ecological contexts.

3.2. MATERIALS AND METHODS

3.2.1. Host collection and sample processing

Hosts were collected opportunistically in the intertidal zones near Oshoro Marine Station, Hokkaido, Japan (43°12'37"N 140°51'25"E) and Clover Point, British Columbia, Canada (48°24'14"N 123°21'00"W) between November 2022 and December 2023 (Table 3.1) from under intertidal rocks and inside tufts of seagrass. Subsequent steps were performed as described in Section 2.2.1.

3.2.2. Electron microscopy

Electron microscopy was performed as described in Section 2.2.2.

3.2.3. Amplification and sequencing of the 18S rRNA gene and ITS region

Gregarine trophozoites were transferred individually to 0.2 ml PCR microcentrifuge tubes and stored at –20°C for 1–5 days. Genomic DNA was then extracted from these samples using a QuickExtract FFPE DNA Extraction Kit (Lucigen, Middlesex, United Kingdom) in line with manufacturer protocol. General and specific primers (Table 3.2) with KOD One® PCR Master Mix (Toyobo, Osaka, Japan) were used in amplification of the 18S rRNA gene (18S) and ITS region. Subsequent steps were performed as described in Section 2.2.3.

3.2.4. Molecular phylogenetic analyses

Phylogenetic analyses were performed as described in Section 2.2.4.

3.2.5. Host identification

Fragments of host tissue remaining after gregarine isolation were preserved in 100% ethanol for barcoding. Host DNA was extracted from samples using the MasterPure Complete

DNA & RNA Purification Kit (LGC Biosearch Technologies, Hoddesdon, United Kingdom). The cytochrome *c* oxidase subunit 1 (COI) gene was amplified using primers polyLCO and polyHCO (Table 3.2) with KOD One® PCR Master Mix (Toyobo, Osaka, Japan). Subsequent steps were performed as described in Section 2.2.5.

3.3. RESULTS

3.3.1. Morphology of *Ferraria* sp. Clade A

Ferraria sp. Clade A trophozoites were teardrop-shaped with a broad anterior, ball-like or broad mucron (Fig. 3.1 A–C), and gliding motility. Trophozoites also possessed longitudinal ridges (Fig. 3.1 A, C–D). Epicytic folds (Fig. 3.1 C, E) ran longitudinally along the cells with a density of 6 folds/µm. Isolates measured 294–309 µm in length ($\bar{x}$ =292 µm; n = 4) and 135–165 µm in width ($\bar{x}$ = 148 µm; n = 4). Spherical nuclei were located along the longitudinal cell axis and measured 35–38 µm in diameter ($\bar{x}$ = 37 µm; n = 3).

3.3.2. Morphology of *Ferraria* sp. Clade B

Ferraria sp. Clade B trophozoites were elongate with a flattened posterior, a conical mucron (Fig. 3.2, Fig. 3.3 A), and a transverse crease near the anterior of the cell (Fig. 3.2 B–C). Mucrons were observed in retracted (Fig. 3.2 A, C) and extended (Fig. 3.2 B) states. Cells had an oval cross-section (Fig. 3.3 B), a visible apicoplast (Fig. 3.3 C), and epicytic folds (Fig. 3.3 A–B, D) that ran longitudinally along the cells with a density of 6 folds/µm. Isolates measured 247–564 µm in length ($\bar{x}$ =388 µm; n = 17) and 63–159 µm in width ($\bar{x}$ = 103 µm; n = 17). Spherical nuclei were found in the posterior half of cells and measured 26–74 µm in diameter ($\bar{x}$ = 41 µm; n = 15).

3.3.3. Morphology of *Paralecudina* sp. Clade A

Paralecudina sp. Clade A trophozoites were elongate (Fig. 3.4 A–B) with a pointed posterior and prominent anterior bulge near the anterior (Fig. 3.4 A). Mucron was occasionally observed in an extended state, and rarely with host tissue still attached (Fig. 3.4 B). Cells had an

oval cross-section (Fig. 3.4 C) and epicytic folds (Fig. 3.4 C–D) that ran longitudinally along the cells with a density of 5 folds/µm. Isolates measured 105–400 µm in length ($\bar{x}$ = 228 µm; *n* = 16) and 13–30 µm in width ($\bar{x}$ = 19 µm; *n* = 16). Ellipsoid nuclei were found in the anterior half of cells, measuring 7–20 µm along the long axis ($\bar{x}$ = 16 µm; *n* = 13) and 5–8 along the short axis ($\bar{x}$ = 12 µm; *n* = 13).

3.3.4. Morphology of *Paralecudina* sp. Clade B

Paralecudina sp. Clade B trophozoites were elongate with a pointed posterior and wide anterior that tapered towards the mucron (Fig. 3.5 A–B). Cells had epicytic folds (Fig. 3.5 B–D, F) that ran longitudinally along the cells with a density of 6 folds/µm. A putative apicoplast was visible (Fig. 3.5 E), and cells had an oval cross-section containing numerous amylopectin granules (Fig. 3.5 F). Isolates measured 270–615 µm in length ($\bar{x}$ = 375 µm; *n* = 18) and 45–114 µm in width ($\bar{x}$ = 82 µm; *n* = 18). Ellipsoid to spherical nuclei were found in the anterior half of cells, measuring 28–54 µm along the long axis ($\bar{x}$ = 38 µm; *n* = 14) and 25–43 µm along the short axis ($\bar{x}$ = 33 µm; *n* = 14).

3.3.5. Morphology of *Paralecudina* sp. Clade C

Paralecudina sp. Clade C trophozoites were elongate with a pointed posterior and prominent anterior bulge (Fig. 3.6 A, B). Cells had epicytic folds (Fig. 3.6 B–C, E–F) that ran longitudinally along the cells with a density of 6 folds/µm. A putative apicoplast was visible (Fig. 3.6 D), and a circular cross-section (Fig. 3.6 E) was seen on TEM. Isolates measured 127–518 µm in length ($\bar{x}$ = 311 µm; *n* = 17) and 24–79 µm in width ($\bar{x}$ = 35 µm; *n* = 17). Ellipsoid to spherical nuclei were found in the anterior half of cells, measuring 14–30 µm along the long axis ($\bar{x}$ = 21 µm; *n* = 16) and 11–25 µm along the short axis ($\bar{x}$ = 14 µm; *n* = 16).

3.3.6. Molecular phylogeny of gregarine apicomplexans

Phylogenetic analysis was performed on a 57-sequence 18S+ITS concatenated alignment of *Trichotokara*, *Ferraria* and *Paralecudina* (Fig. 3.7) sequences. Distantly related marine gregarines and chromerids (*Metzidium orientale, Chromera velia*, and *Vitrella*

brassicaformis) were included as an outgroup. All *Ferraria* sequences from Oshoro (Hokkaido) formed a strongly supported clade sister to *Trichotokara*, with *Ferraria* sp. Clade B sequences forming a strongly supported clade to the exclusion of *Ferraria* sp. Clade A. *Paralecudina* sequences formed a strongly supported clade sister to the clade formed by *Ferraria* and *Trichotokara*, and contained separate lineages of *P. anankea* (one sequence), *Paralecudina* sp. Clade A *(P. polymorpha;* 16 single-cell isolates from the present work; two from Leander et al., (2003)), *Paralecudina* sp. Clade B (10 single-cell isolates), and *Paralecudina* sp. Clade C (10 single-cell isolates). *Paralecudina* sp. Clade A sequences from western Canada formed a strongly supported clade sister to a clade of paralecudinids from Oshoro (Hokkaido). This moderately supported clade of Japanese paralecudinids contained nested *Paralecudina* sp. Clades B and C, both of which formed under strong support.

3.3.7. Molecular phylogeny of host material

Phylogenetic analysis of a 102-sequence COI alignment (Fig. 3.8) included representatives from polychaete families Nereididae, Eunicidae, and Lumbrineridae. Host material for *Ferraria* sp. Clades A and B was recovered within a strongly supported clade along with *Marphysa victori*. Host material for *Paralecudina* spp. Clades A through C was recovered nested within a strongly supported clade composed exclusively of *Lumbrineris japonica*/*L*. cf. *japonica*. Sipunculid sequences were included as an outgroup.

3.4. DISCUSSION

3.4.1. *Ferraria* highlights a trend of eunicid specialization among marine gregarines

This study adds new insight into the taxonomic boundaries and host associations among marine gregarines in the genus *Ferraria*. Gregarine species known to parasitize *Marphysa* (eunicid) worms include *Ferraria cornucephali* Setna, 1931, *Bhatiella marphysae* Setna, 1931, *Gopaliella marphysae* Ganapati, Kalavati, and Sundaram, 1974, and *Viviera marphysae* Schrével, 1963 (Table 3.3). In addition, *Cotyloepimeritus iwamusii* Tsugawa 1944 was collected

from *Marphysa* hosts around southern Japan during the early 20th century. This genus has been attributed the taxonomic authority Hoshide, 1935 despite being proposed as novel by Tsugawa (1944, p.223) (Tsugawa appears to be a former surname of Hyoma Hoshide). The only evidence I was able to find in support of the Hoshide, 1935 taxonomic authority is a claimed date of discovery by Hoshide (1957): "I discovered a parasite which resembles to the above from *Marphysa iwamusi* IZUKA and reported as *Cotyloepimeritus iwamusii* in 1935." (p.106). Later, *Cotyloepimeritus iwamusii* was re-classified as *Ferraria iwamusi* with the final "i" dropped and with a clear distinction drawn between this taxon and *F. cornucephala* from India (Hoshide, 1957). Sixteen years after this, subspecies nomenclature for *F. cornucephala iwamusi* appeared in print (Hoshide, 1973). This subspecies nomenclature was perpetuated in later works (Elbarhoumi and Zghal, 2010; Desportes and Schrével, 2013). For these reasons, the present work interprets Hoshide (1973)'s taxonomic view to include subspecies *F. cornucephala cornucephala* (India) and *F. cornucephala iwamusi* (southern Japan).

Data from the present study suggest that *F. cornucephala iwamusi* is actually two phylogenetically and morphologically distinct organisms rather than immature and mature forms (Hoshide, 1973) of the same organism. Line drawings (Tsugawa, 1944; Hoshide, 1957) and light micrographs (Hoshide, 1973) of "mature" *F. cornucephala iwamusi* closely match the bulbous anterior, longitudinal ridges, and tapered posterior seen with *F.* sp. Clade A (Fig. 3.1, Fig. 3.9). Similarly, line drawings and light micrographs of the "immature" form (Hoshide 1957; Hoshide, 1973) reflect the elongate shape, transverse crease, and telescoping mucron observed among *F.* sp. Clade B isolates (Fig. 3.2, Fig. 3.9). A species-level difference between *F. iwamusi* (Hoshide, 1957) and *F. cornucephala* (Setna, 1931) cannot currently be made because there is no available molecular data from the *F. cornucephala* type locality.

Ferraria sp. Clades A and B are distinguishable from other *Marphysa*-inhabiting gregarines as well. With respect to locality, *Ferraria cornucephali*, *Bhatiella marphysae*, and *Gopaliella marphysae* were described from India. In addition, *Viviera marphysae* was described

from France (Table 3.3). Morphologically, *F. cornucephali* is similar in shape to *F.* sp. Clade B but is recorded as being more rounded and clearly cephaline (having a distinct head-like region separated by a septum) (Setna, 1931). *Bhatiella marphysae* is more elliptical than *F.* sp. Clade B in morphology, and displays a wrinkled membrane (Elbarhoumi and Zghal, 2010) not present in the isolates of this study. *Gopaliella marphysae* trophozoites slightly resemble *F.* sp. Clade B but are more elongate and have a distinct flower-like mucron (Ganapati et al., 1974). *Viviera marphysae* vaguely resembles *F.* sp. Clade A in morphology, but with a more angular center section and more elongate, pointed posterior (Schrével, 1963).

Genus *Trichotokara* Rueckert and Leander, 2010 also specializes in eunicid polychaetes, and includes *T. nothriae* from *Nothria conchylega* (western Canada), *T. japonica* from *Nothria* cf. *otsuchiensis* (southern Japan), and *T. eunicae* from *Eunice valens* (western Canada) (Table 3.3). Phylogenetically, *F.* sp. Clades A and B are distinct from *Trichotokara*, which form a separate clade (Fig. 3.7). Morphologically, *F.* sp. Clade A is tear-shaped (Fig. 3.1), and *F.* sp. Clade B is elongate (Fig. 3.2, Fig. 3.9), differing from the guitar-shaped *T. nothriae*, elongate *T. japonica*, and bulbous *T. eunicae*. Mucron morphology further differentiates these species: *F.* sp. Clade A has a ball-like or broad mucron and *F.* sp. Clade B has a conical mucron, while *T. nothriae* has an elongate mucron with hair-like projections, *T. japonica* has an elongate mucron with antler-like projections, and *T. eunicae* has a bulbous mucron (Table 3.3). This discovery and taxonomic revision better reflects the diversity of marine gregarines that parasitize eunicid polychaetes.

3.4.2. Cryptic diversity and the biogeography of *Paralecudina*

Cryptic diversity is prevalent among marine gregarines, having been observed in the genera *Lecudina* (Rueckert et al., 2011; Odle et al., 2024), *Selenidium* (Wakeman and Leander, 2013b), and now *Paralecudina*. Initially described as *Lecudina polymorpha* by Schrével (1963, 1969), *Paralecudina polymorpha* Rueckert, Wakeman, and Leander, 2013 (presumed to be the identity of *Paralecudina* sp. Clade A) is reported to possess multiple morphotypes: a larger,

ellipsoid (type 1) trophozoite and a slender, elongate (type 2) trophozoite with an anterior bulge (Leander et al., 2003b). However, upon re-sampling the initial locality (western Canada) of these isolates, I was unable to obtain type 1 morphotypes. Regardless, a strong similarity in morphology (Fig. 3.10) and host preference (*Lumbrineris japonica*) was observed (Fig. 3.8) between *P.* sp. Clade A from western Canada and *P.* sp. Clades B and C from northern Japan (Oshoro). These *Paralecudina* clades formed exclusive, strongly supported sister clades sharply delineated by locality (Fig. 3.7), suggesting allopatric speciation as a biodiversity driver in this case. The remaining member, *P. anankae* Iritani, Wakeman and Leander, 2018, forms a clade sister to a clade containing all other known *Paralecudina* (Fig. 3.7) and was isolated from *Lumbrineris inflata* (Iritani et al., 2018b)—a closely related polychaete host.

Novel *Paralecudina* biodiversity from the present work includes *P.* sp. Clades B and C, both collected from northern Japan (Oshoro). *Paralecudina* sp. Clade B has a rounded posterior and ellipsoid-to-spherical nucleus, contrasting with the pointed posteriors and solely ellipsoidal nuclei seen with *P.* sp. Clade C, *P. polymorpha/P. s*p. Clade A, and *P. anankae* (Table 3.4). These four taxa also share a similar epicytic fold density of 5 to 6 folds/µm (Table 3.4). *Paralecudina* sp. Clade C is morphologically distinct from *P.* sp. Clade B by the presence of an anterior bulge and a slimmer, elongate body (Fig. 3.10), and from *P. anankea* by its lack of a spindle-like form (Iritani et al., 2018b). All members of this clade share a rounded mucron (Schrével, 1969; Leander et al., 2003; Rueckert et al., 2010; Rueckert et al., 2013) except for *P. anankae*, which has a tapered mucron (Table 3.4). Based on these observations and a clearly distinct phylogeny recovered from 18S and ITS (Fig. 3.7, Fig. 3.10) molecular data, *P.* sp. Clades B and C are likely novel species.

CHAPTER 4. Early branching lecudinids reveal novel biodiversity and host-linked speciation in Pacific marine gregarines

SUMMARY

Marine gregarines, particularly early branching lecudinids, display unique adaptations that may provide clues about early apicomplexan parasitism. In this study, I describe four novel clades of marine gregarines collected from tidal zone invertebrates in the northern Pacific Ocean. These clades are distinguished by their morphological traits, host specificity, and molecular phylogenetic placement. Notably, Lecudinidae sp. Clade A, isolated from an ostracod, represents a potential first of its kind. Lecudinidae spp. Clades B and C, meanwhile, were isolated from a *Glycera* bloodworm and cirratulid, respectively. A novel clade of *Difficilina* is also introduced, notably collected from a terebellid polychaete rather than the typical nemertean host type. These findings together suggest that host affiliation, more than biogeography, is a key driver of speciation among early lecudinids.

4.1. INTRODUCTION

Apicomplexans are unicellular parasites that infect animals (Levine, 1970). Research on apicomplexans tends to focus on lineages such as *Plasmodium*, *Toxoplasma*, and *Babesia* due to their roles in the diseases malaria (Kolawole et al., 2023), toxoplasmosis (Adem and Ame, 2023), and babesiosis (Kuibagarov et al., 2023), respectively. However, these lineages represent only a small fraction of the overall apicomplexan diversity. Regarding the biodiversity of this group, apicomplexa is comprised of an estimated 350 genera (Adl et al., 2019). Yet, likely fewer than 1% of apicomplexans have been described in the literature (Morrison, 2009). This estimate

implies the existence of hundreds of thousands to potentially millions of yet-undiscovered species.

Marine gregarines represent a highly diverse and evolutionarily significant group of apicomplexans, likely among the earliest to have evolved (Théodoridès, 1984; Leander, 2008). Among these are the lecudinids: a group of marine gregarines known to exhibit unique variations in both form and motility. For instance, *Veloxidium leptosynaptae* moves via a unique thrashing movement (Wakeman and Leander, 2012), while other genera such as *Pterospora* and *Lithocystis* have formed specialized membrane structures such as branching digits, irregular surface elevations, (Landers and Leander, 2005), and star-shaped ridges (Coulon and Jangoux, 1987). These innovations highlight the success of early marine gregarines in occupying the full range of invertebrate hosts. Nevertheless, available molecular and biogeographical data remain limited to no more than around 100 species (Wakeman et al., 2021), hindering a full understanding of lecudinid evolution.

In this study, I describe four novel clades of marine gregarines—three broadly within Lecudinidae and one specifically within *Difficilina*—collected from intertidal invertebrates in the northern Pacific Ocean. These clades are distinguished by morphological traits, host specificity, and molecular phylogenetics. Lecudinidae spp. Clades B and C were isolated from a *Glycera* bloodworm and cirratulid, respectively. Additionally, *Difficilina* sp. Clade A, recovered from a terebellid polychaete, represents the first known member of its genus to infect annelids rather than nemerteans. Notably, Lecudinidae sp. Clade A was isolated from an ostracod host, likely marking the first recorded gregarine association with this arthropod lineage.

4.2. MATERIALS AND METHODS

4.2.1 Host collection and sample processing

Hosts were collected opportunistically in the intertidal zones near Oshoro Marine Station (43°12'37"N 140°51'25"E) in Hokkaido (Japan), Mizunashikaihin (41°48'40"N

141°11'3"E) in Hakodate, Hokkaido (Japan), around Hanaguri (34°18'04"N 132°50'20"E) in Hiroshima, Japan, and Crescent City (41°44'12"N 124°11'40"E), California (United States) between November 2022 and October 2023 (Table 4.1) from under intertidal rocks and inside tufts of seagrass. Subsequent steps were performed as described in Section 2.2.1.

4.2.2. Electron microscopy

Electron microscopy was performed as described in Section 2.2.2.

4.2.3. Amplification and sequencing of the 18S rRNA gene

Gregarine trophozoites were transferred individually to 0.2 ml PCR microcentrifuge tubes and stored at –20°C for 1–5 days. Genomic DNA was then extracted from these samples using a QuickExtract FFPE DNA Extraction Kit (Lucigen, Middlesex, United Kingdom) in line with manufacturer protocol. General and specific primers (Table 4.2) with KOD One® PCR Master Mix (Toyobo, Osaka, Japan) were used in amplification of the 18S rRNA gene. Subsequent steps were performed as described in Section 2.2.3.

4.2.4. Molecular phylogenetic analyses

Phylogenetic analyses were performed as described in Section 2.2.4.

4.2.5. Host identification

Fragments of host tissue remaining after gregarine isolation were preserved in 100% ethanol for barcoding. Host DNA was extracted from samples using the MasterPure Complete DNA & RNA Purification Kit (LGC Biosearch Technologies, Hoddesdon, United Kingdom). The cytochrome *c* oxidase subunit 1 (COI) gene was amplified using primers polyLCO and polyHCO (Table 4.2) with KOD One® PCR Master Mix (Toyobo, Osaka, Japan). Subsequent steps were performed as described in Section 2.2.5.

4.3. RESULTS

4.3.1. Morphology of Lecudinidae sp. Clade A

Lecudinidae sp. Clade A trophozoites were bean-shaped with a broadly rounded anterior

and posterior (Fig. 4.1 A–C). Centrally located amylopectin granules, as well as putative apicoplasts and lipid droplets, were visible within a round TEM cross-section (Fig. 4.1 E–F). Epicytic folds (Fig. 4.1 C–E) ran longitudinally along the cells with a density of 1.5 folds/µm. Isolates measured 60–120 µm in length ($\bar{x}$ = 81.6 µm; *n* = 3) and 30–85 µm in width ($\bar{x}$ = 55 µm; *n* = 3). Spherical nuclei were in the cell anterior and measured 20 µm in diameter ($\bar{x}$ = 20 µm; *n* = 1).

4.3.2. Morphology of Lecudinidae sp. Clade B

Lecudinidae sp. Clade B possessed elongate trophozoite pairs in lateral syzygy (Fig. 4.2 A–B); single trophozoites were not observed. Trophozoites actively moved in a dynamic wave-like motion (undulating) passing across the length of the trophozoite. Epicytic folds ran longitudinally along the cells (Fig. 4.2 A–B, B inset). Folds were broadly spaced at the lobular bulge with a density of 1 fold/µm (Fig. 4.2 B inset). Isolates measured 130–270 µm in length (x = 193 µm, *n* = 6) and 30–50 µm in width (x = 41 µm, *n* = 6). Spherical nuclei measured 10–15 µm in diameter (x = 11.25 µm, *n* = 4). Nuclear position was not fixed to a specific location but rather moved with the motion of the cell.

4.3.3. Morphology of *Difficilina* sp. Clade A

Difficilina sp. Clade A contained oval to crescent-shaped (Fig. 4.3 A–B, E) trophozoites measuring 45–60 µm in length ($\bar{x}$ = 50 µm, *n* = 3) and 15–25 µm in width ($\bar{x}$ = 20 µm, *n* = 3). Nuclei were not visible, and cell mucrons had a papillary morphology (Fig. 4.3 A–B, E). Isolates were surrounded by short folds with a density of 4 folds/µm at the widest part of the cell (Fig. 4.3 C, D).

4.3.4. Morphology of Lecudinidae sp. Clade C

Lecudinidae sp. Clade C trophozoites were club-shaped with a rounded posterior and mucron (Fig. 4.4 A–B, D). Cells had a circular cross-section (Fig. 4.4 E) and epicytic folds (Fig. 4.4 C–F) that ran longitudinally along the cells with a density of 3.3 folds/µm. Numerous amylopectin granules (Fig. 4.4 E), mitochondria at the cytoplasmic periphery, and an inner

membrane complex (Fig. 4.4 F) were visible by TEM. Isolates measured 225–360 µm in length ($\bar{x}$ = 293.3 µm; *n* = 6) and 70–100 µm in width ($\bar{x}$ = 83.3 µm; *n* = 6). Spherical nuclei were found in the central to anterior portion of cells and measured 30–40 µm in diameter ($\bar{x}$ = 37.5 µm; *n* = 4).

4.3.5. Molecular phylogeny of gregarine apicomplexans

Phylogenetic analysis of a 69-sequence 18S alignment (Fig. 4.5) included *Amplectina,* archigregarines (*Devanium, Metzidium,* and *Selenidium*), chromerids, *Cuspisella, Lankesteria, Lecudina,* paralecudinids, *Sphinctocystis*, *Trichotokara*, and early branching lecudinid genera *Difficilina, Lithocystis, Urospora,* and *Veloxidium*. Lecudinidae sp. Clades A (Hiroshima) and B (Oshoro) formed distinct, strongly supported clades that branched from the *Lankesteria*/*Lecudina* lineage before *Difficilina*, *Lithocystis*, and *Pterospora*. *Difficilina* sp. Clade A (northern California) was strongly supported as sister to *Difficilina tubulani*, nested within a well-supported *Difficilina* + *Urospora* clade. This clade diverged early along the *Lankesteria*/*Lecudina* lineage, before *Sphinctocystis* and *Amplectina*, and included Lecudinidae sp. Clade C (Hakodate), which also formed a strongly supported monophyletic group.

4.3.6. Molecular phylogeny of host material

Phylogenetic analysis of an 81-sequence COI alignment (Fig. 4.6) included representatives from major marine invertebrate groups, including Arenicolidae, Capitellidae Chaetopteridae, Cirratulidae, Decapoda, Eunicidae, Glyceridae, Lumbrineridae, Maldanidae, Mollusca, Nereididae, Orbiniidae, Ostracoda, Sipunculidae, and Terebelliformia. Hosts of Lecudinidae sp. Clade A were placed within a moderately supported clade (ML:85/PP:1.00) composed exclusively of Ostracoda sequences. Hosts of Lecudinidae sp. Clade B were nested within a strongly supported *Glycera* clade. *Difficilina* sp. Clade A host material was recovered within a Terebelliformia clade, and hosts of Lecudinidae sp. Clade C were placed within a strongly supported Cirratulidae clade. Cnidarian sequences served as the outgroup.

4.4. DISCUSSION

4.4.1. Novel gregarine biodiversity from the Pacific Ocean

Lecudinidae spp. Clades A–C were recovered among other marine gregarines that diverge early in the lecudinid lineage. Comparing these novel clades to their close relatives *Pterospora* Labbé and Racovitza, 1897, *Urospora* Schneider, 1875, and *Lithocystis* Giard, 1876, minimal similarity was seen beyond the peristaltic motility shared by Lecudinidae sp. Clade B. Lecudinidae sp. Clade B had a dynamic peristaltic movement that appeared as a lobular bulge passing in a repeating wave from anterior to posterior, then returning. *Pterospora* (Landers and Leander, 2005), *Urospora* (Diakin et al., 2016), and *Lithocystis* (Coulon and Jangoux, 1987), which inhabit the coeloms of hosts, also move by peristalsis. However, peristalsis in these genera is more sporadic than with Lecudinidae sp. Clade B. Furthermore, *Pterospora* is only known from maldanid hosts (Landers and Leander, 2005); *Urospora* infects a range of host phyla including echinoderms, annelids (e.g., sipunculids and oligochaetes), and nemerteans (Desportes and Schrével, 2013; Diakin et al., 2016); and *Lithocystis* has only been reported from echinoderms (Coulon and Jangoux, 1987). None of the present novel clades were collected from these host groups.

Trophozoites of Lecudinidae sp. Clade A were bean-shaped, had short folds, and were densely colored (Fig. 4.1), while Lecudinidae sp. Clade C trophozoites more closely resembled members of *Lecudina* or *Lankesteria* with their elongate body, long epicytic folds, and translucent mucron (Fig. 4.4). Epicytic folds on Lecudinidae sp. Clades A and B were short and broadly spaced (1–1.5 folds/µm), while the longer folds on Lecudinidae sp. Clade C were denser (3 folds/µm) (Table 4.3). In contrast, *Pterospora* has cross-hatching patterns with bifurcating digits (Landers and Leander, 2005), *Urospora* has relatively moderately spaced folds (2 fold/µm), and *Lithocystis* has membrane crenulations (Coulon and Jangoux, 1987) (Table 4.4).

Difficilina sp. Clade A shared gliding motility with other *Difficilina* Simdyanov, 2009 species but were otherwise phylogenetically and morphologically distinct. Phylogenetically, *D.*

sp. Clade A formed a clade with other *Difficilina* and *Urospora* sequences under strong support. Although 18S sequences were not available for type species *D. cerebratuli* Simdyanov, 2009, the morphology of *D.* sp. Clade A sets it apart from other *Difficilina* species. *Difficilina* sp. Clade A had a papillary mucron and blunt posterior, distinguishing it from *D. cerebratuli* (tapered posterior), as well as *D. paranemertis* and *D. tubulani* (rounded mucrons, tapered posteriors) (Table 4.3). Biogeographically, *D.* sp. Clade A (northern California) does share a similar region and latitude with *D. paranemertis* and *D. tubulani* (western Canada). However, it is physically distant from the type locality of *D. cerebratuli* described from northwestern Russia (White Sea) (Simdyanov, 2009).

4.4.2. Lecudinidae spp. Clades A–C highlight a trend of diverse annelid and crustacean host specialization among early branching lecudinids

Host affiliation also distinguished Lecudinidae sp. Clades A through C and *Difficilina* sp. Clade A from their close relatives. Lecudinidae sp. Clade A (Table 4.1) was isolated from an ostracod host (Ostracoda Latreille, 1802), a group seemingly without any record of gregarine association. Ostracods are small (1–2 mm) crustaceans with calcified, bivalved carapaces that fossilize well (Foote and Sepkoski, 1999), inhabit nearly all aquatic environments worldwide (Oakley et al., 2013), and include some species that display a trademark bioluminescence (Hensley et al., 2023). Despite their prevalence across aquatic habitats, parasitism in ostracods is not commonly observed (Bruvo et al., 2011). Together, these facts suggest that the discovery of Lecudinidae sp. Clade A represents a first in the field of marine gregarines.

Lecudinidae sp. Clade B was collected from a *Glycera* Lamarck, 1818 bloodworm (Table 4.1). Other gregarines found in *Glycera* bloodworms include *Ceratospora* Schneider, 1892, *Gonospora* Schneider, 1875, *Lecudina legeri* Brasil, 1909, and *L. amphora* Hoshide, 1957. However, Lecudinidae sp. Clade B is distinct from these other organisms in the following ways. *Ceratospora* has distinct membrane protrusions and fronto-frontal syzygy (Léger, 1892) rather than lateral syzygy observed in Lecudinidae sp. Clade B. *Gonospora* exhibits larger trophozoites

than Lecudinidae sp. Clade B, which are up to 1000 µm or more in length (Pixell-Goodrich, 1916). These traits contrast with the bulbous shape and shorter length of Lecudinidae sp. Clade B, which ranged between 130–270 µm (Table 4.3). Biogeographically, *Ceratospora* and *Gonospora* have been reported in Europe from northern France (Léger, 1892) to the Mediterranean Sea (Pixell-Goodrich, 1916): an entirely different ocean basin from which Lecudinidae sp. Clade B was found (northwestern Pacific Ocean). Additionally, *Lecudina legeri* and *L. amphora* possess different morphologies and host preferences from Lecudinidae sp. Clade B (Desportes and Schrével, 2013).

Lecudinidae sp. Clade C and *Difficilina* sp. Clade A were associated with terebellid hosts (Table 4.1). Lecudinidae sp. Clade C was isolated from a cirratulid polychaete—a host type associated with many (typically archigregarine) species (Desportes and Schrével, 2013; Wakeman, 2020; Lax et al., 2024). Meanwhile, *Difficilina* sp. Clade A was found in a polychaete, marking the first time a *Difficilina* species has been described from an annelid. To date, all *Difficilina* species have been isolated from ribbon worms (Nemertea) (Simdyanov, 2009; Rueckert et al., 2010).

4.4.3. Novel biogeographical insights on the distribution of early branching lecudinids

While geographic isolation and long-distance relocation may help shape marine gregarine biogeography (Lohan et al., 2017), the present data suggests that host association is the dominant factor driving speciation. These novel Lecudinidae sp. clades from Hiroshima (Clade A), Oshoro Bay (Clade B), and Mizunashikaihin, Hakodate (Clade C) are located along different currents: the Kuroshio Current which flows along the south of Japan (Qiu, 2001), the Tsushima Current which flows along northern Hokkaido (Yabe et al., 2021), and the Tsugaru Current which passes eastbound between Honshu and Hakodate (Yasui et al., 2022), respectively. It is therefore plausible that invertebrates (and the gregarines within them) living along these regions of fast-moving seawater could share a similar biogeographic range. In the present study, host identity appeared more influential on the observed species diversity. Each clade was associated with a

distinct invertebrate group. Specifically, Clade A came from an ostracod, Clade B from a *Glycera* polychaete, Clade C from a cirratulid polychaete, and *Difficilina* sp. Clade A from a different terebellid polychaete (Fig. 4.6). Strong correlation between novel clade and host group seen in these data supports the idea that host specificity is the dominant variable driving speciation among early branching lecudinids.

CHAPTER 5. Expanded *Lankesteria* phylogeny shows correlation with order-level classification of ascidian hosts

SUMMARY

Gregarines (Apicomplexa), a group of single-cell parasitic eukaryotes that undergo complex life cycles within invertebrate hosts, include the genus *Lankesteria* found exclusively within ascidians (tunicates). This study describes five novel clades of *Lankesteria* from tunicates, identified through a combination of morphological traits, SSU (18S) rRNA, and host COI phylogenetic analysis. Novel clades presented herein are distinguished by morphology (e.g., trophozoite form, epicytic fold density, and mucron shape), molecular evidence, and host group affiliations. Results presented herein demonstrate that *Lankesteria* clades show a clear association to specific tunicate orders (Phlebobranchia, Stolidobranchia, and Aplousobranchia). Overall, these findings support the idea that host identity plays a strong role in driving gregarine speciation.

5.1. INTRODUCTION

Gregarines (Apicomplexa) are remarkable for their ability to thrive in diverse environments from marine and freshwater to terrestrial ecosystems (Desportes and Schrével, 2013). However, research has largely centered on vertebrate-infecting species due to their relevance to human health and agriculture (Rueckert et al., 2015; Wakeman et al., 2021; Park and Leander, 2024a), leaving marine gregarine biodiversity comparatively neglected (Morrison, 2009). Marine gregarines infect a wide range of ocean-dwelling invertebrates, including ascidians (Ciancio et al., 2001; Desportes and Schrével, 2013; Rueckert et al., 2015; Iritani et al., 2021). Tunicates (ascidians) fall within the taxonomic class Ascidiacea Blainville, 1824, and are

also known as sea squirts, sea pineapples, or in Japanese as *hoya*.

A single genus of marine gregarines, *Lankesteria* (Mingazzini, 1891*)*, is conventionally associated with ascidian hosts (Ormières, 1964). Over 40 species of *Lankesteria* have been described (Desportes and Schrével, 2013), yet currently only 14 species (*Lankesteria abbotti, L. ascidiae, L. chelyosomae, L. cystodytae, L. didemni, L. dolabra, L. halocynthiae, L. herdmaniae, L. hesperidiiformis, L. kaiteriteriensis, L. metandrocarpae, L. pollywoga, L.* cf. *ritterellae,* and *L. savignyii*) have associated molecular data available to the scientific community. In the greater eugregarine context, a shared evolutionary origin between tunicate-parasitizing *Lankesteria* and polychaete-parasitizing *Lecudina* has been hypothesized (Leander et al., 2006). This hypothesis was introduced around the same time SSU rRNA molecular data began to drive the study of marine gregarine biodiversity (Wakeman and Leander, 2012; Rueckert et al., 2013; Schrével et al., 2016; Simdyanov et al., 2017).

In the present study, I characterize five novel clades of *Lankesteria* from tunicate hosts using both morphological traits and SSU rRNA phylogenies. Beyond describing this novel diversity, I examine how patterns of *Lankesteria* speciation correspond to host group identity. Results from this work reveal a strong congruence between *Lankesteria* clades and major tunicate taxa Phlebobranchia, Stolidobranchia, and Aplousobranchia, highlighting host identity as a driver of gregarine diversification. Overall, this study provides new insight into the co-evolutionary dynamics of ascidian–gregarine associations and expands our understanding of the forces shaping marine gregarine biodiversity.

5.2. MATERIALS AND METHODS

5.2.1. Host collection and sample processing

Hosts were collected opportunistically in the intertidal zones near Hakodate Port (41°46'29"N 140°42'38"E), Shibetsu Port (43°40'5"N 145°7'51"E), and Wakkanai Port (45°24'15"N 141°40'41"E) in Hokkaido (Japan), Ishigaki Port (24°20'41"N 124°8'45"E) on

Ishigaki Island (Japan), and Hawaii Beach (28°22'47"N 130°0'51"E) on Kikai Island (Japan) between May and September of 2023 (Table 5.1) from buoys and submerged mooring lines. Subsequent steps were performed as described in Section 2.2.1.

5.2.2. Electron microscopy

Electron microscopy was performed as described in Section 2.2.2.

5.2.3. Amplification and sequencing of the 18S rRNA gene

Gregarine trophozoites were transferred individually to 0.2 ml PCR microcentrifuge tubes and stored at –20°C for 1–5 days. Genomic DNA was then extracted from these samples using a QuickExtract FFPE DNA Extraction Kit (Lucigen, Middlesex, United Kingdom) in line with manufacturer protocol. General and specific primers (Table 5.2) with KOD One® PCR Master Mix (Toyobo, Osaka, Japan) were used in amplification of the 18S rRNA gene. Subsequent steps were performed as described in Section 2.2.3.

5.2.4. Molecular phylogenetic analyses

Phylogenetic analyses were performed as described in Section 2.2.4.

5.2.5. Host identification

Fragments of host tissue remaining after gregarine isolation were preserved in 100% ethanol for barcoding. Host DNA was extracted from samples using the MasterPure Complete DNA & RNA Purification Kit (LGC Biosearch Technologies, Hoddesdon, United Kingdom). The cytochrome *c* oxidase subunit 1 (COI) gene was amplified using an initial primer set of DinF and NuxR1 followed by a nested primer set of CatF1 and UxR1 (Table 5.2) with KOD One® PCR Master Mix (Toyobo, Osaka, Japan). Subsequent steps were performed as described in Section 2.2.5.

5.3. RESULTS

5.3.1. Morphology of *Lankesteria* sp. Clade A

Lankesteria sp. Clade A trophozoites were oblong with a tapered mucron (Fig. 5.1 A–B)

and moved with gliding motility. Epicytic folds ran longitudinally along the cells with a density of 0.4 folds/µm, and isolates were covered in beaded strands of (suspected) foreign material (Fig. 5.1 C). Isolates measured 18–24 µm in length ($\bar{x}$ = 20.7 µm; *n* = 4) and 9–10 µm in width ($\bar{x}$ = 9.8 µm; *n* = 4). Spherical nuclei were in the cell center and measured 2–3 µm in diameter ($\bar{x}$ = 2.5 µm; *n* = 2).

5.3.2. Morphology of *Lankesteria* sp. Clade B

Lankesteria sp. Clade B trophozoites were elongate with a rounded posterior, a proboscis-like mucron (Fig. 5.2 A–B, D), and exhibited gliding motility. Epicytic folds (Fig. 5.2 C–D) ran longitudinally along the cells with a density of 3 folds/µm. Isolates measured 62–135 µm in length ($\bar{x}$ =106 µm; *n* = 19) and 10–18 µm in width ($\bar{x}$ = 14.1 µm; *n* = 19). Spherical or ellipsoid nuclei were in the anterior of the cell and measured 5–12 µm in diameter ($\bar{x}$ = 6.4 µm; *n* = 12).

5.3.3. Morphology of *Lankesteria* sp. Clade C

Lankesteria sp. Clade C trophozoites were elongate with a pointed posterior, a bulbous and hooked mucron (Fig. 5.3 A–B, D), and moved with gliding motility. Epicytic folds (Fig. 5.3 C–D) ran longitudinally along the cells with a density of 4 folds/µm. Isolates measured 95–130 µm in length ($\bar{x}$ =111.8 µm; *n* = 6) and 20–30 µm in width ($\bar{x}$ = 24.8 µm; *n* = 6). Ellipsoid nuclei were in the anterior of the cell, measuring 14–20 µm ($\bar{x}$ = 17 µm; *n* = 2) along the long axis and 6–7 µm ($\bar{x}$ = 6.5 µm; *n* = 2) along the short axis.

5.3.4. Morphology of *Lankesteria* sp. Clade D

Lankesteria sp. Clade D trophozoites were elongate with a rounded posterior and cylindrically protruding mucron (Fig. 5.4 A–B, D), and exhibited gliding motility. Epicytic folds (Fig. 5.4 C–D) ran longitudinally along the cells with a density of 3 folds/µm. Isolates measured 86–125 µm in length ($\bar{x}$ =105.3 µm; *n* = 4) and 25–32 µm in width ($\bar{x}$ = 29.3 µm; *n* = 4). Spherical nuclei were in the anterior of the cell, measuring 15–25 µm ($\bar{x}$ = 18.3 µm; *n* = 3) in diameter.

5.3.5. Morphology of *Lankesteria* sp. Clade E

Lankesteria sp. Clade E trophozoites were elongate with a tapered posterior and beak-like mucron (Fig. 5.5 A–B, D), and exhibited gliding motility. Epicytic folds (Fig. 5.5 C–D) ran longitudinally along the cells with a density of 4 folds/µm. Isolates measured 105–110 µm in length ($\bar{x}$ =106.6 µm; *n* = 3) and 24–30 µm in width ($\bar{x}$ = 26 µm; *n* = 3). Spherical nuclei were in the anterior of the cell, measuring 9–12.3 µm ($\bar{x}$ = 10.7 µm; *n* = 2) in diameter.

5.3.6. Molecular phylogeny of gregarine apicomplexans

Phylogenetic analysis of a 74-sequence 18S alignment (Fig. 5.6) included *Lithocystis*, *Pterospora*, *Difficilina*, *Urospora*, *Amplectina*, *Lecudina*, and *Lankesteria*. All *Lankesteria* sequences, except *L. pollywoga*, formed a moderately supported (ML:59/PP:--) clade sister to *Lecudina* Clade A. Within this clade, *Lankesteria* sp. Clade A (Hakodate, Hokkaido) was strongly supported as sister to *L. hesperidiiformis*, together forming a clade sister to *Lankesteria* sp. Clade B (Hakodate, Oshoro, and Shibetsu, Hokkaido). *Lankesteria* spp. Clades C (Ishigaki) and D (Kikai) were recovered as strongly supported clades sister to each other, forming a broader clade under moderate support (ML:71/PP:0.99). *Lankesteria* sp. Clade E (Ishigaki) formed a strongly supported clade sister to *L. dolabra*, and the two taxa together formed a broader clade that was also recovered under strong support. *Veloxidium leptosynaptae*, a distantly related marine gregarine, was included as an outgroup.

5.3.7. Molecular phylogeny of host material

Phylogenetic analysis of an 85-sequence COI alignment (Fig. 5.7) included representatives from major tunicate lineages: Aplousobranchia, Doliolida, Fritillariidae, Kowalevskiidae, Oikopleuridae, Phlebobranchia, Pyrosomida, Salpida, and Stolidobranchia. *Lankesteria* spp. Clade A and B hosts were recovered within separate, strongly supported clades which included *Ascidia aspersa* and *A. zara*, respectively. These host clades were both nested within a moderately supported Phlebobranchia clade (ML:57/PP:--). Hosts of *Lankesteria* spp. Clades C–E were recovered within a moderately supported clade (ML:56/PP:--) of

Stolidobranchia sequences. Mollusks were included as an outgroup.

5.4. DISCUSSION

5.4.1. Novel biodiversity among gregarines from tunicates

These morphological and molecular analyses present five novel *Lankesteria* clades, each likely representing a distinct species. These clades exhibit clear differences in trophozoite morphology and host specificity within their characteristic host niche of ascidians (tunicates). *Lankesteria* sp. Clade A trophozoites were the smallest observed (18–24 µm), and were distinguished by an oblong shape, the presence of numerous beaded strands (Fig. 5.1), and low-density epicytic folds (0.4 folds/µm) (Table 5.3). This clade was recovered as sister to *L. hesperidiiformis* (Fig. 5.6) but with a different host association than *L. hesperidiiformis*. Further distinguishing these sister clades, *Lankesteria* sp. Clade A was found in a phlebobranch (Phlebobranchia Lahille, 1886) tunicate while *L. hesperidiiformis* (Rueckert et al., 2015) was collected from the Aplousobranchia Lahille, 1886 (Moreno and Rocha, 2008) tunicate *Distaplia occidentalis* (Mastrototaro and Brunetti, 2006). During the present phylogenetic analysis of host COI data, a monophyletic clade of Aplousobranchia sequences was recovered under weak statistical support, while two (polyphyletic) clades of Phlebobranchia were recovered under moderate support (Fig. 5.7). Paraphyly observed among these tunicate groups highlights the value of paired isolate-host phylogenetic comparison when studying marine gregarines, as omitting this analysis can lead to an overlooked coevolutionary context. Overall, these differences support *Lankesteria* sp. Clade A as a novel member of the genus.

Lankesteria sp. Clade B (Hakodate, Wakkanai, and Shibetsu, Hokkaido), also from phlebobranch tunicates (Fig. 5.7, Table 5.3), exhibited elongate cells (62–135 µm), a rounded posterior, and a proboscis-like mucron. Together with a phylogenetic position sister to the *L.* sp. Clade A + *L. hesperidiiformis* lineage, these data suggest *L.* sp. Clade B is distinct from its close relatives.

Lankesteria sp. Clade C, found in Stolidobranchia Lahille, 1886 hosts from Ishigaki Island (Japan), is morphologically distinct due to its hooked, bulbous mucron (Fig. 5.3) and high epicytic fold density (4 folds/μm). Phylogenetically, this novel clade was recovered as sister to *Lankesteria* sp. Clade D. Similarly, *Lankesteria* sp. Clade D trophozoites were collected from Stolidobranchia hosts (Kikai Island, Japan), and had an elongate form with a cylindrically protruding mucron (Fig. 5.4). *Lankesteria* sp. Clade E, also from a Stolidobranchia host (Ishigaki), was characterized by a triangular, beak-like mucron (Fig. 5.5). These isolates formed a strongly supported clade sister to *L. dolabra*, indicating that Clade E represents a unique *Lankesteria* lineage. Biogeography further supports the distinctness of *Lankesteria* sp. Clade E from *L. dolabra,* as *L. dolabra* was described from New Zealand (Iritani et al., 2021) in the southern hemisphere whereas *L.* sp. Clade E was collected from Ishigaki Island in the northern hemisphere.

5.4.2. Host phylogeny strongly coincides with *Lankesteria* speciation patterns

Novel diversity seen among *Lankesteria* spp. Clades A–E demonstrates a strong pattern of gregarine speciation mirroring host phylogeny (Table 5.4). In the present work, *L.* spp. Clades A and B (Table 5.4 Group A, Fig. 5.8) were found in phlebobranch hosts, while *L.* spp. Clades C–E were restricted to stolidobranch hosts (Table 5.4 Group D, Fig. 5.8). A distinct clade (Table 5.4 Group D, Fig. 5.8) of *Lankesteria* comprising *L.* spp. Clades C, D, E, *L. abbotti, L. herdmaniae, L. kaiteriteriensis, L. metandrocarpae, L. halocynthiae*, and *L. dolabra* was consistently associated with stolidobranch tunicate hosts. Moreover, *L. ascidiae, L. savignyii,* and *L. chelyosomae* formed a clade (Table 5.4 Group C, Fig. 5.8) and were all isolated from phlebobranch hosts, while *L. didemni* along with three lineages of *L. cystodytae* formed a grouping (Table 5.4 Group B, Fig. 5.8) of sequences all associated with aplousobranch tunicates. Exceptions to this pattern include *L. hesperidiiformis* and *L.* cf. *ritterellae*, which are members of Group A and D, respectively (Fig. 5.8), but were isolated from aplousobranch tunicates. More work is needed to help resolve why some *Lankesteria* members appear to deviate from this

largely consistent pattern of speciation.

CHAPTER 6. Pacific marine gregarines from lumbrinerid polychaetes display speciation linked to biogeography and host phylogeny

SUMMARY

Marine gregarines, especially those from the genus *Lecudina*, exhibit extensive morphological and ecological diversity. This study explores *Lecudina* species parasitizing lumbrinerid polychaetes from northern Japan and the western United States using a combination of morphological and molecular data. Here, I uncover cryptic diversity within *Lecudina* Clade B among two novel clades (*Lecudina* sp. Clade A and *Lecudina* sp. Clade B) that share similar biogeographies, morphologies, and host preferences despite being phylogenetically distinct. These results emphasize how both host association and biogeography impact speciation among some marine gregarines.

6.1. INTRODUCTION

Apicomplexans are single-cell animal parasites (Levine, 1970). Several well-studied core apicomplexan lineages, such as those causing malaria (*Plasmodium*; Kolawole et al., 2023), toxoplasmosis (*Toxoplasma*; Adem and Ame, 2023), and babesiosis (*Babesia*; Kuibagarov et al., 2023), have gained attention primarily due to their significant impact on human health and livestock. However, Apicomplexa as a whole are an exceptionally diverse group, comprising roughly 350 known genera (Adl et al., 2019). Morrison (2009) argued that because of their often host-specific nature, only a small fraction—likely less than 1%—of apicomplexan diversity has been formally described. This suggests the existence of hundreds of thousands, if not millions, of yet-undiscovered species. Apicomplexans have diversified across a wide range of animal hosts in

marine (Dubey et al., 2003), freshwater (Molla et al., 2013), terrestrial (McAllister et al., 1995; Chen et al., 1997), and even extremophile environments (Moreira and López-García, 2003; Wakeman et al., 2018). Nevertheless, marine apicomplexans, especially those infecting invertebrates, remain under-explored because they do not directly affect public health or agriculture.

A substantial portion of known apicomplexan diversity is found within the gregarines—parasites of invertebrates that include at least 1600 described species (Levine, 1988; Desportes and Schrével, 2013). Gregarines serve as valuable models in evolutionary biology for several reasons: 1) they represent early-diverging apicomplexan lineages (Schrével et al., 2016); 2) they include both morphologically conservative and highly specialized taxa (Leander, 2008; MacGregor and Thomasson, 1965; Valigurová et al., 2013; Paskerova et al., 2018); 3) they occupy marine, freshwater, and terrestrial environments; 4) they infect a wide range of invertebrate hosts (Levine, 1977; Levine, 1979; Valigurová and Koudela, 2005), and have even been found in amphibians during development (Chambouvet et al., 2016); 5) they are highly host-specific; and 6) they typically require only a single host to complete their life cycle (Lee et al., 2000). Additionally, recent studies have emphasized the importance of gregarines in understanding the evolution of organelle function, parasitism, and early alveolate diversification (Gubbels and Duraisingh, 2012; Templeton and Pain, 2016; Mathur et al., 2021).

Marine gregarines are especially intriguing due to their diversity and evolutionary relevance, as they are thought to be among the earliest gregarines to have evolved (Théodoridès, 1984; Leander, 2008). One key group, the lecudinids (particularly genus *Lecudina*) exhibit broad morphological diversity (Leander et al., 2006; Rueckert et al., 2011b). Some lecudinid species display distinctive locomotor and structural adaptations, such as the thrashing motility of *Veloxidium leptosynaptae* with its transverse membrane striations (Wakeman and Leander, 2012), or the folded membranes of many *Lecudina* species that facilitate gliding motility (Leander, 2008; Rueckert et al., 2010; Rueckert et al., 2011b; Park and Leander, 2024a). Other

derived marine genera, including *Pterospora*, *Lithocystis*, and *Lankesteria*, exhibit specialized membrane features like cross-hatches (Landers and Leander, 2005), crenulations (Coulon and Jangoux, 1987), and knob-like surface protrusions (Rueckert et al., 2015; Iritani et al., 2021), respectively. Overall, the lecudinids are a successful group of marine parasites that have demonstrated an ability to adapt to a wide variety of hosts. However, much of the available information on marine gregarines is limited to morphological descriptions. Indeed, fewer than 100 species are supported by molecular data (Wakeman et al., 2021).

Historically limited availability of molecular data has posed a major obstacle to making informed species-level comparisons. Without this ability to compare, it is difficult to elucidate the patterns behind their speciation, host association, and biogeographic distribution. However, efforts to integrate morphological observations with modern molecular datasets continue (Rueckert et al., 2011; Simdyanov et al., 2015; Diakin et al., 2016; Schrével et al., 2016; Rueckert and Horák, 2017; Iritani et al., 2021; Wakeman et al., 2021), and have even begun to reveal hidden (cryptic) biodiversity among some of these organisms (Rueckert et al., 2013).

This study focuses on marine lecudinid gregarines that parasitize lumbrinerid polychaetes —a lineage of worms that has been often overlooked in molecular gregarine research. In particular, I examine *Lecudina* diversity across the northern Pacific Ocean, specifically targeting specimens from northern Japan and the western United States. Using morphological techniques (light and electron microscopy) together with molecular phylogenetic analysis of small subunit (18S) rRNA, internal transcribed spacer (ITS) rRNA, and host cytochrome *c* oxidase I (COI) genes, this study contributes to resolving the taxonomy, biogeography, and evolutionary relationships of understudied marine gregarines from lumbrinerid worms.

6.2. MATERIALS AND METHODS

6.2.1. Host collection and sample processing

Hosts were collected opportunistically in the intertidal zones near Crescent City

(41°44'12"N 124°11'40"E), California (United States) and Clover Point, British Columbia, Canada (48°24'14"N 123°21'00"W) between January and December 2023 (Table 6.1) from under intertidal rocks and inside tufts of seagrass. Subsequent steps were performed as described in Section 2.2.1.

6.2.2. Electron microscopy

Electron microscopy was performed as described in Section 2.2.2.

6.2.3. Amplification and sequencing of the 18S rRNA gene and ITS region

Gregarine trophozoites were transferred individually to 0.2 ml PCR microcentrifuge tubes and stored at –20°C for 1–5 days. Genomic DNA was then extracted from these samples using a QuickExtract FFPE DNA Extraction Kit (Lucigen, Middlesex, United Kingdom) in line with manufacturer protocol. General and specific primers (Table 6.2) with KOD One® PCR Master Mix (Toyobo, Osaka, Japan) were used in amplification of 18S and ITS rRNA regions. Subsequent steps were performed as described in Section 2.2.3.

6.2.4. Molecular phylogenetic analyses

Phylogenetic analyses were performed as described in Section 2.2.4.

6.2.5. Host identification

Fragments of host tissue remaining after gregarine isolation were preserved in 100% ethanol for barcoding. Host DNA was extracted from samples using the MasterPure Complete DNA & RNA Purification Kit (LGC Biosearch Technologies, Hoddesdon, United Kingdom). The COI gene was amplified using primers polyLCO and polyHCO (Table 6.2) with KOD One® PCR Master Mix (Toyobo, Osaka, Japan). Subsequent steps were performed as described in Section 2.2.5.

6.3. RESULTS

6.3.1. Morphology of *Lecudina* sp. Clade A

Lecudina sp. Clade A trophozoites were elongate with a nipple-like mucron (Fig. 6.1 A–

C) and moved with gliding motility. Numerous amylopectin granules (Fig. 6.1 D) and a mitochondrion (Fig. 6.1 E) were visible on TEM cross-section. Epicytic folds (Fig. 6.1 D, F) ran longitudinally along the cells with a density of 4 folds/µm. Isolates measured 52–150 µm in length ($\bar{x}$ = 86 µm; *n* = 7) and 10–20 µm in width ($\bar{x}$ = 15 µm; *n* = 7). Spherical nuclei were in the cell anterior and measured 6–10 µm in diameter ($\bar{x}$ = 7.4 µm; *n* = 7).

6.3.2. Morphology of *Lecudina* sp. Clade B

Lecudina sp. Clade B trophozoites were elongate (Fig. 6.2 A–B), measuring 200–420 µm in length ($\bar{x}$ = 270 µm, *n* = 6) and 30–70 µm in width ($\bar{x}$ = 43.3 µm, *n* = 6). The cells possessed a rounded mucron (Fig. 6.2 A–B) and spherical nucleus located in the anterior third of the cell (Fig. 6.2 A). Nuclei measured 18–22 µm in diameter ($\bar{x}$ = 20 µm, *n* = 3). Externally, isolates were covered in longitudinally-running epicytic folds with a density of 4 folds/µm at the widest part of the cell (Fig. 6.2 C–D). Cell body was ovaloid in cross-section (Fig. 6.2 D).

6.3.3. Molecular phylogeny of gregarine apicomplexans

Phylogenetic analysis was performed on a 52-sequence alignment composed of 18S+ITS concatenated sequences from *Lecudina* sp. Clades A (western Canada) and B (northern California), as well as 18S sequences encompassing *Loxomorpha*, *Cuspisella*, *Lithocystis*, *Pterospora*, *Difficilina*, *Urospora*, *Sphinctocystis*, *Amplectina*, *Lankesteria*, and *Lecudina* (Fig. 6.3). Distantly related marine gregarines and alveolates (*Chromera velia*, *Metzidium orientale,* and *Vitrella brassicaformis*) were included as an outgroup. Concatenated *Lecudina* sp. Clade A sequences from western Canada formed a strongly supported clade sister to a clade of *Lecudina* sp. Clade B and one *L. longissima* sequence (Fig. 6.3).

6.3.4. Molecular phylogeny of host material

Phylogenetic analysis of a 25-sequence COI alignment (Fig. 6.4) included representatives from polychaete families Eunicidae, Lumbrineridae, and Nereididae. Host material for *Lecudina* sp. Clades A and B was recovered nested within a moderately supported (ML:73/PP:0.99) clade composed exclusively of Lumbrineridae sequences. *Lecudina* sp. Clade

A host material formed a strongly supported clade with *Lumbrineris tetraura,* and *Lecudina* sp. Clade B host material formed a strongly supported clade with *Lumbrineris japonica*. Sipunculid sequences were included as an outgroup.

6.4. DISCUSSION

6.4.1. Biogeography and cryptic lineages in *Lecudina* Clade B

Genus *Lecudina* is one of the most species-rich groups of gregarine apicomplexans. Historically, this apparent diversity was partly the result of traditional taxonomy that lumped most eugregarine-like species together (Levine, 1976). However, molecular data have since revealed cryptic diversity within the group. For example, *Lecudina polymorpha* was reassigned to *Paralecudina polymorpha* (Rueckert et al., 2013) in light of an updated 18S-based phylogeny. In an effort to account for these unresolved taxonomic boundaries, the term "lecudinid" is often used as a general group label (Wakeman, 2020; Odle et al., 2024). Among the lecudinids, members of *Lecudina* Clade B—namely *L*. sp. Clade A and *L. longissima*/*L*. sp. Clade B (Fig. 6.3)—are now known to also display cryptic diversity.

Lecudina sp. Clade A, is proposed here based primarily on phylogenetic evidence. This clade was recovered under strong support and is nested within the broader *Lecudina* Clade B (Fig. 6.3), which is also strongly supported. Morphologically, *L*. sp. Clade A only differs slightly from close relatives *L. caspera* (tapered posterior) and *L. longissima* (pointed posterior) by having a rounded posterior (Table 6.3). Meanwhile, *Lecudina* sp. Clade B was sampled from northern California where isolates were identified using host ecology, light microscopy, and molecular phylogeny. These samples were morphologically indistinguishable from *L. longissima* collected in Japan (Tsugawa, 1944; Hoshide, 1957), western Canada (Rueckert et al., 2010), and southern California (Levine, 1974). Phylogenetic analysis of 18S+ITS sequences revealed that *Lecudina* sp. Clade B isolates from northern California formed a strongly supported clade along with one *L. longissima* sequence from western Canada (Fig. 6.3).

6.4.2. Host association and its role in *Lecudina* speciation

A key driver of diversity among lecudinids appears to be host specialization. Lecudinid gregarines have undergone extensive radiation through marine invertebrates, including echinoderms (Leander et al, 2006), polychaetes (Rueckert et al., 2013; Wakeman and Leander, 2013), and tunicates (Mita et al., 2012; Rueckert et al., 2015; Iritani et al., 2021). *Lecudina* Clade B is herein associated strictly with lumbrinerid polychaetes (Family: Lumbrineridae Schmarda, 1861) (Table 6.3). Close relatives such as *L. phyllochaetopteri* from *Phyllochaetopterus prolifica* (Family: Chaetopteridae Audouin and Milne Edwards, 1833) and *L.* cf. *arabellae* from *Arabella iricolor* (Park and Leander, 2024a) are documented, but they do not inhabit lumbrinerid worms (Table 6.3) nor do they share a strongly supported clade with members of *Lecudina* Clade B (Fig. 6.3).

Other lecudinids that parasitize lumbrinerids include *L. brasili* (India) and *L. laubieri* (France), but these taxa are morphologically distinct from *L.* sp. Clade A (Table 6.3). For example, *L. brasili* has a tapered rather than nipple-like mucron, and *L. laubieri* has a long, proboscis-like mucron. Together, these findings indicate that host specificity (particularly within Lumbrineridae) along with biogeography help to contextualize the biodiversity observed among *Lecudina* Clade B.

CHAPTER 7. Pacific marine gregarines from nereidid polychaetes display novel biodiversity and cryptic speciation

SUMMARY

Marine gregarines are a diverse group of unicellular apicomplexan parasites known for their host specificity. This study explores the biodiversity and speciation patterns of *Lecudina* species which parasitize nereidid polychaetes from northern Japan and the western United States. Using a combination of morphological analysis (light and electron microscopy) and molecular phylogenetic techniques (18S rRNA gene sequencing), this study uncovers cryptic diversity within *Lecudina* Clade A, revealing several novel nested clades. Here, I demonstrate a strong preference for nereidid hosts among a subset of *Lecudina* species and identify a strong biogeographical link with their phylogeny. Molecular evidence shows that *Lecudina* spp. Clades C through G form a distinct monophyletic group within *Lecudina* Clade A along with type species *L. pellucida*. I also report evidence for a *Lecudina tuzetae* species complex spanning the globe. Overall, this work provides new insight into the evolutionary and biogeographical dynamics of *Lecudina*, contributing to the broader understanding of marine gregarine biodiversity.

7.1. INTRODUCTION

Gregarines, a subset of apicomplexans that specialize on invertebrate hosts, are considered evolutionarily successful for their prevalence across a wide range of hosts inhabiting marine (Leander, 2006; Rueckert et al., 2013; Wakeman, 2020), freshwater (Molla et al., 2013), terrestrial (Chen et al., 1997), and extreme (Wakeman et al., 2018) environments. Gregarines are also highly biodiverse, with over 1600 described species (Levine, 1988; Desportes and Schrével,

2013). Indeed, gregarines are found in nearly all invertebrate phyla (Levine, 1977; Levine, 1979; Valigurová and Koudela, 2005; Desportes and Schrével, 2013), and sometimes even in amphibian larvae (Chambouvet et al., 2016).

As one of the earliest branching apicomplexan lineages (Leander, 2008; Schrével et al., 2016), gregarines are regarded as a living glimpse into the evolution of parasitism. Genus *Lecudina* and related lecudinids are especially notable for their biodiversity and derived adaptations. *Lecudina* species, for instance, use highly folded membranes to produce gliding motility (Leander et al., 2003b; Leander, 2008). Other genera such as *Pterospora*, *Lithocystis*, and *Lankesteria* have derived membrane features such as cross-hatches, crenulations, and knob-like protrusions (Coulon and Jangoux, 1987; Landers and Leander, 2005; Rueckert et al., 2015; Iritani et al., 2021), reflecting their adaptation to different host environments.

Most marine gregarines have been described solely through morphology, with fewer than 100 species supported by molecular data (Wakeman et al., 2021). This has prompted efforts to integrate historical morphological descriptions with modern genetic analysis (Rueckert et al., 2011; Simdyanov et al., 2015; Diakin et al., 2016; Schrével et al., 2016; Rueckert and Horák, 2017; Iritani et al., 2021; Wakeman et al., 2021). These efforts have begun to uncover gregarine biodiversity hidden among visually similar yet genetically unique (cryptic) species (Rueckert et al., 2013). In the present study, I investigate *Lecudina* biodiversity and speciation across the northern Pacific Ocean by examining marine gregarines from polychaete hosts in northern Japan and the western United States using a combination of light and electron microscopy alongside 18S rRNA (isolate) and COI (host) gene phylogenetics.

7.2. MATERIALS AND METHODS

7.2.1. Host collection and sample processing

Hosts were collected opportunistically in the intertidal zones near Oshoro Marine Station (43°12'37"N 140°51'25"E) in Hokkaido (Japan), Ogamimaru Port (26°41'28"N

127°59'54"E) on Okinawa Island (Japan), Kabira Bay (24°26'46"N 124°8'25"E) on Ishigaki Island (Japan), Hanaguri (34°18'04"N 132°50'20"E) in Hiroshima (Japan), and Crescent City (41°44'12"N 124°11'40"E), California (United States) between November 2022 and January 2024 (Table 7.1) from under intertidal rocks and inside tufts of seagrass. Subsequent steps were performed as described in Section 2.2.1.

7.2.2. Electron microscopy

Electron microscopy was performed as described in Section 2.2.2.

7.2.3. Amplification and sequencing of the 18S rRNA gene

Gregarine trophozoites were transferred individually to 0.2 ml PCR microcentrifuge tubes and stored at –20°C for 1–5 days. Genomic DNA was then extracted from these samples using a QuickExtract FFPE DNA Extraction Kit (Lucigen, Middlesex, United Kingdom) in line with manufacturer protocol. General and specific primers (Table 7.2) with KOD One® PCR Master Mix (Toyobo, Osaka, Japan) were used in amplification of the 18S rRNA gene. Subsequent steps were performed as described in Section 2.2.3.

7.2.4. Molecular phylogenetic analyses

Phylogenetic analyses were performed as described in Section 2.2.4.

7.2.5. Host identification

Fragments of host tissue remaining after gregarine isolation were preserved in 100% ethanol for barcoding. Host DNA was extracted from samples using the MasterPure Complete DNA & RNA Purification Kit (LGC Biosearch Technologies, Hoddesdon, United Kingdom). The cytochrome *c* oxidase subunit 1 (COI) gene was amplified using primers polyLCO and polyHCO (Table 7.2) with KOD One® PCR Master Mix (Toyobo, Osaka, Japan). Subsequent steps were performed as described in Section 2.2.5.

7.3. RESULTS

7.3.1. Morphology of *Lecudina* sp. Clade C

Lecudina sp. Clade C trophozoites were elliptical in shape, possessing a wide central region that tapered to a rounded anterior and posterior (Fig. 7.1 A–C). Isolates measured 75–100 µm in length ($\bar{x}$ = 82 µm, *n* = 5), 45–60 µm in width ($\bar{x}$ = 51 µm, *n* = 5), and possessed a spherical nucleus measuring 14–20 µm in diameter ($\bar{x}$ = 17 µm, *n* = 3). Gliding motility was also noted. Epicytic folds ran longitudinally along the cells with a density of 2 folds/µm at the widest part of the cell (Fig. 7.1 D–E).

7.3.2. Morphology of *Lecudina* sp. Clade D

Lecudina sp. Clade D trophozoites had a rounded posterior and narrowed at the anterior end (Fig. 7.2 A). Light micrographs showed a centrally located, spherical nucleus and rounded mucron (Fig. 7.2 A). Cells were either centrally wide, cascading, or pear-like in shape, and exhibited gliding motility. Longitudinal epicytic folds surrounded the cells with a density of 2 folds/µm at the widest part of the cell (Fig. 7.2 B–D, F–G). Isolates measured 60–80 µm in length ($\bar{x}$ = 67 µm, *n* = 4) and 33–40 µm in width ($\bar{x}$ = 37 µm, *n* = 4). Nuclei measured 10–12.5 µm in diameter ($\bar{x}$ = 11.67 µm, *n* = 3). Cross-sections were circular with amylopectin granules concentrated towards the central axis of the cell (Fig. 7.2 C). Organelles such as the Golgi apparatus, mitochondria, as well as lipid droplets were observed near the cell membrane (Fig. 7.2 E–F). Additionally, rippled dense structures were visible at the terminal ends of epicytic folds (Fig. 7.2 G).

7.3.3. Morphology of *Lecudina* sp. Clade E

Lecudina sp. Clade E trophozoites were ellipsoid or circular with a tapered posterior rounded at the end and a mucron that was either rounded or button-like (Fig. 7.3 A–B, D–E). Longitudinal epicytic folds ran along the cells with a density of 1.3 folds/µm (Fig. 7.3 C–E), and gliding motility was observed. Isolates measured 125–190 µm in length ($\bar{x}$ =155 µm; *n* = 6) and 40–110 µm in width ($\bar{x}$ = 85 µm; *n* = 6). Spherical nuclei were found centrally, measuring 23–27 µm in diameter ($\bar{x}$ = 25 µm; *n* = 3).

7.3.4. Morphology of *Lecudina* sp. Clade F

Lecudina sp. Clade F trophozoites displayed ellipsoid, pear-shaped, and centrally constricted morphotypes. All morphotypes had a rounded posterior and conspicuous mucron, with the mucron observed in both retracted (Fig. 7.4 A, E) and extended (Fig. 7.4 B, D) positions. Longitudinal epicytic folds ran along the cells with a density of 2.1 folds/µm (Fig. 7.4 C–E), and gliding motility was observed. Isolates measured 40–72 µm in length ($\bar{x}$ =53.1 µm; *n* = 7) and 28–34 µm in width ($\bar{x}$ = 29.7 µm; *n* = 7). Spherical nuclei were found in the center of the cells, measuring 9–11 µm in diameter ($\bar{x}$ = 10 µm; *n* = 4).

7.3.5. Morphology of *Lecudina* sp. Clade G

Lecudina sp. Clade G trophozoites were pear-shaped with a rounded posterior and narrow, rounded mucron (Fig. 7.5 A–D, F). Cells had epicytic folds (Fig. 7.5 E–F) that ran longitudinally along the cells with a density of 1.3 folds/µm. Isolates measured 25–34 µm in length ($\bar{x}$ = 28.2 µm; *n* = 6) and 14–21 µm in width ($\bar{x}$ = 18 µm; *n* = 6). Spherical nuclei were found in the center of the cells, measuring 6–8 µm in diameter ($\bar{x}$ = 7 µm; *n* = 4).

7.3.6. Molecular phylogeny of gregarine apicomplexans

Phylogenetic analysis of an 80-sequence 18S alignment (Fig. 7.6) included archigregarines (*Devanium*, *Metzidium*, and *Selenidium*), *Trichotokara*, *Filipodium*, *Platyproteum*, *Paralecudina*, *Cuspisella*, *Loxomorpha*, early branching lecudinids (*Veloxidium*, *Lithocystis*, *Pterospora*, *Difficilina*, *Urospora*), *Sphinctocystis*, *Amplectina*, *Lecudina*, and *Lankesteria*. *Lecudina* Clade A, which was strongly supported, included *L.* cf. *platynereidis*, *L. pellucida*, and *Lecudina* spp. Clades C (northern California), D (Oshoro), E (Hiroshima), F (Ishigaki), and G (Okinawa). Clade C was recovered as a strongly supported monophyletic group, forming a strongly supported clade along with sequences from *L. tuzetae*/*L.* cf. *tuzetae* and one environmental sequence (Fig. 7.6). Clades D–G each formed strongly supported monophyletic groups nested within a moderately supported clade (ML:72/PP:0.99) that also included *L. pellucida*. Distantly related alveolates (*Chromera velia* and *Vitrella brassicaformis*) were included as an outgroup.

7.3.7. Molecular phylogeny of host material

Phylogenetic analysis of a 53-sequence COI alignment (Fig. 7.7) included representatives from the polychaete families Eunicidae and Nereididae. Host material for *Lecudina* spp. Clades C–G was recovered within a strongly supported Nereididae clade. Host material from *L*. sp. Clade C was recovered as sister to *Nereis eakini*, together forming a clade under strong support. Host material from *L*. spp. Clades D and E formed a strongly supported clade along with *Perinereis wilsoni*, while hosts from *L*. spp. Clades F and G formed a strongly supported clade with *Perinereis kaustiana*. Sipunculid sequences served as the outgroup.

7.4. DISCUSSION

7.4.1. Novel gregarine biodiversity from around Japan and the Pacific Ocean

Trophozoites of *Lecudina* spp. Clades D through G morphologically resembled *L. pellucida* Mingazzini, 1891 (Vivier, 1968) as well as *L*. sp. Clade C isolates from northern California (present work), western Canada (Rueckert et al., 2011b), and the English Channel (Schrével et al., 2016). Epicytic fold densities among these clades ranged from 1–3 folds/µm, posteriors and mucrons were consistently rounded, and spherical nuclei were located centrally with a diameter from 10–20 µm in length (Table 7.3). Isolates of *Lecudina* spp. Clades C through G all exhibited gliding motility, which is consistent with other members of *Lecudina* (Desportes and Schrével, 2013).

Lecudina sp. Clade E was notably larger than the other clades, with trophozoites ranging 125–190 µm in length. Cells were ellipsoid or circular in shape (Fig. 7.3). Epicytic folds were present along the length of the cell body with a density of 1.3 folds/µm, which was lower than in Clades C, D, and F. Centrally positioned spherical nuclei of *L*. sp. Clade E were among the largest observed among these *Lecudina* clades (Table 7.3), measuring 23–27 µm in diameter.

Lecudina sp. Clade F trophozoites were morphologically variable, appearing ellipsoid, pear-shaped, or constricted at the center (Fig 7.4). These trophozoites were also smaller than

those of Clades C through E, measuring 40–72 µm in length, and epicytic folds were among the densest recorded in this group (2.1 folds/µm). *Lecudina* sp. Clade G represented the smallest morphotype observed, with trophozoites measuring only 25–34 µm in length ($\bar{x}$ = 28.2 µm, n = 6) and 14–21 µm in width ($\bar{x}$ = 18 µm, n = 6). Despite their reduced size, these cells possessed morphological traits characteristic of *Lecudina* Clade A, including longitudinal epicytic folds (1.3 folds/µm), central, spherical nuclei, a pear-like (or lemon-like) shape (Fig. 7.5), and gliding motility. Furthermore, phylogenetic analysis (Fig. 7.6) grouped *Lecudina* sp. Clades C through G with *L. pellucida*, placing these novel lecudinids firmly within *Lecudina* Clade A. These observations, combined with a shared preference for nereidid hosts, strongly suggest *Lecudina* spp. Clades C through G are all novel members of the broader *Lecudina* Clade A.

7.4.2. Characteristic host preference among members of *Lecudina* Clade A

Close phylogenetic relationships among these clades can be largely explained by their characteristic preference for nereidid polychaete hosts (Fig. 7.7), specifically the genera *Nereis* and *Perinereis* (Schrével, 1963; Vivier, 1968; Schrével et al., 2016). Indeed, the results of this study reinforce the idea that *Lecudina* clades closely related to type species *L. pellucida* all share an affinity for nereidid hosts. Other lecudinids inhabiting nereidid worms, such as *L. pelmatomorpha* and *L. caudata*, have been described from the English Channel (Schrével, 1963) and southern Japan (Hoshide, 1977), respectively. However, a lack of molecular data for these species prevents comparative analysis. Given the data currently available on this group, a preference for nereidid hosts appears to be a defining feature of *Lecudina* Clade A.

7.4.3. Novel biogeographical insights into the distribution of *Lecudina*

The present study contains some of the first molecular data from around Japan that belongs to *Lecudina* Clade A (Fig. 7.6). Other such data from around Japan largely focuses on archigregarines (Wakeman, 2020) or the eugregarine genus *Lankesteria* (Iritani et al., 2021). Closer comparison of *L.* sp. Clade C sequences suggests a strong biogeographical influence on the observed phylogenetic topology (Fig. 7.8). Specifically, sequences from western Canada

(highlighted peach), northern California (highlighted pink), and northern France (highlighted red) all formed distinct sub-clades within the larger *Lecudina tuzetae* clade (Fig. 7.8). Jump dispersal is one explanation for how these *L*. cf. *tuzetae* populations were founded. For example, freight shipping across the Panama Canal has been implicated in the dispersal of protists (Lohan et al., 2017). It is also worth considering that nereidid polychaetes are a cosmopolitan group and can be found in a variety of marine habitats (Özpolat et al., 2021). Therefore, it is reasonable to surmise that *Lecudina tuzetae* is currently undergoing an allopatric speciation event that has resulted in yet-unexplored biodiversity.

CHAPTER 8. General conclusion

This project investigated the speciation patterns of marine gregarines through a multi-faceted analysis of their biodiversity, host associations, and biogeographic distributions across the Pacific Ocean. Focusing on gregarine lineages mainly from polychaetes and tunicates, this project examined how host identity and geographic isolation shape speciation among these understudied unicellular parasites.

In Chapter 2, novel lineages of archigregarines from polychaete hosts around Japan were discovered, with new clades of *Lunidium*, *Metzidium*, and *Devanium* characterized by varying morphology and host associations. Chapter 3 explored the cryptic diversity of paralecudinid gregarines, uncovering novel clades of *Ferraria* and *Paralecudina* while also offering a taxonomic revision in light of new molecular evidence. Chapter 4 focused on early branching lecudinids, identifying four novel clades with unique morphologies, phylogenetic lineages, and host associations with polychaetes (and even one ostracod). In Chapter 5, five new clades of *Lankesteria* were identified from tunicates. Phylogenetic relationships among these *Lankesteria* clades closely mirrored those of their ascidian hosts, clearly demonstrating the marine gregarine tendency towards host specialization. Chapter 6 discussed cryptic diversity in *Lecudina* clades from lumbrinerid polychaetes collected in northern Japan and the western United States, finding both host specialization and biogeographical range as contributors to speciation in this group. Finally, Chapter 7 investigated *Lecudina* gregarines infecting nereidid polychaetes and identified several novel clades within *Lecudina* Clade A. Data from this chapter demonstrated a strong host preference for nereidid worms and a global species complex associated with *Lecudina tuzetae*.

Together, the chapters of this dissertation offer a phylogenetic perspective on the biogeography, biodiversity, and evolutionary history of marine gregarines. From archigregarines to *Lecudina*, the combined use of light and electron microscopy with molecular evidence allows

us to see that both host phylogeny and biogeography play critical roles in explaining the rich biodiversity of marine gregarines. Hopefully, this work inspires continued study into the biodiversity of marine gregarines.

REFERENCES

Adem, D. and Ame, M., 2023. Toxoplasmosis and its significance in public health: a review. *Journal of Biomedical and Biological Sciences*, *2*(1), pp.1–20.

Adl, S.M., Bass, D., Lane, C.E., Lukeš, J., Schoch, C.L., Smirnov, A., Agatha, S., Berney, C., Brown, M.W., Burki, F. and Cárdenas, P., 2019. Revisions to the classification, nomenclature, and diversity of eukaryotes. *Journal of Eukaryotic Microbiology*, *66*(1), pp.4–119.

Alié, A., Hiebert, L.S., Simion, P., Scelzo, M., Prünster, M.M., Lotito, S., Delsuc, F., Douzery, E.J., Dantec, C., Lemaire, P. and Darras, S., 2018. Convergent acquisition of nonembryonic development in styelid ascidians. *Molecular Biology and Evolution*, *35*(7), pp.1728–1743.

Audouin, J.V. and Milne-Edwards, H., 1833. Classification des Annélides et description de celles qui habitent les côtes de la France. *Annales des Sciences Naturelles*, *30*, pp.411–425.

Berthold, A.A., 1827. *Latreille's Natuerliche Familien der Tierreichs, aus dem Franzgsischen mit Anmerkungen und Zusaetzen.* Weimar: Industrie Comptoirs.

Bhatia, B.L. and Setna, S.B., 1938. On some gregarine parasites from certain polychete worms from the Andaman Islands. *Proceedings of the Indian Academy of Sciences*, *8*(3), pp.231–242.

Blainville, H.D., 1818. Mémoire sur la classe des Sétipodes, partie des vers à sang rouge de M. Cuvier, et des Annélides de M. de Lamarck. *Bulletin des Sciences, par la Société Philomatique de Paris*, *1818*(3), pp.78-85.

Blainville, H.D., 1824. *Appendice au Traité Zoologique et Physiologique sur les Vers Intestinaux de M. Bremser*. Paris: Grundler, p.522.

Boisard, J. and Florent, I., 2020. Why the –omic future of Apicomplexa should include gregarines. *Biology of the Cell*, *112*(6), pp.173–185.

Brasil, L., 1909. Documents sur quelques Sporozoaires d'Annélides. *Archiv für Protistenkunde*, *16*, pp.106–142.

Bruvo, R., Adolfsson, S., Symonova, R., Lamatsch, D.K., Schön, I., Jokela, J., Butlin, R.K. and Müller, S., 2011. Few parasites, and no evidence for *Wolbachia* infections, in a freshwater ostracod inhabiting temporary ponds. *Biological Journal of the Linnean Society*, *102*(1), pp.208–216.

Canales-Aguirre, C.B., Rozbaczylo, N. and Hernández, C.E., 2011. Genetic identification of benthic polychaetes in a biodiversity hotspot in the southeast Pacific. *Revista de Biología Marina y Oceanografía*, *46*(1), pp.89–94.

Carr, C.M., Hardy, S.M., Brown, T.M., Macdonald, T.A. and Hebert, P.D., 2011. A tri-oceanic perspective: DNA barcoding reveals geographic structure and cryptic diversity in Canadian polychaetes. *PLOS ONE*, *6*, e22232.

Carus, J.V., 1863. Vermes. In: Peters, W.C.H., Carus, J.V. and Gerstäcker, C.E.A. (eds.) *Handbuch der Zoologie*. Leipzig: Wilhelm Engelmann, pp.422–484.

Caullery, M. and Mesnil, F., 1914. Sur les Metchnikovellidae et autre Protistes des Grégarines d'Annélides. *Comptes Rendus de Séances de la Société de Biologie*, *77*, pp.527–532.

Cavalier-Smith, T., 1999. Principles of protein and lipid targeting in secondary symbiogenesis: euglenoid, dinoflagellate, and sporozoan plastid origins and the eukaryote family tree. *Journal of Eukaryotic Microbiology*, *46*(4), pp.347–366.

Chait, E., Page, G. and Hunkapiller, M., 1988. Battle of the DNA sequencers. *Nature*, *333*(6172), pp.477–478.

Chambouvet, A., Valigurová, A., Pinheiro, L.M., Richards, T.A. and Jirků, M., 2016. *Nematopsis temporariae* (Gregarinasina, Apicomplexa, Alveolata) is an intracellular infectious agent of tadpole livers. *Environmental Microbiology Reports*, *8*(5), pp.675–

679.

Chen, W.J., Wu, S.T., Chow, C.Y. and Yang, C.H., 1997. Sporogonic development of the gregarine *Ascogregarina taiwanensis* (Lien and Levine) (Apicomplexa: Lecudinidae) in its natural host *Aedes albopictus* (Skuse) (Diptera: Culicidae). *Journal of Eukaryotic Microbiology*, *44*(4), pp.326–331.

Chittavichai, T., Sathitnaitham, S., Utthiya, S., Prompichai, W., Prommarit, K., Vuttipongchaikij, S. and Wonnapinij, P., 2025. Limitations of 18S rDNA sequence in species-level classification of dictyostelids. *Microorganisms, 13*(2), p.275.

Ciancio, A., Scippa, S. and Cammarano, M., 2001. Ultrastructure of trophozoites of the gregarine *Lankesteria ascidiae* (Apicomplexa: Eugregarinida) parasitic in the ascidian *Ciona intestinalis* (Protochordata). *European Journal of Protistology*, *37*(3), pp.327–336.

Coulon, P. and Jangoux, M., 1987. Gregarine species (Apicomplexa) parasitic in the burrowing echinoid *Echinocardium cordatum*: occurrence and host reaction. *Diseases of Aquatic Organisms, 2*, pp.135–145.

Cox, F.E.G., 1994. The evolutionary expansion of the Sporozoa. *International Journal for Parasitology, 24*(8), pp.1301–1316.

Desportes, I. and Schrével, J., 2013. *Treatise on Zoology: Anatomy, Taxonomy, Biology. The Gregarines (2 vols): The Early Branching Apicomplexa.* Leiden, Netherlands: De Gruyter Brill.

Diakin, A., Paskerova, G.G., Simdyanov, T.G., Aleoshin, V.V. and Valigurová, A., 2016. Morphology and molecular phylogeny of coelomic gregarines (Apicomplexa) with different types of motility: *Urospora ovalis* and *U. travisiae* from the polychaete *Travisia forbesii*. *Protist*, *167*, pp.279–303.

Diakin, A., Wakeman, K.C. and Valigurová, A., 2017. Description of *Ganymedes yurii* sp. n. (Ganymedidae), a new gregarine species from the Antarctic amphipod *Gondogeneia* sp. (Crustacea). *Journal of Eukaryotic Microbiology*, *64*(1), pp.56–66.

Dubey, J.P., Zarnke, R., Thomas, N.J., Wong, S.K., van Bonn, W., Briggs, M., Davis, J.W., Ewing, R., Mense, M., Kwok, O.C.H. and Romand, S., 2003. *Toxoplasma gondii*, *Neospora caninum*, *Sarcocystis neurona*, and *Sarcocystis canis*-like infections in marine mammals. *Veterinary Parasitology*, *116*, pp.275–296.

Dufour, L., 1828. Note sur la grégarine, nouveau genre de ver qui vit en troupeau dans les intestins de divers insectes. *Annales des Sciences Naturelles*, *13*, pp.366–368.

Elbarhoumi, M. and Zghal, F., 2010. Présence de trois espèces de grégarines (Apicomplexa: Eugregarinorida) chez l'annélide polychète *Marphysa sanguinea* (Montagu, 1815) dans le lac de Tunis. *Parasite*, *17*(1), pp.71–75.

Escalante, A.A. and Ayala, F.J., 1995. Evolutionary origin of *Plasmodium* and other Apicomplexa based on rRNA genes. *Proceedings of the National Academy of Sciences*, *92*(13), pp.5793–5797.

Field, K.G., Olsen, G.J., Lane, D.J., Giovannoni, S.J., Ghiselin, M.T., Raff, E.C., Pace, N.R. and Raff, R.A., 1988. Molecular phylogeny of the animal kingdom. *Science*, *239*(4841), pp.748–753.

Field, S.G. and Michiels, N.K., 2006. Acephaline gregarine parasites (*Monocystis* sp.) are not transmitted sexually among their lumbricid earthworm hosts. *Journal of Parasitology*, *92*(2), pp.292–297.

Foote, M. and Sepkoski, J.J., 1999. Absolute measures of the completeness of the fossil record. *Nature*, *398*(6726), pp.415–417.

Frolova, E.V., Paskerova, G.G., Smirnov, A.V. and Nassonova, E.S., 2021. Molecular phylogeny and new light microscopic data of *Metchnikovella spiralis* (Microsporidia: Metchnikovellidae), a hyperparasite of eugregarine *Polyrhabdina* sp. from the polychaete *Pygospio elegans*. *Parasitology*, *148*(7), pp.779–786.

Frolova, E.V., Paskerova, G.G., Smirnov, A.V. and Nassonova, E.S., 2022. *Metchnikovella dobrovolskiji* sp. nov. (Microsporidia: Metchnikovellida), a parasite of archigregarines

Selenidium pygospionis from the polychaete *Pygospio elegans*. *Protistology*, *16*(3), pp.226–235.

Frolova, E.V., Paskerova, G.G., Smirnov, A.V. and Nassonova, E.S., 2023. Diversity, distribution, and development of hyperparasitic microsporidia in gregarines within one super-host. *Microorganisms*, *11*(1), p.152.

Gaber, I. and Elghazaly, M., 2021. First record of two sabelline fan-worms in the tunic of the exotic sea squirt *Cnemidocarpa amphora* (Kott, 1992) (Stolidobranchia, Styelidae) from the Mediterranean Sea off Alexandria, Egypt. *Egyptian Journal of Aquatic Research*, *47*(2), pp.185–190.

Ganapati, P.N., Kalavati, C. and Sundaram, P.S., 1974. On a new multisegmented gregarine, *Gopaliella marphysae* n. gen., n. sp. from the gut of a polychete worm, *Marphysa gravelyi*. *Archiv für Protistenkunde*, *116*, pp.244–250.

Giard, A., 1876. Sur une nouvelle espèce de Psorospermie (*Lithocystis schneideri*) parasite de l'*Echinocardium cordatum*. *Comptes rendus de l'Académie des Sciences*, *32*, pp.1208–1210.

Giard, A., 1884. Note sur un nouveau groupe de Protozoaires parasites des Annelides et sur quelques points de l'histoire des Gregarines. *Association française pour l'avancement des sciences, Congrès de Blois, Compte-Rendu. 12:* 192.

Goodrich, H.P., 1949. *Heliospora* ng and *Rotundula* ng, gregarines of *Gammarus pulex*. *Journal of Cell Science*, *3*(9), pp.27–35.

Gordon, T., Manni, L. and Shenkar, N., 2019. Regeneration ability in four stolidobranch ascidians: ecological and evolutionary implications. *Journal of Experimental Marine Biology and Ecology*, *519*, p.151184.

Granthom-Costa, L.V., Resende de Messano, L.V., Padula, V., Silva Oliveira, F.A., Fabian Messano, H. and Coutinho, R., 2023. First record of a *Didemnum carpet* ascidian from the southwestern Atlantic Ocean. *BioInvasions Record*, *12*(3), pp.753–763.

Grassé P-P., 1953. Classe des grégarinomorphes (*Gregarinomorpha*, n. nov., Gregarinae Haeckel, 1866; gregarinidea Lankester, 1885; grégarines des auteurs). In: Grassé P-P editor. *Traité de Zoologie*. Paris: Masson. pp.590–690.

Gray, M.W., 2017. Lynn Margulis and the endosymbiont hypothesis: 50 years later. *Molecular Biology of the Cell*, *28*(10), pp.1285–1287.

Green, B.R., 2011. After the primary endosymbiosis: An update on the chromalveolate hypothesis and the origins of algae with Chl c. *Photosynthesis Research*, *107*, pp.103–115.

Gubbels, M.J. and Duraisingh, M.T., 2012. Evolution of apicomplexan secretory organelles. *International Journal for Parasitology*, *42*, pp.1071–1081.

Haeckel, E., 1866. *Generelle Morphologie der Organismen: Allgemeine Grundzüge der organischen Formen-Wissenschaft, mechanisch begründet durch die von Charles Darwin reformierte Descendenz-Theorie*. Berlin: de Gruyter.

Hensley, N.M., Rivers, T.J., Gerrish, G.A., Saha, R. and Oakley, T.H., 2023. Collective synchrony of mating signals modulated by ecological cues and social signals in bioluminescent sea fireflies. *Proceedings of the Royal Society B*, *290*(2011), p.20232311.

Hoshide, H., 1957. Studies on the cephaline gregarines of Japan (II) : Description of those belonging to the families Lecudinidae, Polyrhabdinidae Cephaloidophoridae and Stenophoridae. *Bulletin of the Faculty of Education, Yamaguchi University*, *6*(2), pp.97–157.

Hoshide, K., 1973. Studies on the fine structure of gregarines. *Bulletin of the Faculty of Education, Yamaguchi University*, *23*, pp.87–90.

Hu, K., Johnson, J., Florens, L., Fraunholz, M., Suravajjala, S., DiLullo, C., Yates, J., Roos, D.S. and Murray, J.M., 2006. Cytoskeletal components of an invasion machine—the apical complex of *Toxoplasma gondii*. *PLOS Pathogens*, *2*(2), p.e13.

Huelsenbeck, J.P. and Ronquist, F., 2001. MRBAYES: Bayesian inference of phylogenetic trees.

Bioinformatics, *17*(8), pp.754–755.

Huxley, J., 1910. On *Ganymedes anaspidis* (nov. gen., nov. sp.), a gregarine from the digestive tract of *Anaspides tasmaniae* (Thompson). *Journal of Cell Science*, *2*(217), pp.155–175.

Huxley, J., 1957. The three types of evolutionary process. *Nature*, *180*(4584), pp.454–455.

Iritani, D., Banks, J.C., Webb, S.C., Fidler, A., Horiguchi, T. and Wakeman, K.C., 2021. New gregarine species (Apicomplexa) from tunicates show an evolutionary history of host switching and suggest a problem with the systematics of *Lankesteria* and *Lecudina*. *Journal of Invertebrate Pathology*, *183*, p.107622.

Iritani, D., Horiguchi, T. and Wakeman, K.C., 2018a. Molecular phylogenetic positions and ultrastructure of marine gregarines (Apicomplexa) *Cuspisella ishikariensis* n. gen., n. sp. and *Loxomorpha* cf. *harmothoe* from western Pacific scaleworms (Polynoidae). *Journal of Eukaryotic Microbiology*, *65*(5), pp.637-647.

Iritani, D., Wakeman, K.C. and Leander, B.S., 2018b. Molecular phylogenetic positions of two new marine gregarines (Apicomplexa)—*Paralecudina anankea* n. sp. and *Lecudina caspera* n. sp.—from the intestine of *Lumbrineris inflata* (Polychaeta) show patterns of co-evolution. *Journal of Eukaryotic Microbiology*, *65*(2), pp.211–219.

Jimi, N., Fujiwara, Y. and Kajihara, H., 2024. Evaluation of "*Cirriformia tentaculata*"(Annelida: Cirratulidae) from Japan as a pollution indicator in marine environments: is it truly a single species?. *Species Diversity*, *29*(2), pp.281–316.

Kalyaanamoorthy, S., Minh, B.Q., Wong, T.K., Von Haeseler, A. and Jermiin, L.S., 2017. ModelFinder: fast model selection for accurate phylogenetic estimates. *Nature Methods*, *14*, pp.587–589.

Katoh, K., Misawa, K., Kuma, K.i. and Miyata, T., 2002. MAFFT: a novel method for rapid multiple sequence alignment based on fast Fourier transform. *Nucleic Acids Research*, *30*, pp.3059–3066.

Keeling, P.J., 2009. Chromalveolates and the evolution of plastids by secondary endosymbiosis

1. *Journal of Eukaryotic Microbiology*, *56*(1), pp.1–8.

Kolawole, E.O., Ayeni, E.T., Abolade, S.A., Ugwu, S.E., Awoyinka, T.B., Ofeh, A.S. and Okolo, B.O., 2023. Malaria endemicity in Sub-Saharan Africa: Past and present issues in public health. *Microbes and Infectious Diseases*, *4*(1), pp.242–251.

Kováčiková, M., Simdyanov, T.G., Diakin, A. and Valigurová, A., 2017. Structures related to attachment and motility in the marine eugregarine *Cephaloidophora* cf. *communis* (Apicomplexa). *European Journal of Protistology*, *59*, pp.1–13.

Kováčiková, M., Paskerova, G.G., Diakin, A., Simdyanov, T.G., Vaškovicová, N. and Valigurová, A., 2019. Motility and cytoskeletal organisation in the archigregarine *Selenidium pygospionis* (Apicomplexa): observations on native and experimentally affected parasites. *Parasitology Research*, *118*, pp.2651–2667.

Koyama, H., Taneda, Y. and Ishii, T., 2012. The postbranchial digestive tract of the ascidian, *Polyandrocarpa misakiensis* (Tunicata: Ascidiacea). *Zoological Science*, *29*(2), pp.97–110.

Kuibagarov, M., Makhamed, R., Zhylkibayev, A., Berdikulov, M., Abdrakhmanov, S., Kozhabayev, M., Akhmetollayev, I., Mukanov, K., Ryskeldina, A., Ramankulov, Y. and Shustov, A., 2023., *Theileria* and *Babesia* infection in cattle–first molecular survey in Kazakhstan. *Ticks and Tick-borne Diseases*, *14*(1), p.102078.

Kuvardina, O.N., Leander, B.S., Aleshin, V.V., Myl'nikov, A.P., Keeling, P.J. and Simdyanov, T.G., 2002. The phylogeny of colpodellids (Alveolata) using small subunit rRNA gene sequences suggests they are the free-living sister group to apicomplexans. *Journal of Eukaryotic Microbiology*, *49*(6), pp.498–504.

Labbé, A. and Racovitza, E.G., 1897. *Pterospora maldaneorum* ng, n. sp., grégarine nouvelle parasite des maldaniens. *Bulletin de la Société zoologique de France*, *22*, pp.92–97.

Lahille, F., 1886. Sur le classification des tuniciers. *Comptes rendus de l'Académie des Sciences*, *16*, pp.1573–1575.

Lamarck, J.B., 1818. *Histoire naturelle des animaux sans vertèbres*. Paris: Deterville/Verdière. Vol 5.

Landers, S.C. and Leander, B.S., 2005. Comparative surface morphology of marine coelomic gregarines (Apicomplexa, Urosporidae): *Pterospora floridiensis* and *Pterospora schizosoma*. *Journal of Eukaryotic Microbiology*, 52, pp.23–30.

Latreille, P.A., 1802. *Histoire Naturelle, Générale et Particulière des Crustacés et des Insectes*. Paris: de L'imprimerie de F. Dufart.

Lax, G., Park, E., Na, I., Jacko-Reynolds, V., Kwong, W.K., House, C.S., Trznadel, M., Wakeman, K., Leander, B.S. and Keeling, P., 2024. Phylogenomic diversity of archigregarine apicomplexans. *Open Biology*, *14*(9), p.240141.

Leander, B.S., 2006. Ultrastructure of the archigregarine *Selenidium vivax* (Apicomplexa)–a dynamic parasite of sipunculid worms (host: *Phascolosoma agassizii*). *Marine Biology Research*, *2*(3), pp.178–190.

Leander, B.S., 2007. Molecular phylogeny and ultrastructure of *Selenidium serpulae* (Apicomplexa, Archigregarinia) from the calcareous tubeworm *Serpula vermicularis* (Annelida, Polychaeta, Sabellida). *Zoologica Scripta*, *36*(2), pp.213–227.

Leander, B.S., 2008. Marine gregarines: evolutionary prelude to the apicomplexan radiation? *Trends in Parasitology*, *24*, pp.60–67.

Leander, B.S. and Keeling, P.J., 2003. Morphostasis in alveolate evolution. *Trends in Ecology & Evolution*, *18*(8), pp.395–402.

Leander, B.S., Clopton, R.E. and Keeling, P.J., 2003a. Phylogeny of gregarines (Apicomplexa) as inferred from small-subunit rDNA and β-tubulin. *International Journal of Systematic and Evolutionary Microbiology*, *53*(1), pp.345–354.

Leander, B.S., Harper, J.T. and Keeling, P.J., 2003b. Molecular phylogeny and surface morphology of marine aseptate gregarines (Apicomplexa): *Selenidium* spp. and *Lecudina* spp. *Journal of Parasitology*, *89*(6), pp.1191–1205.

Leander, B.S., Lloyd, S.A., Marshall, W. and Landers, S.C., 2006. Phylogeny of marine gregarines (Apicomplexa)—*Pterospora*, *Lithocystis* and *Lankesteria*—and the origin(s) of coelomic parasitism. *Protist*, *157*, pp.45–60.

Lee, J.J., Leedale, G.F. and Bradbury, P., 2000. *The Illustrated Guide to the Protozoa, 2nd edn*. Lawrence, Kansas: Allen Press.

Léger, L., 1892. *Recherches sur les Grégarines*. Poitiers, France: Typographie Oudin et cie, 3, pp.1–183.

Léger, L., 1900. Sur Une nouveau sporozoite des larves de dipteres (Schizocystis). *Comptes rendus de l'Académie des Sciences, 131*, pp.722–724.

Léger, L. and Duboscq, O., 1917. Sporozoaires de *Glossobalanus minutus* Kow., *Selenidium metchnikowi* n. sp. *Annals d'Institut Pasteur, 31*, pp.60–74.

Levine N.D., 1970. *Taxonomy of the Sporozoa.* In: Proceedings of the Second International Congress of Parasitology. Lawrence, Kansas: Allen Press. pp. 208–209.

Levine, N.D., 1971. Taxonomy of the archigregarinorida and selenidiidae (Protozoa, Apicomplexa). *The Journal of Protozoology, 18*(4), pp.704–717.

Levine, N.D., 1974. Gregarines of the genus *Lecudina* (Protozoa, Apicomplexa) from Pacific Ocean polychaetes. *Journal of Protozoology, 21*, pp.10–12.

Levine, N.D., 1976. Revision and checklist of the species of the aseptate gregarine genus *Lecudina. Transactions of the American Microscopical Society, 95*, pp.695–702.

Levine, N.D., 1977. Checklist of the species of the aseptate gregarine family Urosporidae. *International Journal for Parasitology*, *7*, pp.101–108.

Levine, N.D., 1979. New genera and higher taxa of septate gregarines (Protozoa, Apicomplexa). *Journal of Protozoology, 26*, pp.532–536.

Levine, N.D., 1988. Progress in taxonomy of the apicomplexan Protozoa. *Journal of Protozoology*, *35*, pp.518–520.

Lim, L. and McFadden, G.I., 2010. The evolution, metabolism and functions of the apicoplast.

Philosophical Transactions of the Royal Society B: Biological Sciences, *365*(1541), pp.749–763.

Lohan, K.M.P., Fleischer, R.C., Torchin, M.E. and Ruiz, G.M., 2017. Protistan biogeography: a snapshot across a major shipping corridor spanning two oceans. *Protist*, *168*(2), pp.183–196.

MacGregor, H.C. and Thomasson, P.A., 1965. The fine structure of two archigregarines, *Selenidium fallax* and *Ditrypanocystis cirratuli*. *Journal of Protozoology*, *12*, pp.438–443.

Mangold, A.J., Bargues, M.D. and Mas-Coma, S., 1997. 18S rRNA gene sequences and phylogenetic relationships of European hard-tick species (Acari: Ixodidae). *Parasitology Research*, *84*, pp.31–37.

Maréchal, E. and Cesbron-Delauw, M.F., 2001. The apicoplast: a new member of the plastid family. *Trends in Plant Science*, *6*(5), pp.200–205.

Mastrototaro, F. and Brunetti, R., 2006. The non-indigenous ascidian *Distaplia bermudensis* in the Mediterranean: comparison with the native species *Distaplia magnilarva* and *Distaplia lucillae* sp. nov. *Journal of the Marine Biological Association of the United Kingdom*, *86*(1), pp.181–185.

Mathur, V., Wakeman, K.C. and Keeling, P.J., 2021. Parallel functional reduction in the mitochondria of apicomplexan parasites. *Current Biology*, *31*, pp.2920–2928.

McAllister, C.T., Upton, S.J., Trauth, S.E. and Dixon, J.R., 1995. Coccidian parasites (Apicomplexa) from snakes in the southcentral and southwestern United States: new host and geographic records. *Journal of Parasitology*, *81*, pp.63–68.

McKinley, K., Tsaousis, A.D. and Rückert, S., 2024. Description and prevalence of gregarines infecting the amphipod *Gammarus pulex*, in the Water of Leith, Scotland, UK. *European Journal of Protistology*, *94*, p.126084.

Meca, M.A., Zhadan, A. and Struck, T.H., 2021. The early branching group of Orbiniida sensu

Struck et al., 2015: Parergodrilidae and Orbiniidae. *Diversity*, *13*(1), p.29.

Mellor, J.S. and Stebbings, H., 1980. Microtubules and the propagation of bending waves by the archigregarine, *Selenidium fallax*. *Journal of Experimental Biology*, *87*(1), pp.149–161.

Meyer, A., Todt, C., Mikkelsen, N.T. and Lieb, B., 2010. Fast evolving 18S rRNA sequences from Solenogastres (Mollusca) resist standard PCR amplification and give new insights into mollusk substitution rate heterogeneity. *BMC Evolutionary Biology*, *10*, pp.1–12.

Mingazzini, P., 1891. Gregarine monocistidee, nuove o poco conosciute, del Golfo di Napoli. *Atti della Accademia Nazionale dei Lincei*, *4*, pp.229–35.

Miroliubova, T.S., Mikhailov, K.V., Simdyanov, T.G., Aleoshin, V.V., Dũng, Đ.T. and Kudriavkina, A.I., 2025. Parasites specific to centipedes form a new major lineage of terrestrial gregarines. *Scientific Reports*, *15*(1), p.192.

Mita, K., Kawai, N., Rueckert, S. and Sasakura, Y., 2012. Large-scale infection of the ascidian *Ciona intestinalis* by the gregarine *Lankesteria ascidiae* in an inland culture system. *Diseases of Aquatic Organisms*, *101*(3), pp.185–195.

Mo, C., Douek, J. and Rinkevich, B., 2002. Development of a PCR strategy for thraustochytrid identification based on 18S rDNA sequence. *Marine Biology*, *140*, pp.883–889.

Molla, S.H., Bandyopadhyay, P.K. and Gürelli, G., 2013. On the occurrence of a Haemogregarinae (Apicomplexa) parasite from freshwater turtles of south 24 Parganas, West Bengal, India. *Türkiye Parazitoloji Dergisi*, *37*, pp.118–122.

Moreira, D. and López-García, P., 2003. Are hydrothermal vents oases for parasitic protists? *Trends in Parasitology*, *19*, pp.556–558.

Moreno, T.R. and Rocha, R.M., 2008. Phylogeny of the Aplousobranchia (Tunicata: Ascidiacea). *Revista Brasileira de Zoologia*, *25*, pp.269–298.

Morrison, D.A., 2009. Evolution of the Apicomplexa: where are we now? *Trends in Parasitology*, *25*, pp.375–382.

Morrison, D.A. and Ellis, J.T., 1997. Effects of nucleotide sequence alignment on phylogeny

estimation: a case study of 18S rDNAs of apicomplexa. *Molecular Biology and Evolution, 14*(4), pp.428–441.

Nakayama, T., Watanabe, S., Mitsui, K., Uchida, H. and Inouye, I., 1996. The phylogenetic relationship between the Chlamydomonadales and Chlorococcales inferred from 18S rDNA sequence data. *Phycological Research, 44,* pp.47–55.

Nguyen, L.T., Schmidt, H.A., von Haeseler, A. and Minh, B.Q., 2015. IQ-TREE: a fast and effective stochastic algorithm for estimating maximum likelihood phylogenies. *Molecular Biology and Evolution, 32*, pp.268–274.

Nishimoto, Y., Arisue, N., Kawai, S., Escalante, A.A., Horii, T., Tanabe, K. and Hashimoto, T., 2008. Evolution and phylogeny of the heterogeneous cytosolic SSU rRNA genes in the genus *Plasmodium*. *Molecular Phylogenetics and Evolution, 47*(1), pp.45–53.

Oakley, T.H., Wolfe, J.M., Lindgren, A.R. and Zaharoff, A.K., 2013. Phylotranscriptomics to bring the understudied into the fold: monophyletic Ostracoda, fossil placement, and pancrustacean phylogeny. *Molecular Biology and Evolution, 30*(1), pp.215–233.

Odle, E., Riewluang, S., Ageishi, K., Kajihara, H. and Wakeman, K.C., 2024. Pacific marine gregarines (Apicomplexa) shed light on biogeographic speciation patterns and novel diversity among early apicomplexans. *European Journal of Protistology*, *94*, p.126080.

Okamoto, N. and Keeling, P.J., 2014. The 3D structure of the apical complex and association with the flagellar apparatus revealed by serial TEM tomography in *Psammosa pacifica*, a distant relative of the Apicomplexa. *PLOS ONE, 9*(1), p.e84653.

Ormières, R., 1964. Recherches sur les sporozoaires parasites des tuniciers. *Vie et Milieu, 15*(4) p.823–946.

Ormières, R., 1979. *Selenidium cantoui* n. sp., a parasitic archigregarine from *Physcosoma granulatum* (Leuckart) (Sipunculid) an ultrastructural study. *Zeitschrift für Parasitenkunde, 61*, pp.13–20.

Özpolat, B.D., Randel, N., Williams, E.A., Bezares-Calderón, L.A., Andreatta, G., Balavoine,

G., Bertucci, P.Y., Ferrier, D.E.K., Gambi, M.C., Gazave, E., Handberg-Thorsager, M., Hardege, J., Hird, C., Hsieh, Y.W., Hui, J., Mutemi, K.N., Schneider, S.Q., Simakov, O., Vergara, H.M., Vervoort, M., Jékely, G., Tessmar-Raible, K., Raible, F. and Arent, D., 2021. The nereid on the rise: *Platynereis* as a model system. *EvoDevo, 12*, p.e10.

Pamungkas, J., Glasby, C.J. and Costello, M.J., 2021. Biogeography of polychaete worms (Annelida) of the world. *Marine Ecology Progress Series*, *657*, pp.147–159.

Park, E. and Leander, B.S., 2024a. Molecular phylogeny of the Lecudinoidea (Apicomplexa): a major group of marine gregarines with diverse shapes, movements and hosts. *Journal of Eukaryotic Microbiology*, *71*(6), p.e13053.

Park, E. and Leander, B., 2024b. Coinfection of slime feather duster worms (Annelida, Myxicola) by different gregarine apicomplexans (*Selenidium*) and astome ciliates reflects spatial niche partitioning and host specificity. *Parasitology*, *151*(4), pp.400–411.

Paskerova, G.G., Miroliubova, T.S., Diakin, A., Kováčiková, M., Valigurová, A., Guillou, L., Aleoshin, V.V. and Simdyanov, T.G., 2018. Fine structure and molecular phylogenetic position of two marine gregarines, *Selenidium pygospionis* sp. n. and *S. pherusae* sp. n., with notes on the phylogeny of Archigregarinida (Apicomplexa). *Protist, 169*, pp.826–852.

Paskerova, G.G., Miroliubova, T.S., Valigurová, A., Janouškovec, J., Kováčiková, M., Diakin, A., Sokolova, Y.Y., Mikhailov, K.V., Aleoshin, V.V. and Simdyanov, T.G., 2021. Evidence from the resurrected family Polyrhabdinidae Kamm, 1922 (Apicomplexa: Gregarinomorpha) supports the epimerite, an attachment organelle, as a major eugregarine innovation. *PeerJ*, *9*, p.e11912.

Patwardhan, A., Ray, S. and Roy, A., 2014. Molecular markers in phylogenetic studies—a review. *Journal of Phylogenetics & Evolutionary Biology*, *2*(2), p.131.

Perkins, F., Barta, J., Clopton, R., Pierce, M. and Upton, S. 2000. Phylum Apicomplexa. In: *The Illustrated Guide to the Protozoa.* Lawrence, Kansas: Allen Press, 2nd edition, pp.190–

304.

Pietluch, F., Mackiewicz, P., Ludwig, K. and Gagat, P., 2024. A new model and dating for the evolution of complex plastids of red alga origin. *Genome Biology and Evolution*, *16*(9), p.evae192.

Pixell-Goodrich, H.L., 1916. Memoirs: the gregarines of *Glycera siphonostoma*. *Journal of Cell Science*, *2*, pp.205–216.

Qiu, B., 2001. Kuroshio and Oyashio currents. *Ocean Currents: A Derivative of the Encyclopedia of Ocean Sciences*, *2*, pp.61–72.

de Queiroz, K., 2007. Species concepts and species delimitation. *Systematic Biology*, *56*(6), pp.879–886.

Ridley, M., 1989. The cladistic solution to the species problem. *Biology and Philosophy*, *4*, pp.1–16.

Rotari, Y.M., Paskerova, G.G. and Sokolova, Y.Y., 2015. Diversity of metchnikovellids (Metchnikovellidae, Rudimicrosporea), hyperparasites of bristle worms (Annelida, Polychaeta) from the White Sea. *Protistology*, *9*(1), pp.50–59.

Rueckert, S. and Horák, A., 2017. Archigregarines of the English Channel revisited: new molecular data on *Selenidium* species including early described and new species and the uncertainties of phylogenetic relationships. *PLOS ONE*, *12*, p.e0187430.

Rueckert, S. and Leander, B.S., 2009. Molecular phylogeny and surface morphology of marine archigregarines (Apicomplexa), *Selenidium* spp., *Filipodium phascolosomae* n. sp., and *Platyproteum* ng and comb. from north-eastern Pacific peanut worms (Sipuncula). *Journal of Eukaryotic Microbiology*, *56*(5), pp.428–439.

Rueckert, S. and Leander, B.S., 2010. Description of *Trichotokara nothriae* n. gen. et sp. (Apicomplexa, Lecudinidae)—an intestinal gregarine of *Nothria conchylega* (Polychaeta, Onuphidae). *Journal of Invertebrate Pathology*, *104*(3), pp.172–179.

Rueckert, S., Chantangsi, C. and Leander, B.S., 2010. Molecular systematics of marine

gregarines (Apicomplexa) from North-eastern Pacific polychaetes and nemerteans, with descriptions of three novel species: *Lecudina phyllochaetopteri* sp. nov., *Difficilina tubulani* sp. nov. and *Difficilina paranemertis* sp. nov. *International Journal of Systematic and Evolutionary Microbiology*, *60*(11), pp.2681–2690.

Rueckert, S., Simdyanov, T.G., Aleoshin, V.V. and Leander, B.S., 2011a. Identification of a divergent environmental DNA sequence clade using the phylogeny of gregarine parasites (Apicomplexa) from crustacean hosts. *PLOS ONE*, *6*, p.e18163.

Rueckert, S., Villette, P.M. and Leander, B.S., 2011b. Species boundaries in gregarine apicomplexan parasites: a case study—comparison of morphometric and molecular variability in *Lecudina* cf. *tuzetae* (Eugregarinorida, Lecudinidae). *Journal of Eukaryotic Microbiology*, *58*, pp.275–283.

Rueckert, S., Wakeman, K.C. and Leander, B.S., 2013. Discovery of a diverse clade of gregarine apicomplexans (Apicomplexa: Eugregarinorida) from Pacific eunicid and onuphid polychaetes, including descriptions of *Paralecudina* n. gen., *Trichotokara japonica* n. sp., and *T. eunicae* n. sp. *Journal of Eukaryotic Microbiology*, *60*(2), pp.121–136.

Rueckert, S., Wakeman, K.C., Jenke-Kodama, H. and Leander, B.S., 2015. Molecular systematics of marine gregarine apicomplexans from Pacific tunicates, with descriptions of five novel species of *Lankesteria*. *International Journal of Systematic and Evolutionary Microbiology*, *65*, 2598–2614.

Saeedi, H., Brandt, A. and Jacobsen, N.L., 2022. Biodiversity and distribution of Isopoda and Polychaeta along the northwestern Pacific and the Arctic Ocean. *Biodiversity Informatics*, *17*, pp.10–26.

Sagan, L., 1967. On the origin of mitosing cells. *Journal of Theoretical Biology*, *14*(3), p.225.

Salonna, M., Gasparini, F., Huchon, D., Montesanto, F., Haddas-Sasson, M., Ekins, M., McNamara, M., Mastrototaro, F. and Gissi, C., 2021. An elongated COI fragment to discriminate botryllid species and as an improved ascidian DNA barcode. *Scientific*

Reports, *11*(1), p.4078.

Sawada, H., Pinto, M.R. and De Santis, R., 1998. Participation of sperm proteasome in fertilization of the phlebobranch ascidian *Ciona intestinalis*. *Molecular Reproduction and Development: Incorporating Gamete Research*, *50*(4), pp.493–498.

Schmarda, L.K., 1861. *Neue Wirbellose Thiere Beobachtet und Gesammelt auf Einer Reise um die Erde 1853 bis 1857*. Leipzig: Wilhelm Engelmann.

Schneider, A., 1875. Contribution à l'histoire des grègarines des invertébrés de Paris et de Roscoff. *Archives de Zoologie Expérimentale et Générale, 4*. pp.493–604.

Schneider, A., 1882. Seconde contribution à l'étude des grégarines. *Archives de Zoologie Expérimentale et Générale*, *10*. pp. 423–450.

Schrével, J., 1963. Grégarines nouvelles de Nereidae et Eunicidae (annélides polychètes). *Comptes Rendus des Séances de la Société de Biologie*, *157*(4), p.814.

Schrével, J., 1969. Recherches sur le cycle des Lecudinidae grégarines parasites d'annélides polychétes. *Protistologica*, *5*, pp.561–588.

Schrével, J., Caigneaux, D., Gros, D. and Philippe, M., 1983. The three cortical membranes of the gregarines: I. Ultrastructural organization of *Gregarina blaberae*. *Journal of Cell Science*, *61*(1), pp.151–174.

Schrével, J., Valigurová, A., Prensier, G., Chambouvet, A., Florent, I. and Guillou, L., 2016. Ultrastructure of *Selenidium pendula*, the type species of archigregarines, and phylogenetic relations to other marine Apicomplexa. *Protist*, *167*(4), pp.339–368.

Seo, S.Y., 2025. Taxonomic review of genus *Chelyosoma* (Phlebobranchia: Corellidae) from Korea. *Animal Systematics, Evolution and Diversity*, *41*(1), pp.89-94.

Setna, S.B., 1931. On three new gregarines, *Bhatiella morphysae*, n. g., n. sp., *Ferraria cornucephali*, n. g, n. sp., and *Extremocystis dendrostomi*, n. g., n. sp., from Indian polychaetes. *Records of the Zoological Survey of India*, pp.203–210.

Simdyanov, T.G., 2009. *Difficilina cerebratuli* gen. et sp. n. (Eugregarinida: Lecudinidae)—a

new gregarine species from the nemertean *Cerebratulus barentsi* (Nemertini: Cerebratulidae). *Parazitologiia, 43,* pp.273–287.

Simdyanov, T.G., and Kuvardina, O., 2007. Fine structure and putative feeding mechanism of the archigregarine *Selenidium orientale* (Apicomplexa: Gregarinomorpha). *European Journal of Protistology*, *43*(1), pp.17–25.

Simdyanov, T.G., Diakin, A.Y. and Aleoshin, V.V., 2015. Ultrastructure and 28S rDNA phylogeny of two gregarines: *Cephaloidophora* cf. *communis* and *Heliospora* cf. *longissima* with remarks on gregarine morphology and phylogenetic analysis. *Acta Protozoologica*, *54*, pp.241–262.

Simdyanov, T.G., Guillou, L., Diakin, A.Y., Mikhailov, K.V., Schrével, J. and Aleoshin, V.V., 2017. A new view on the morphology and phylogeny of eugregarines suggested by the evidence from the gregarine *Ancora sagittata* (Leuckart, 1860) Labbé, 1899 (Apicomplexa: Eugregarinida). *PeerJ*, *5*, p.e3354.

Simdyanov, T.G., Paskerova, G.G., Valigurová, A., Diakin, A., Kováčiková, M., Schrével, J., Guillou, L., Dobrovolskij, A.A. and Aleoshin, V.V., 2018. First ultrastructural and molecular phylogenetic evidence from the blastogregarines, an early branching lineage of plesiomorphic Apicomplexa. *Protist*, *169*(5), pp.697–726.

Sokolova, Y.Y., Paskerova, G.G., Rotari, Y.M., Nassonova, E.S. and Smirnov, A.V., 2013. Fine structure of *Metchnikovella incurvata* Caullery and Mesnil 1914 (Microsporidia), a hyperparasite of gregarines *Polyrhabdina* sp. from the polychaete *Pygospio elegans*. *Parasitology*, *140*(7), pp.855–867.

Sokolova, Y.Y., Paskerova, G.G., Rotari, Y.M., Nassonova, E.S. and Smirnov, A.V., 2014. Description of *Metchnikovella spiralis* sp. n. (Microsporidia: Metchnikovellidae), with notes on the ultrastructure of metchnikovellids. *Parasitology*, *141*(8), pp.1108–1122.

Stebbings, H., Boe, G.S. and Garlick, P.R., 1974. Microtubules and movement in the archigregarine, *Selenidium fallax*. *Cell and Tissue Research*, *148*, pp.331–345.

Takano, Y. and Horiguchi, T., 2005. Acquiring scanning electron microscopical, light microscopical and multiple gene sequence data from a single dinoflagellate cell. *Journal of Phycology*, *42*(1), pp.251–256.

Templeton, T.J. and Pain, A., 2016. Diversity of extracellular proteins during the transition from the 'proto-apicomplexan' alveolates to the apicomplexan obligate parasites. *Parasitology 143*, pp.1–17.

Théodoridès, J., 1984. The phylogeny of the Gregarinia (Sporozoa). *Origins of Life*, *13*, pp.339–342.

Théodorides, J. and Desportes, I., 1968. Sur trois Grégarines parasites d'Invertebrés marins. *Bulletin de l'Institut Océanographique de Monaco, 1387*, pp.1–11.

Tsugawa, H., 1944. Nihonsan tamourui ni kisei suru shinzokuchuurui ni tsuite (On eugregarine parasites of polychaetes from Japan). *Bulletin of the Faculty of Science Hiroshima University*, *6*, pp.218–230.

Valigurová, A. and Florent, I., 2021. Nutrient acquisition and attachment strategies in basal lineages: a tough nut to crack in the evolutionary puzzle of Apicomplexa. *Microorganisms*, *9*(7), p.1430.

Valigurová, A. and Koudela, B., 2005. Fine structure of trophozoites of the gregarine *Leidyana ephestiae* (Apicomplexa: Eugregarinida) parasitic in *Ephestia kuehniella* larvae (Lepidoptera). *European Journal of Protistology, 41*, pp.209–218.

Valigurová, A., Diakin, A., Seifertová, M., Vaškovicová, N., Kováčiková, M. and Paskerova, G.G., 2023. Dispersal and invasive stages of *Urospora* eugregarines (Apicomplexa) from brown bodies of a polychaete host. *Journal of Invertebrate Pathology*, *201*, p.107997.

Valigurová, A., Vaškovicova, N., Musilová, N. and Schrével, J., 2013. The enigma of eugregarine epicytic folds: where gliding motility originates? *Frontiers in Zoology*, *10*, p.e57.

Vivier, E., 1968. L'organisation ultrastructurale corticale de la gregarine *Lecudina pellucida*; ses

rapports avec l'alimentation et la locomotion. *Journal of Protozoology, 15,* pp.230–246.

Wakeman, K.C., 2020. Molecular phylogeny of marine gregarines (Apicomplexa) from the Sea of Japan and the Northwest Pacific including the description of three novel species of *Selenidium* and *Trollidium akkeshiense* n. gen. n. sp. *Protist, 171*(1), p.125710.

Wakeman, K.C. and Leander, B.S., 2012. Molecular phylogeny of Pacific archigregarines (Apicomplexa), including descriptions of *Veloxidium leptosynaptae* n. gen., n. sp., from the sea cucumber *Leptosynapta clarki* (Echinodermata), and two new species of *Selenidium*. *Journal of Eukaryotic Microbiology*, *59*, pp.232–245.

Wakeman, K.C. and Leander, B.S., 2013a. Identity of environmental DNA sequences using descriptions of four novel marine gregarine parasites, *Polyplicarium* n. gen. (Apicomplexa), from capitellid polychaetes. *Marine Biodiversity*, *43*, pp.133–147.

Wakeman, K.C. and Leander, B.S., 2013b. Molecular phylogeny of marine gregarine parasites (apicomplexa) from tube-forming polychaetes (Sabellariidae, Cirratulidae, and Serpulidae), including descriptions of two new species of *Selenidium*. *Journal of Eukaryotic Microbiology*, *60*(5), pp.514–525.

Wakeman, K.C., Heintzelman, M.B. and Leander, B.S., 2014a. Comparative ultrastructure and molecular phylogeny of *Selenidium melongena* n. sp. and *S. terebellae* Ray 1930 demonstrate niche partitioning in marine gregarine parasites (Apicomplexa). *Protist*, *165*(4), pp.493–511.

Wakeman, K.C., Hiruta, S., Kondo, Y. and Ohtsuka, S., 2021. Evidence for host jumping and diversification of marine cephaloidophorid gregarines (Apicomplexa) between two distantly related animals, viz., crustaceans and salps. *Protist, 172*, p.e125822.

Wakeman, K.C., Reimer, J.D., Jenke-Kodama, H. and Leander, B.S., 2014b. Molecular phylogeny and ultrastructure of *Caliculium glossobalani* n. gen. et sp. (Apicomplexa) from a Pacific *Glossobalanus minutus* (Hemichordata) confounds the relationships between marine and terrestrial gregarines. *Journal of Eukaryotic Microbiology, 61*(4),

pp.343–353.

Wakeman, K.C., Yabuki, A., Fujikura, K., Tomikawa, K. and Horiguchi, T., 2018. Molecular phylogeny and surface morphology of *Thiriotia hyperdolphinae* n. sp. and *Cephaloidophora oradareae* n. sp. (Gregarinasina, Apicomplexa) isolated from a deep sea *Oradarea* sp. (Amphipoda) in the West Pacific. *Journal of Eukaryotic Microbiology*, *65*(3), pp.372–381.

Watson, J.D. and Crick, F.H., 1953. Molecular structure of nucleic acids: a structure for deoxyribose nucleic acid. *Nature*, *171*(4356), pp.737–738.

Wolters, J., 1991. The troublesome parasites—molecular and morphological evidence that Apicomplexa belong to the dinoflagellate-ciliate clade. *Biosystems*, *25*(1-2), pp.75–83.

Wu, S., Xiong, J. and Yu, Y., 2015. Taxonomic resolutions based on 18S rRNA genes: a case study of subclass Copepoda. *PLOS ONE*, *10*(6), p.e0131498.

Yabe, I., Kawaguchi, Y., Wagawa, T. and Fujio, S., 2021. Anatomical study of Tsushima warm current system: determination of principal pathways and its variation. *Progress in Oceanography*, *194*, p.102590.

Yamaguchi, A. and Horiguchi, T., 2005. Molecular phylogenetic study of the heterotrophic dinoflagellate genus *Protoperidinium* (Dinophyceae) inferred from small subunit rRNA gene sequences. *Phycological Research*, *53*, pp.30–42.

Yasui, T., Abe, H., Hirawake, T., Sasaki, K.I. and Wakita, M., 2022. Seasonal pathways of the Tsugaru warm current revealed by high-frequency ocean radars. *Journal of Oceanography*, *78*(2), pp.103–119.

Zeng, L., Jacobs, M.W. and Swalla, B.J., 2006. Coloniality has evolved once in stolidobranch ascidians. *Integrative and Comparative Biology*, *46*(3), pp.255–268.

Zhadan, A., Stupnikova, A. and Neretina, T., 2015. Orbiniidae (Annelida: Errantia) from Lizard Island, Great Barrier Reef, Australia with notes on orbiniid phylogeny. *Zootaxa*, *4019*(1), pp.773–801.

FIGURES

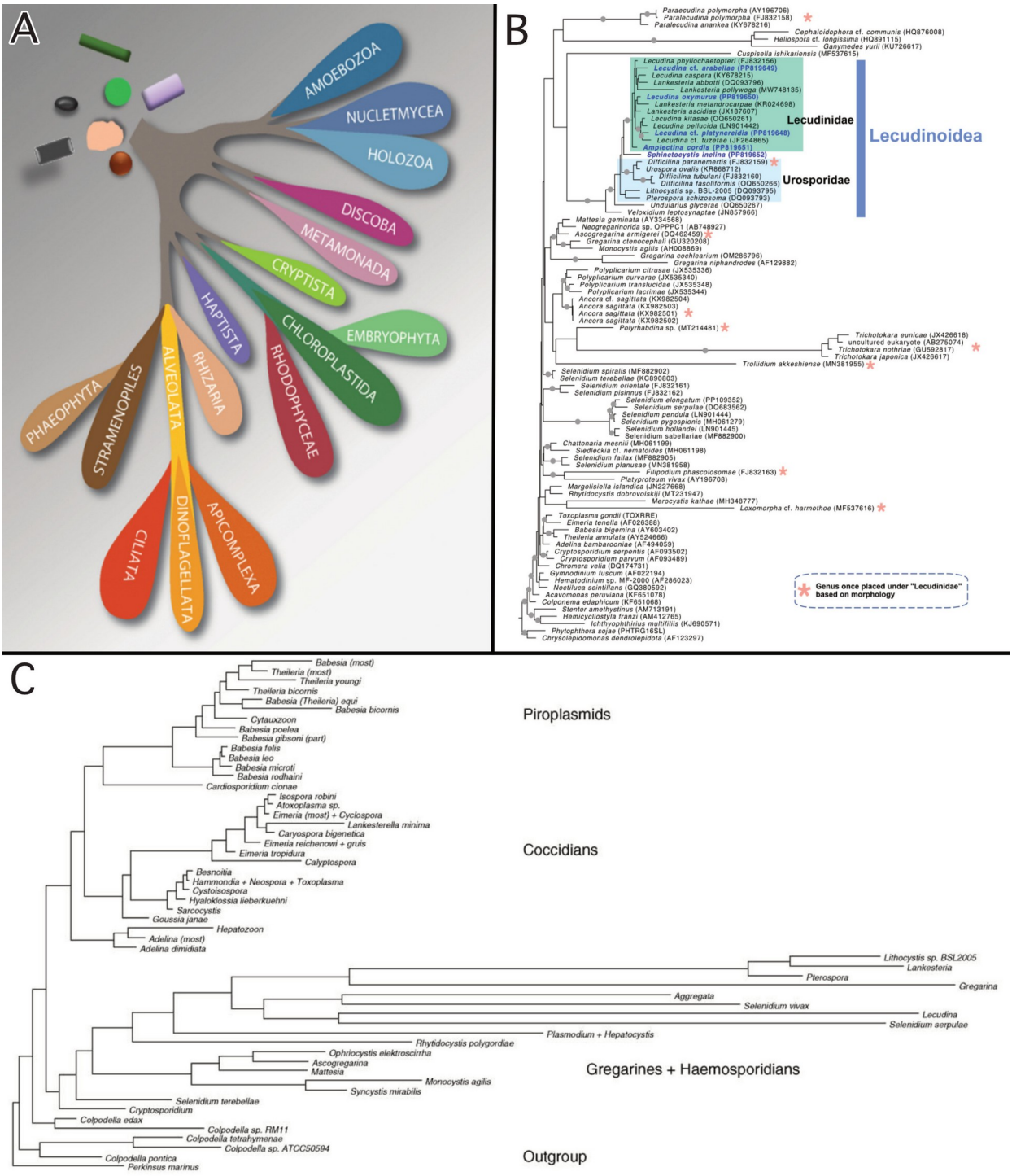

Figure 1.1. Prior phylogenetic analyses of apicomplexan molecular data. (A) Generalized tree of protists placing Apicomplexa as a distinct alveolate lineage. Image modified from Adl et al. (2019). **(B)** Maximum Likelihood (ML) tree focusing on lecudinid marine gregarines. Image modified from Park and Leander (2024a). **(C)** A more general ML tree showing the relative evolutionary positions of piroplasmids, coccidians, haemosporidians, and gregarines. Image modified from Morrison, 2009.

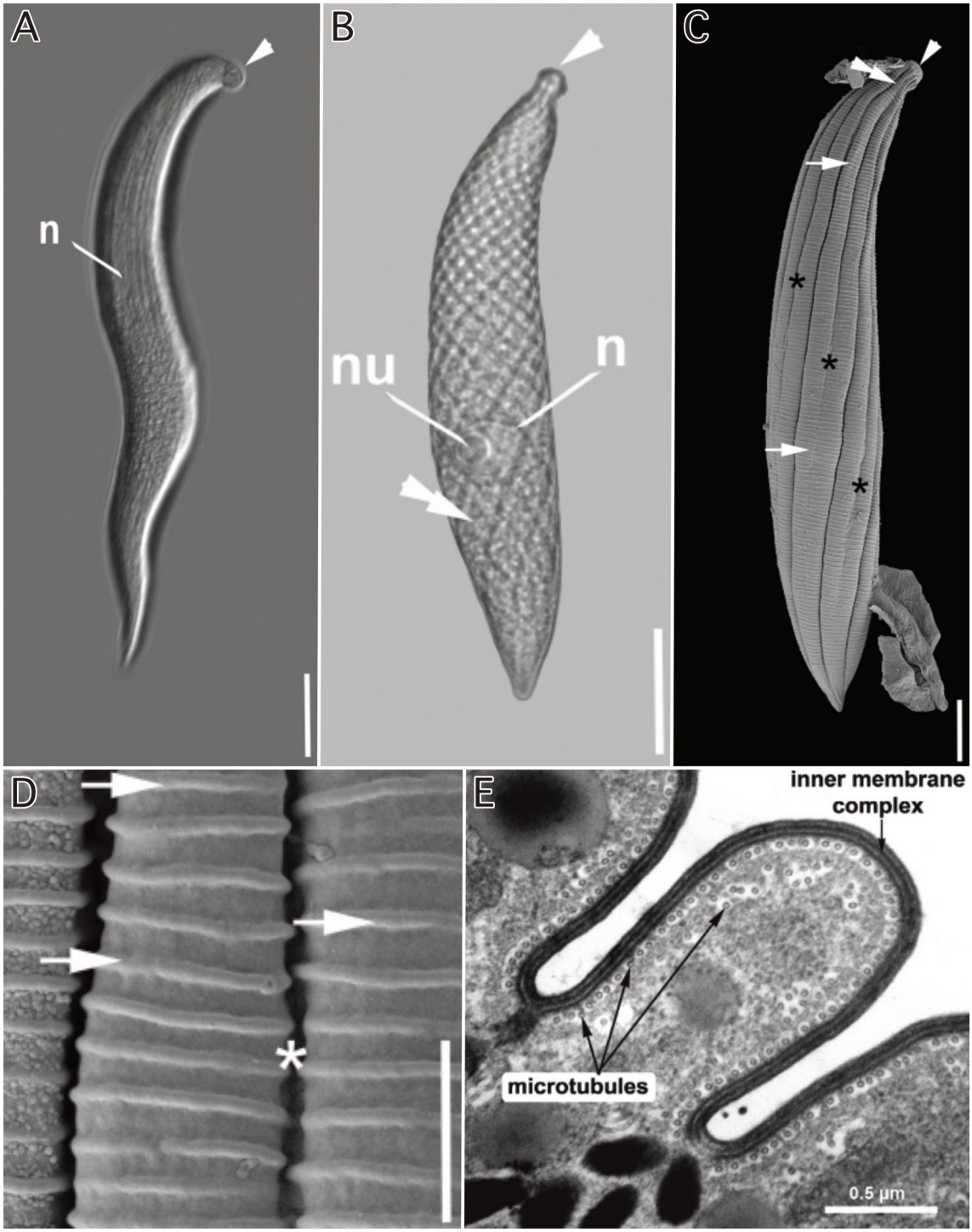

Figure 1.2. Examples of morphological diversity observed among archigregarines. (A) Light microscopy image of vermiform *Selenidium* trophozoite with labeled nucleus (n) and visible mucron (white arrowhead). Scale bar = 20 µm. Image modified from Rueckert and Horák (2017). **(B)** Light microscopy image of *Selenidium* trophozoite with labeled nucleus (n), nucleolus (nu), mucron (white arrowhead), and epicytic folds (double arrowhead). Scale bar = 25 µm. Image modified from Rueckert et al., 2017. **(C)** Scanning electron micrograph (SEM) image of *Selenidium* trophozoite with visible mucron (white arrowhead), broad epicytic folds (white arrows) and fold grooves (asterisks). Scale bar = 10 µm. Image modified from Rueckert and Horák (2017). **(D)** An SEM image showing transverse epicytic folds on a *Selenidium* trophozoite (white arrows) and deep inter-fold grooves (asterisk). Scale bar = 2 µm. Image modified from Rueckert and Horák (2017). **(E)** Transmission electron microscopy image of inner membrane complex and underlying microtubule network within *Selenidium* isolate. Image modified from Leander (2008) (originally from Leander (2007)).

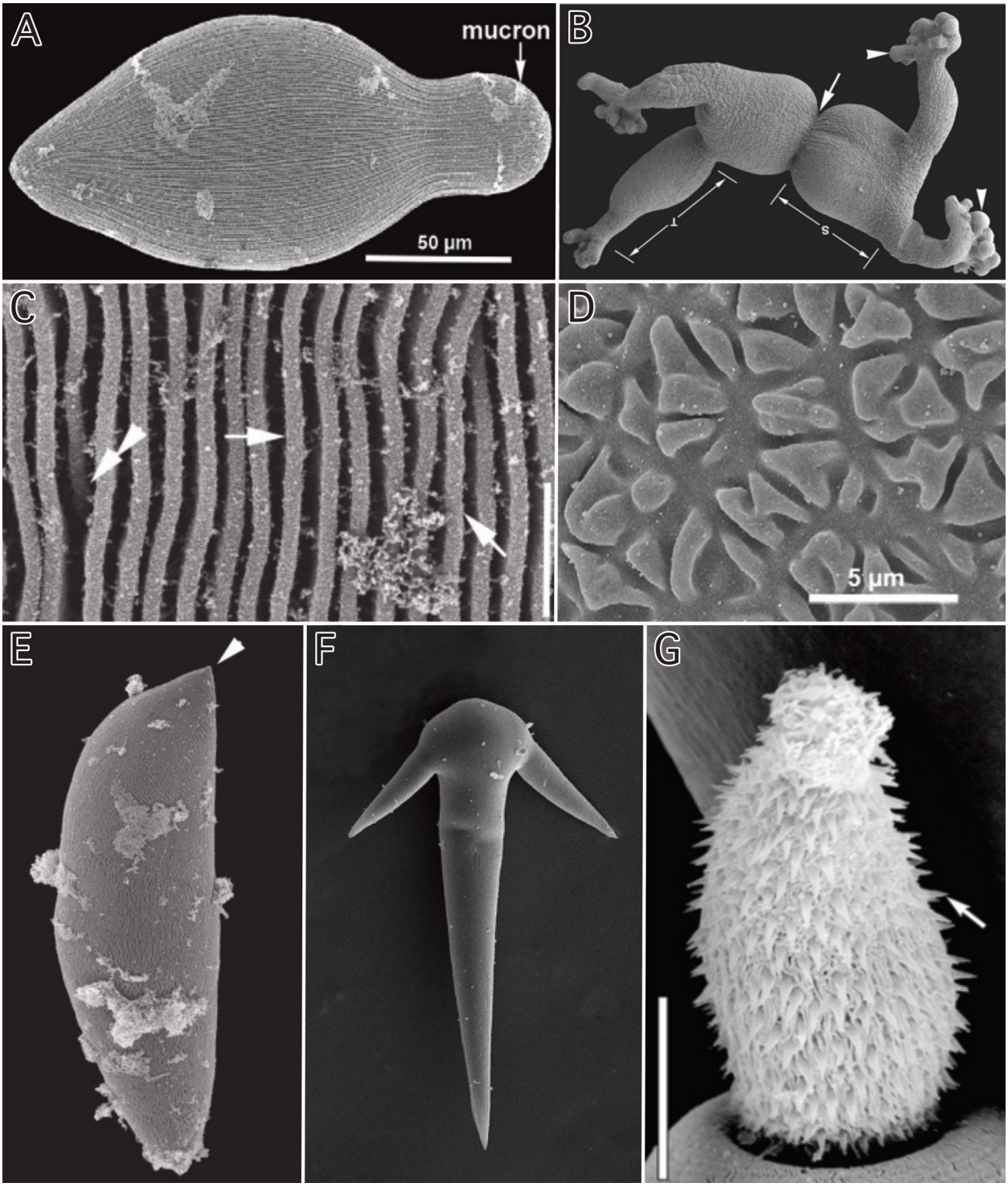

Figure 1.3. Examples of morphological diversity observed among eugregarines. (A) Whole cell scanning electron microscopy (SEM) image of *Lecudina* cf. *tuzetae* trophozoite with mucron (white arrow). Image modified from Leander (2008). **(B)** An SEM image of two *Pterospora* trophozoites in syzygy (white arrow). Branching digits indicated by white arrowhead. Image modified from Landers and Leander (2005). **(C)** High-magnification SEM image of dense longitudinal epicytic folds. Single fold indicated by white arrows. Early terminating fold indicated by double white arrowhead. Scale bar = 1 µm. Image modified from Rueckert et al. (2015). **(D)** High-magnification SEM image of *Pterospora* cell surface showing crenulations. Image modified from Landers and Leander (2005). **(E)** An SEM image of *Lankesteria* trophozoite with pointed mucron (white arrowhead). Image modified from Rueckert et al. (2015). **(F)** An SEM image of anchor-like *Ancora* cell anterior. Image modified from Simdyanov et al. (2017). **(G)** High-magnification SEM image of *Cuspisella* mucron with extended attachment organ (white arrow). Scale bar = 20 µm. Image modified from Iritani et al. (2018a).

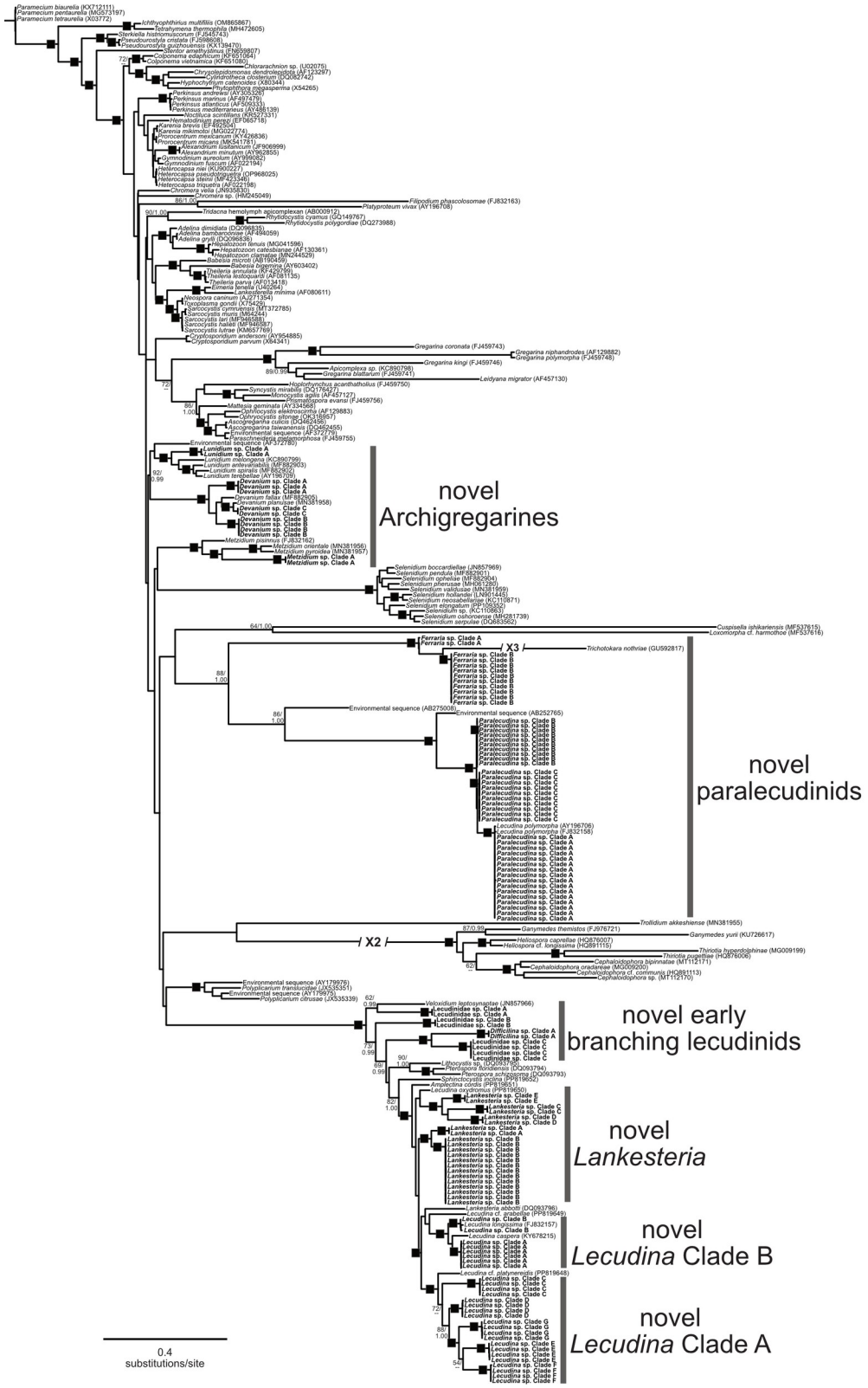

Figure 1.4. Maximum-Likelihood (ML) marine gregarine tree inferred from small subunit 18S (and some concatenated 18S+ITS) rRNA gene sequences. Bootstrap values >50 and Bayesian Posterior Probabilities (PP) >0.95 are shown adjacent to nodes (ML/PP). Black squares indicate statistical support ≥95/0.99. Scale bar represents the inferred evolutionary distance as a rate of base substitutions per site. Gregarine groups explored in this project are labeled with vertical gray bars. Novel sequences presented in this study are written in bold text.

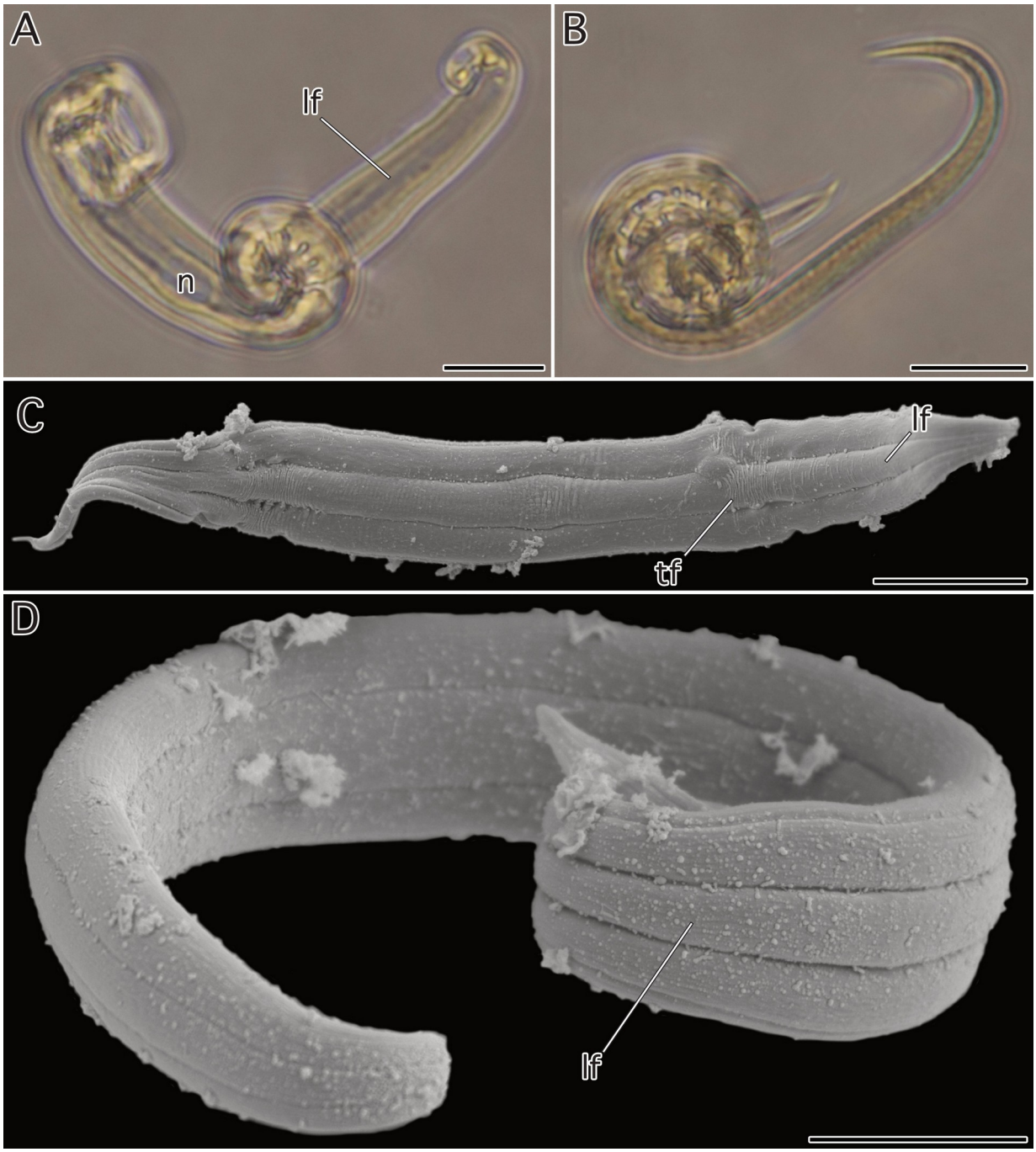

Figure 2.1. Light and electron micrographs of *Lunidium* sp. Clade A isolates. (A–B) Light micrograph showing a nucleus (n), lateral fold (lf), and a view of the broad **(A)** and narrow **(B)** aspects of the cell. **(C)** Scanning electron microscopy (SEM) image showing general trophozoite morphology, longitudinal folds (lf), and transverse folds (tf). **(D)** SEM image showing curled state and broad longitudinal folds (lf) with a low density. Scale bars: A–D = 20 µm.

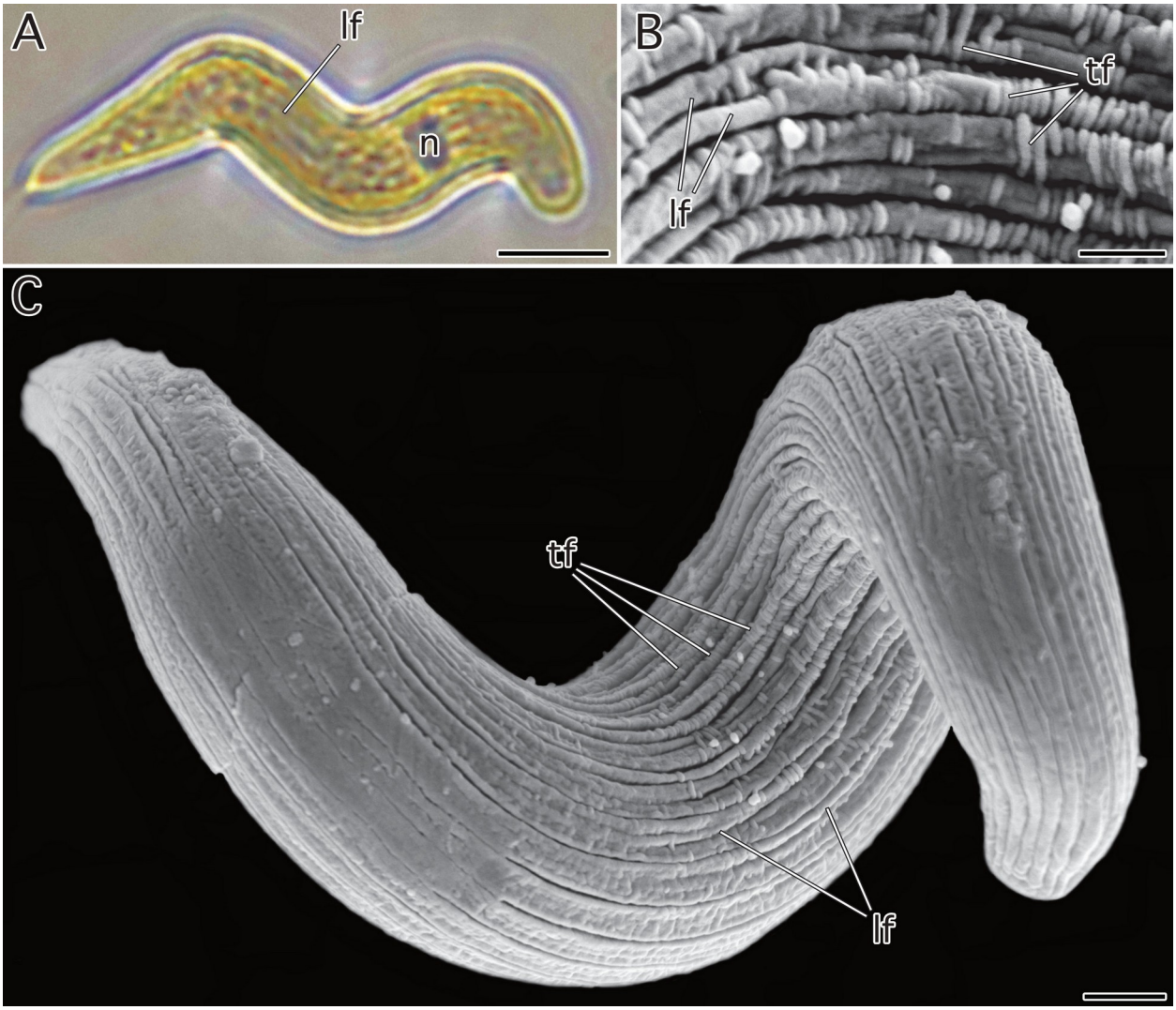

Figure 2.2. Light and electron micrographs of *Metzidium* sp. Clade A isolates. Anterior ends (mucrons) are oriented to the right. **(A)** Light micrograph showing a nucleus (n) and longitudinal fold (lf). **(B)** Scanning electron microscopy (SEM) image of trophozoite surface, showing longitudinal folds (lf) with density of 1.2 folds/µm as well as transverse (tf) epicytic folds. **(C)** SEM image showing general trophozoite morphology, longitudinal folds (lf), and transverse folds (tf). Scale bars: A = 10 µm; B = 2 µm; C = 5 µm.

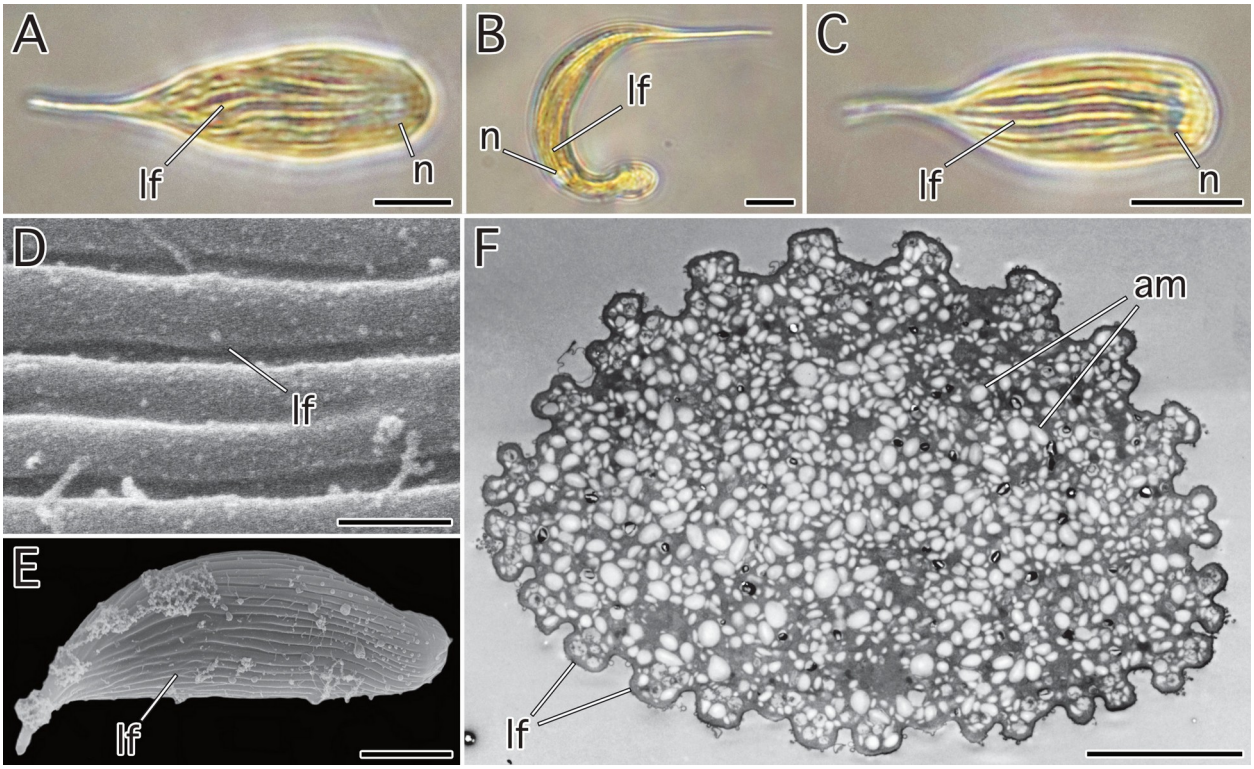

Figure 2.3. Light and electron micrographs of *Devanium* sp. Clade A isolates. Anterior ends (mucrons) are oriented to the right. **(A–C)** Light micrographs showing the nucleus (n) and longitudinal folds (lf). **(D)** Scanning electron microscopy (SEM) image showing detailed view of longitudinal folds (lf) with density of 1.1 folds/µm. **(E)** SEM image showing general trophozoite morphology and longitudinal folds (lf). **(F)** Transmission electron microscopy (TEM) cross-section showing elliptical section with longitudinal folds (lf) and numerous amylopectin granules (am). Scale bars: A–C = 20 µm; D = 1 µm; E–F = 10 µm.

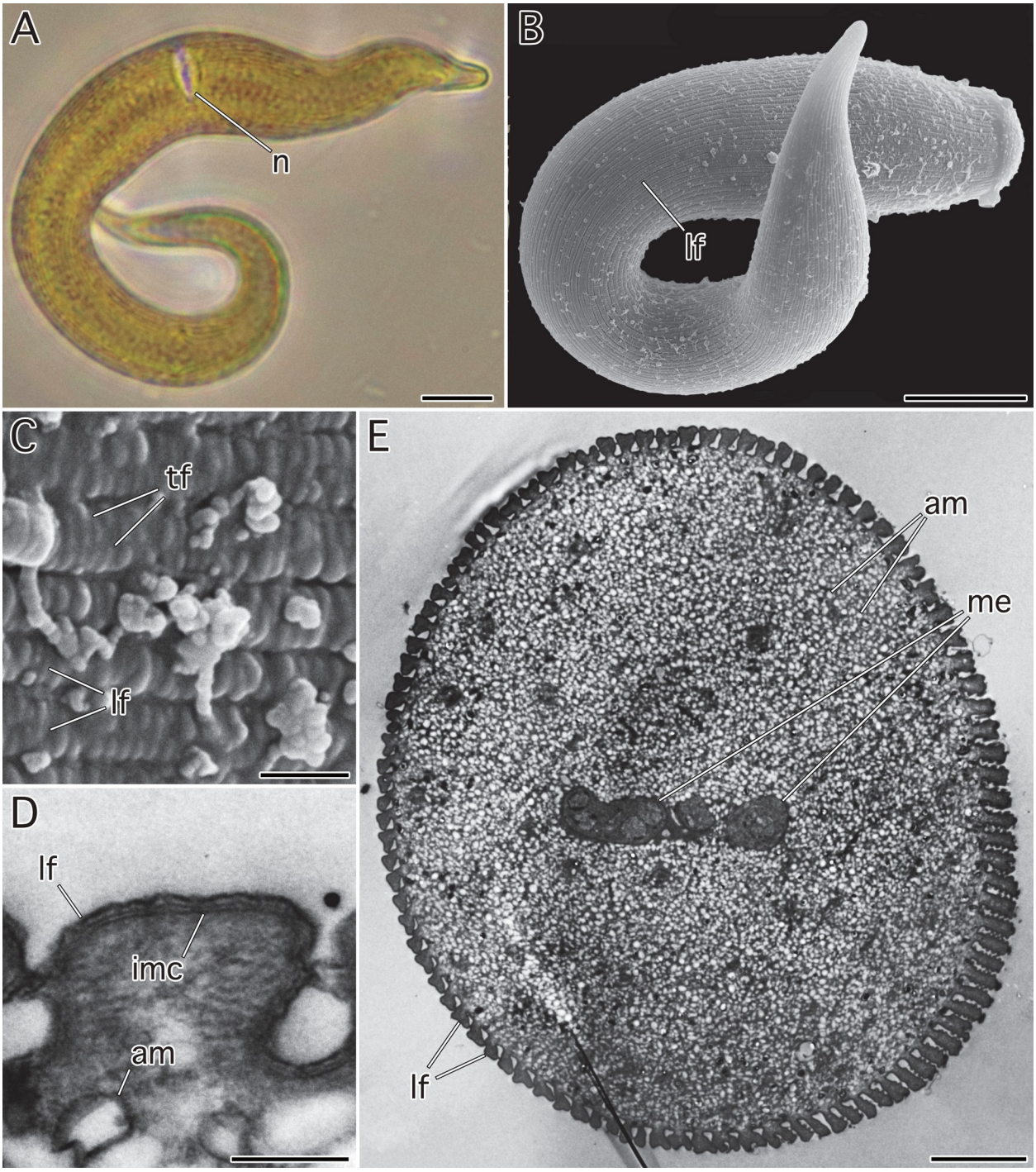

Figure 2.4. Light and electron micrographs of *Devanium* sp. Clade B isolates. Anterior ends (mucrons) are oriented to the right. **(A)** Light micrograph showing nucleus (n). **(B)** Scanning electron microscopy (SEM) image showing general trophozoite morphology and longitudinal folds (lf). **(C)** SEM image showing detailed view of transverse folds (tf) and longitudinal folds (lf) with density of 1.7 folds/µm. **(D)** High-magnification transmission electron microscopy (TEM) image of longitudinal epicytic folds, with visible amylopectin granule (am), longitudinal fold (lf), and inner membrane complex (imc). **(E)** Circular TEM cross-section showing longitudinal folds (lf), numerous amylopectin granules (am), and metchnikovellid hyperparasite infection (me). Scale bars: A–B = 20 µm; C = 1 µm; D = 500 nm; E = 5 µm.

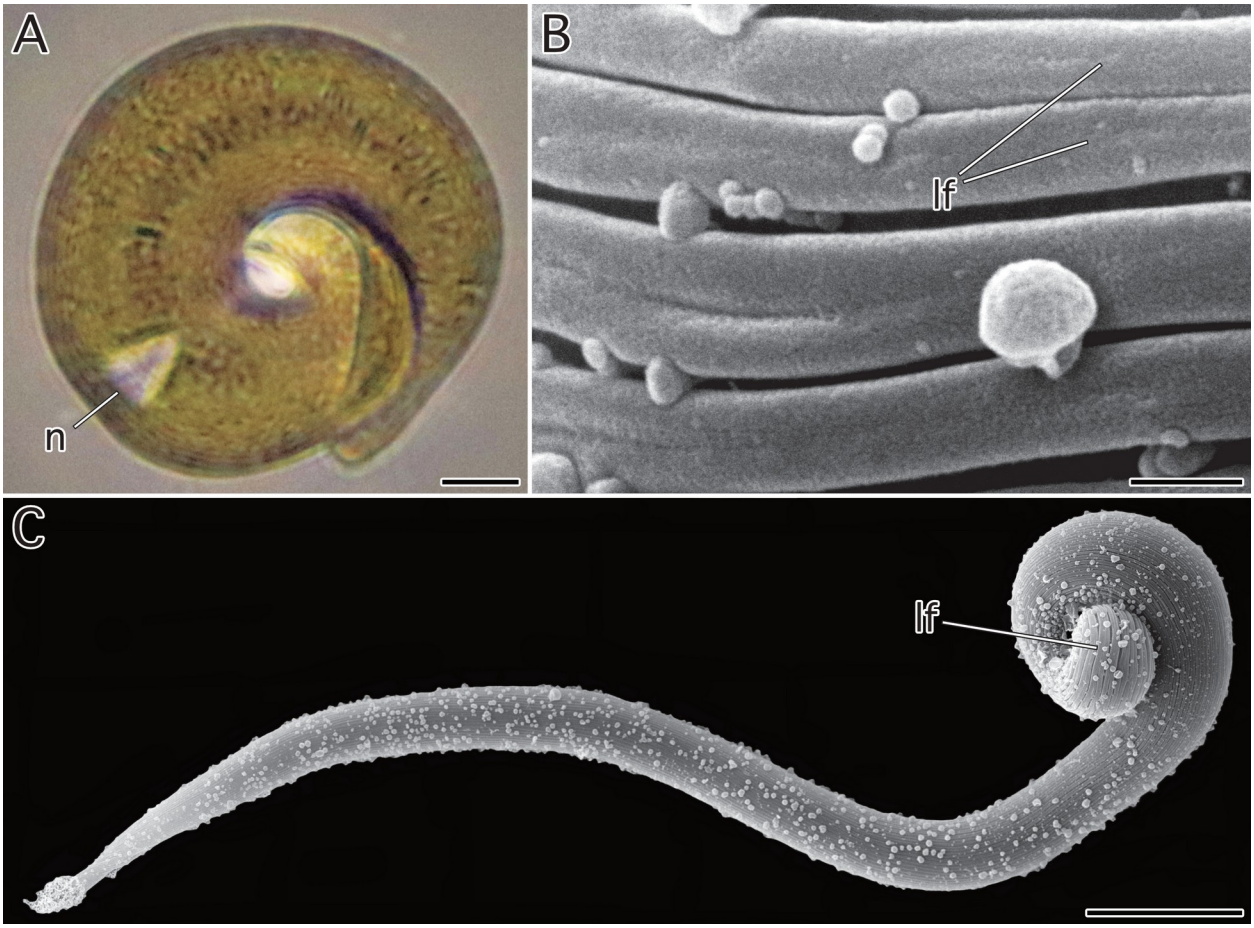

Figure 2.5. Light and electron micrographs of *Devanium* sp. Clade C isolates. (A) Light micrograph showing nucleus (n). **(B)** Scanning electron microscopy (SEM) image of trophozoite surface, showing longitudinal folds (lf) with density of 1.4 folds/µm. **(C)** Whole-body SEM image showing general trophozoite morphology and longitudinal folds (lf). Scale bars: A = 10 µm; B = 1 µm; C = 20 µm.

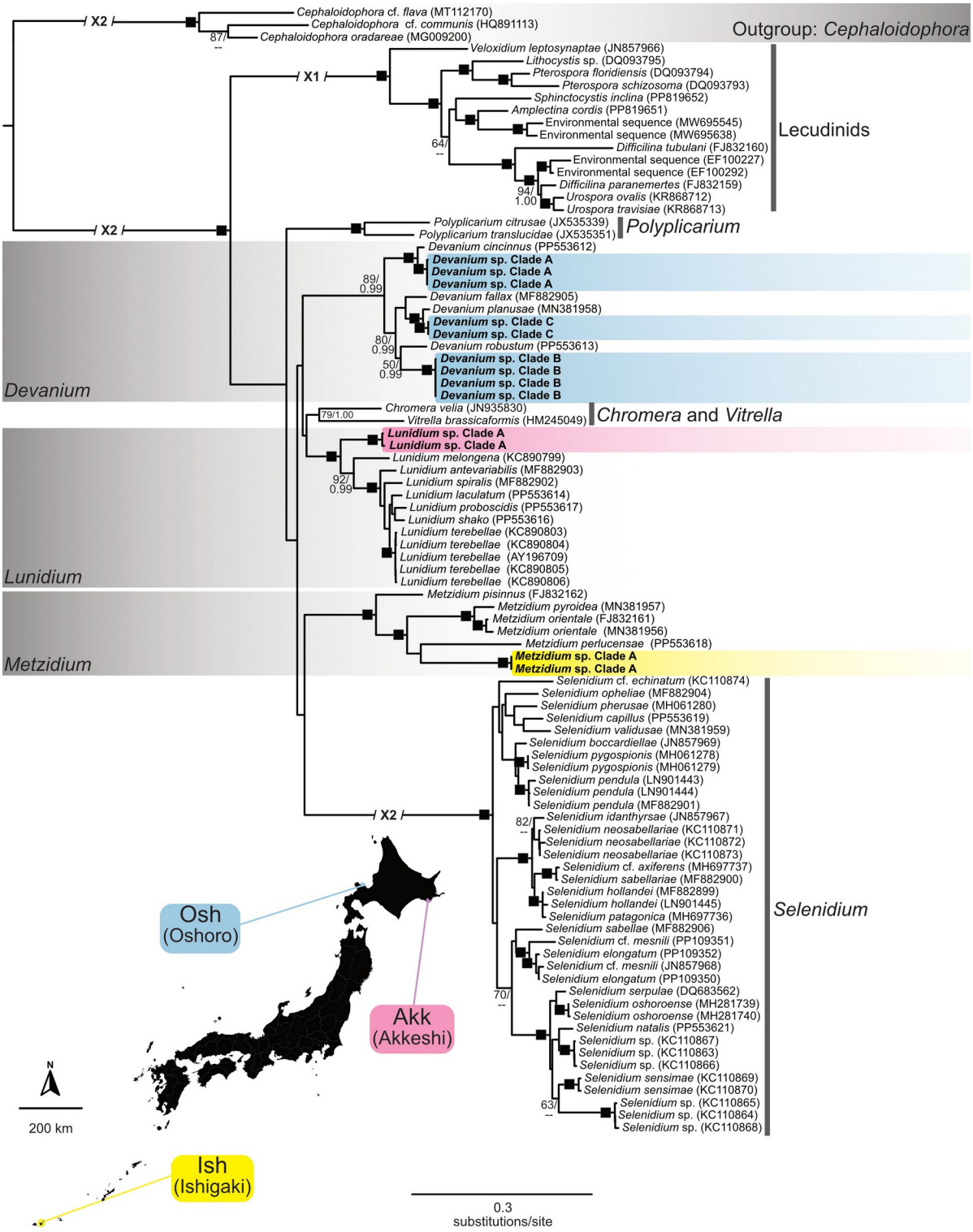

Figure 2.6. Maximum-Likelihood (ML) marine gregarine tree inferred from 18S rRNA gene sequences. *Lunidium* sp. Clade A sequences include concatenated ITS region. Bootstrap values >50 and Bayesian Posterior Probabilities (PP) >0.95 are shown adjacent to nodes (ML/PP). Black squares indicate statistical support ≥95/0.99. Scale bar represents the inferred evolutionary distance as a rate of base substitutions per site. Clades containing novel molecular data are colored to indicate locality. Novel sequences presented in this study are written in bold text.

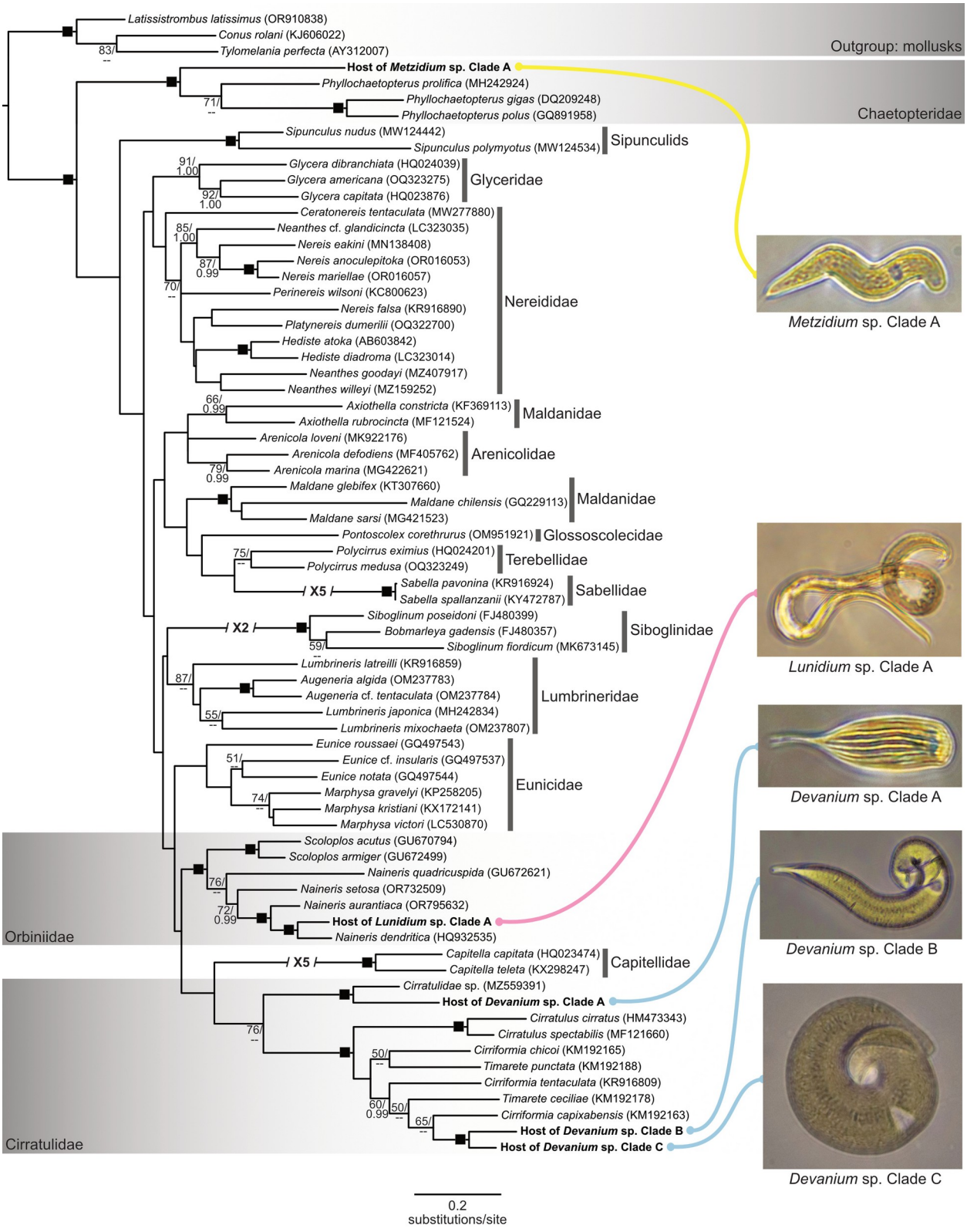

Figure 2.7. Maximum-Likelihood (ML) polychaete host tree inferred from COI gene sequences. Bootstrap values >50 and Bayesian Posterior Probabilities (PP) >0.95 are shown adjacent to nodes (ML/PP). Scale bar represents the inferred evolutionary distance as a rate of base substitutions per site. Host sequences are colored to distinguish locality. Novel sequences presented in this study are written in bold text.

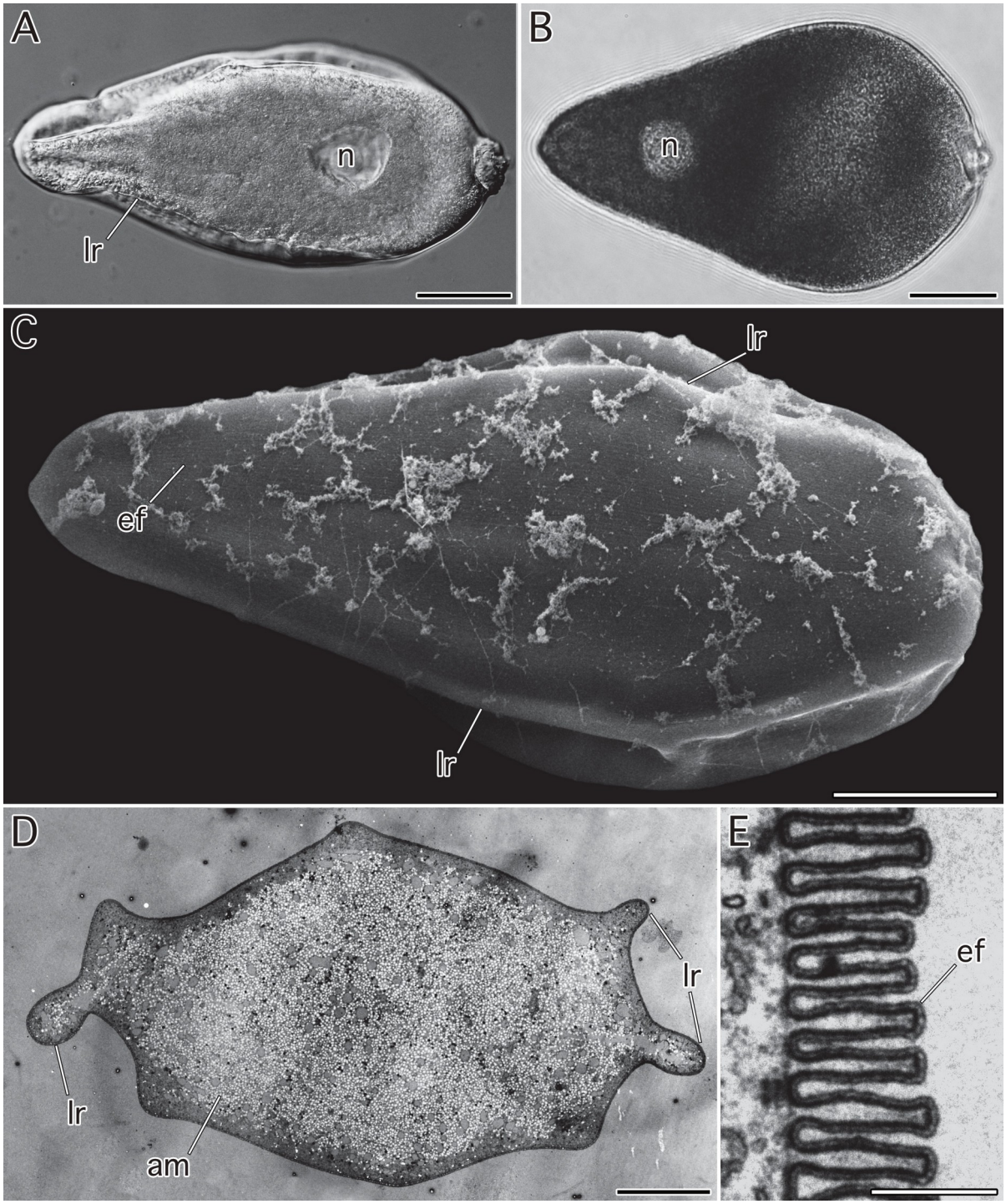

Figure 3.1. Light and electron micrographs of *Ferraria* sp. Clade A isolates. Anterior ends (mucrons) are oriented to the right. **(A)** Differential interference contrast (DIC) micrograph showing nucleus (n) and longitudinal ridge (lr). **(B)** Light micrograph showing the nucleus (n). **(C)** Scanning electron microscopy image showing general trophozoite morphology, epicytic folds (ef), and longitudinal ridges (lr). **(D)** Transmission electron microscopy (TEM) cross-section showing longitudinal ridges (lr) and numerous amylopectin granules (am). **(E)** High-magnification TEM image showing epicytic folds (ef) with density of 6 folds/µm. Scale bars: A–C = 50 µm; D = 20 µm; E = 500 nm.

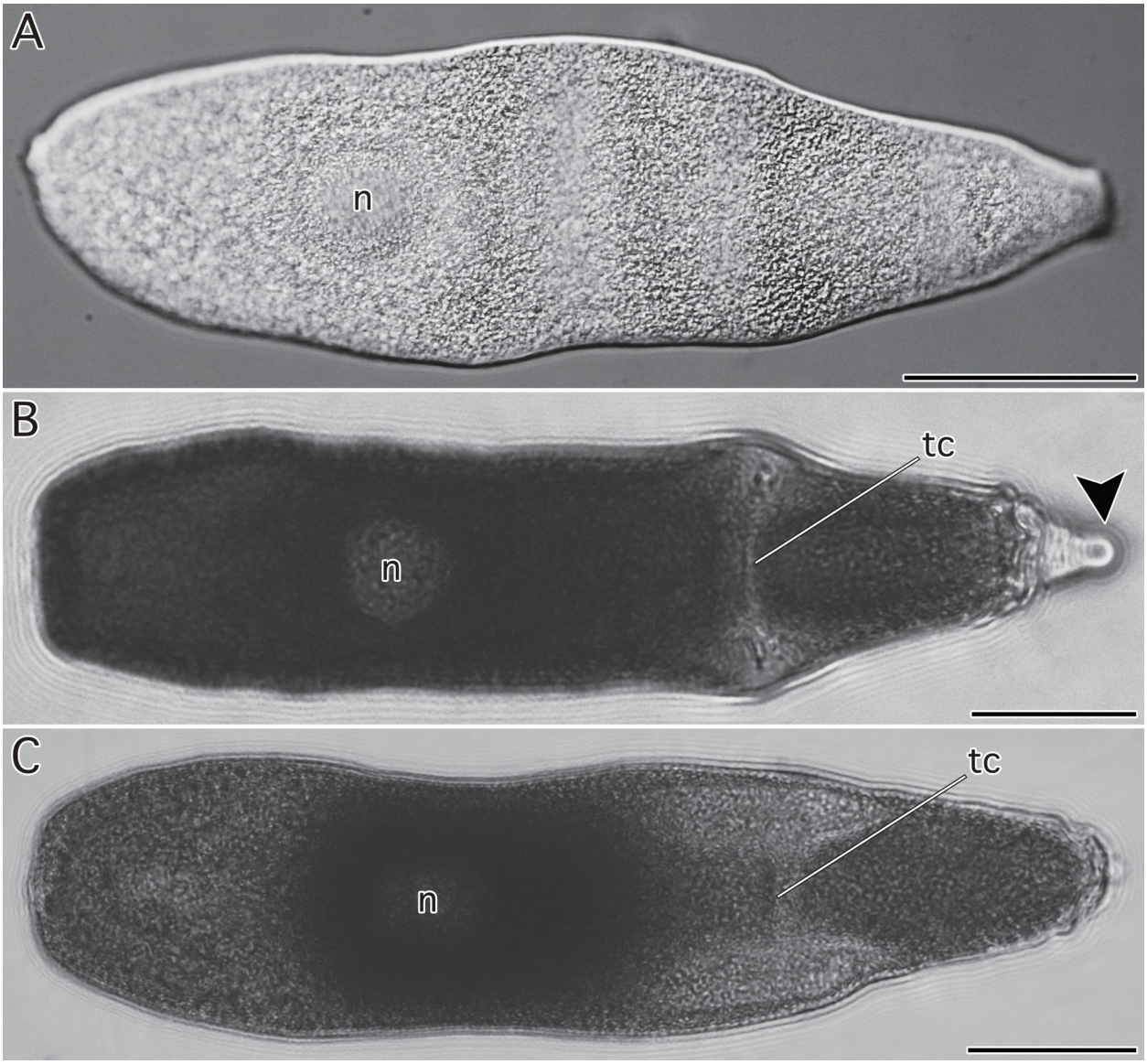

Figure 3.2. Light micrographs of *Ferraria* sp. Clade B. Anterior ends (mucrons) are oriented to the right. **(A)** Differential interference contrast (DIC) micrograph showing the nucleus (n). **(B)** Light micrograph showing nucleus (n), transverse crease (tc), and extended mucron (black arrow). **(C)** Light micrograph showing nucleus (n) and transverse crease (tc). Scale bars: A–C = 100 µm.

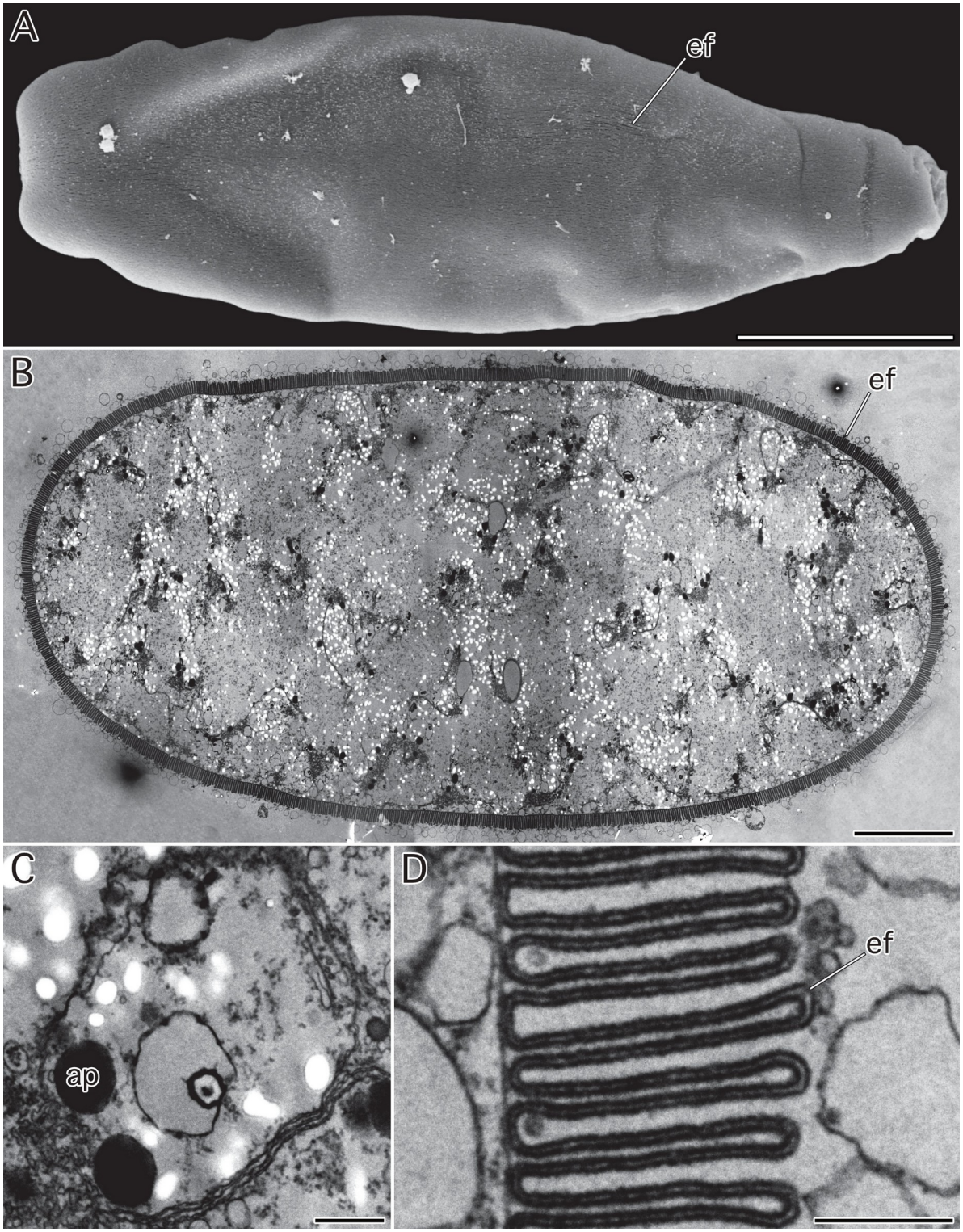

Figure 3.3. Electron micrographs of *Ferraria* sp. Clade B. Anterior ends (mucrons) are oriented to the right. **(A)** Scanning electron microscopy image showing general trophozoite morphology and epicytic folds (ef). **(B)** Transmission electron microscopy (TEM) cross-section showing the elliptical shape of the trophozoite and epicytic folds (ef). **(C)** High-magnification TEM image showing putative apicoplast (ap). **(D)** High-magnification TEM image showing epicytic folds (ef) with density of 6 folds/µm. Scale bars: A = 100 µm; B = 10 µm; C–D = 500 nm.

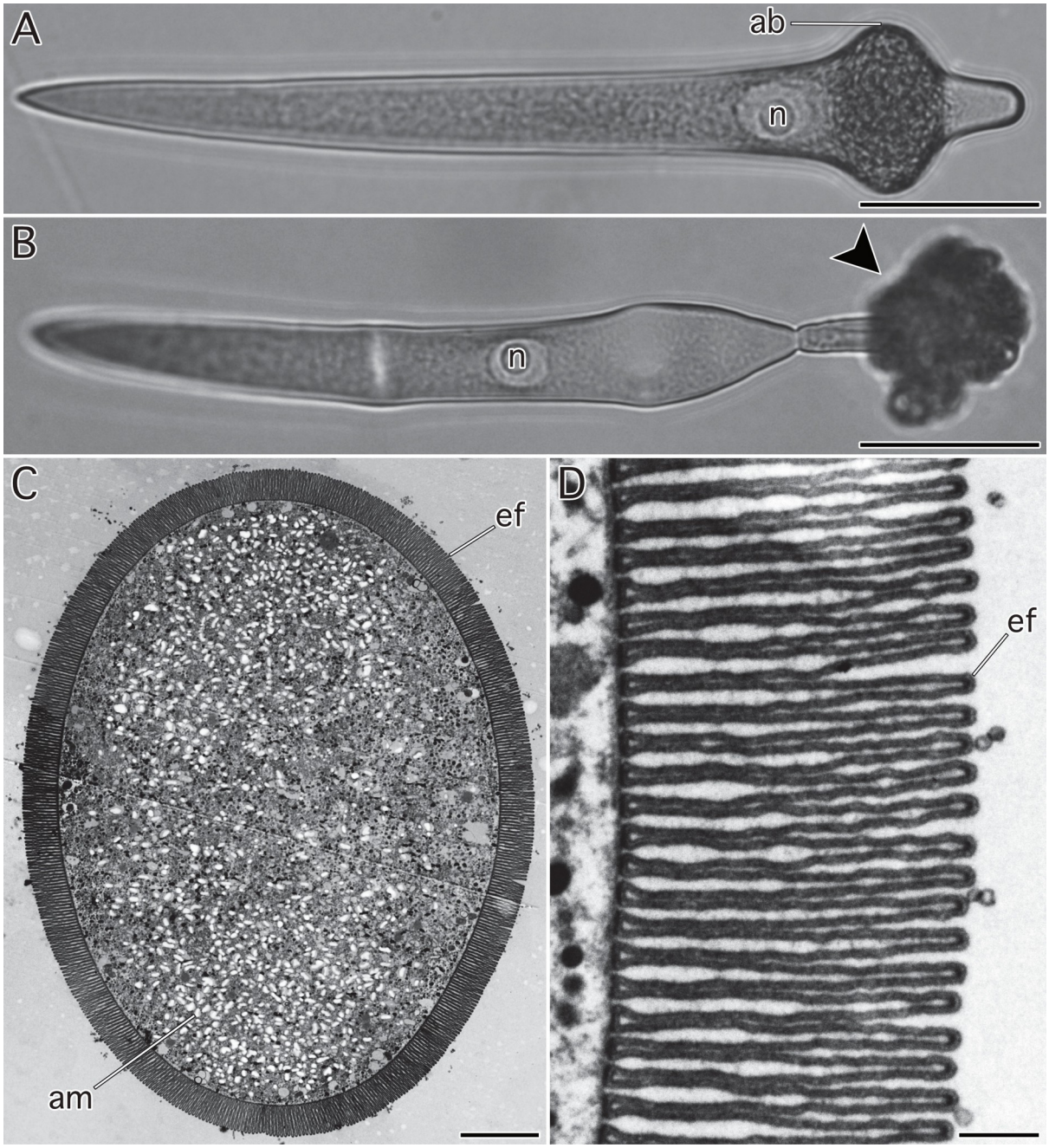

Figure 3.4. Light and transmission electron micrographs of *Paralecudina* sp. Clade A. Anterior ends (mucrons) are oriented to the right. **(A)** Light micrograph showing nucleus (n) and anterior bulge (ab). **(B)** Light micrograph showing nucleus (n) and extended mucron (black arrow). **(C)** Transmission electron micrograph (TEM) cross-section showing the elliptical shape of the trophozoite, epicytic folds (ef), and amylopectin granules (am). **(D)** High-magnification TEM image showing epicytic folds (ef) with density of 5 folds/µm. Scale bars: A–B = 100 µm; C = 5 µm; D = 500 nm.

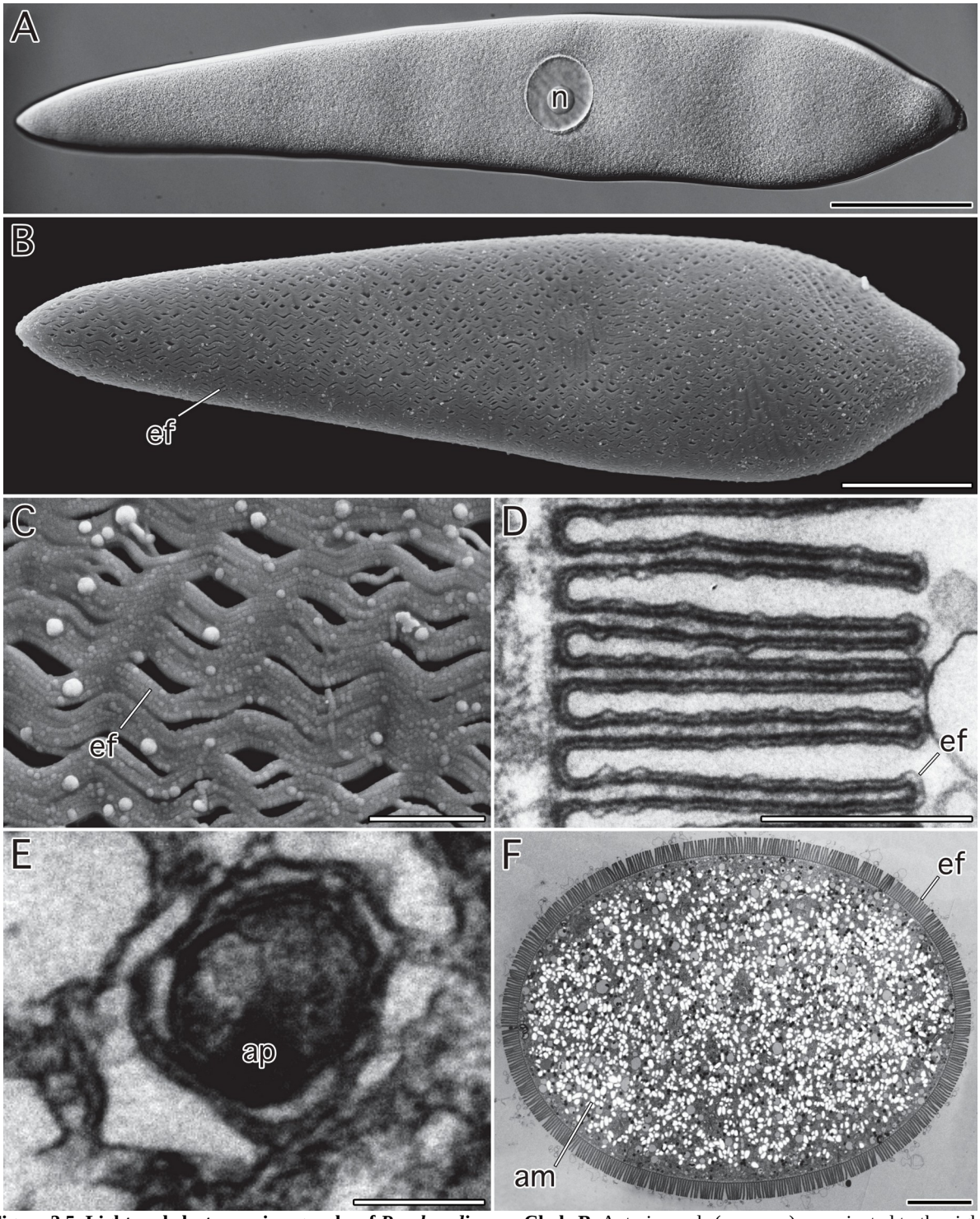

Figure 3.5. Light and electron micrographs of *Paralecudina* sp. Clade B. Anterior ends (mucrons) are oriented to the right. **(A)** Differential interference contrast (DIC) micrograph showing the nucleus (n). **(B)** Scanning electron microscopy (SEM) image showing general trophozoite morphology and epicytic folds (ef). **(C)** High-magnification SEM image showing epicytic folds (ef). **(D)** Transmission electron micrograph (TEM) image showing epicytic folds (ef) with density of 6 folds/µm. **(E)** High-magnification TEM image showing putative apicoplast (ap). **(F)** A TEM cross-section showing the ellipsoid shape of the trophozoite, epicytic folds (ef), and numerous amylopectin granules (am). Scale bars: A–B = 50 µm; C = 5 µm; D = 500 nm; E = 250 nm; F = 3 µm.

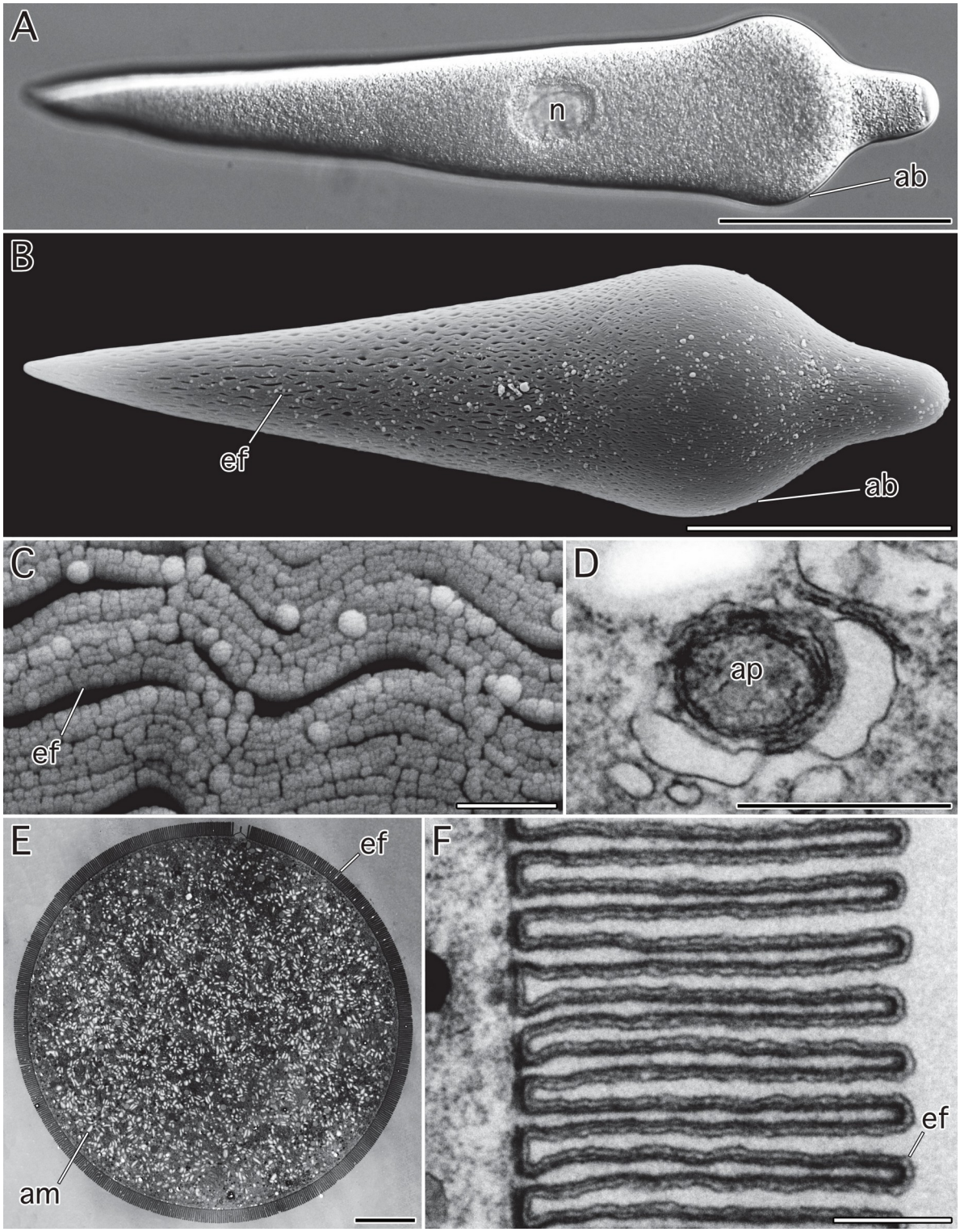

Figure 3.6. Light and electron micrographs of *Paralecudina* sp. Clade C. Anterior ends (mucrons) are oriented to the right. **(A)** Differential interference contrast (DIC) micrograph showing nucleus (n) and anterior bulge (ab). **(B)** Scanning electron microscopy (SEM) image showing general trophozoite morphology, epicytic folds (ef), and anterior bulge (ab). **(C**) High-magnification SEM image showing epicytic folds (ef). (**D)** High-magnification transmission electron microscopy (TEM) image showing putative apicoplast (ap). **(E)** A TEM cross-section showing the circular shape of the trophozoite, epicytic folds (ef), and numerous amylopectin granules (am). **(F)** High-magnification TEM image showing epicytic folds (ef) with density of 5 folds/µm. Scale bars: A–B = 50 µm; C = 1 µm; D = 500 nm; E = 5 µm; F = 500 nm.

Figure 3.7. Maximum-Likelihood (ML) marine gregarine tree inferred from concatenated small subunit 18S and ITS rRNA gene sequences. Bootstrap values >50 and Bayesian Posterior Probabilities (PP) >0.95 are shown adjacent to nodes (ML/PP). Black squares indicate statistical support ≥95/0.99. Scale bar represents the inferred evolutionary distance as a rate of base substitutions per site. Clades containing novel molecular data are colored to indicate locality. Novel sequences presented in this study are written in bold text.

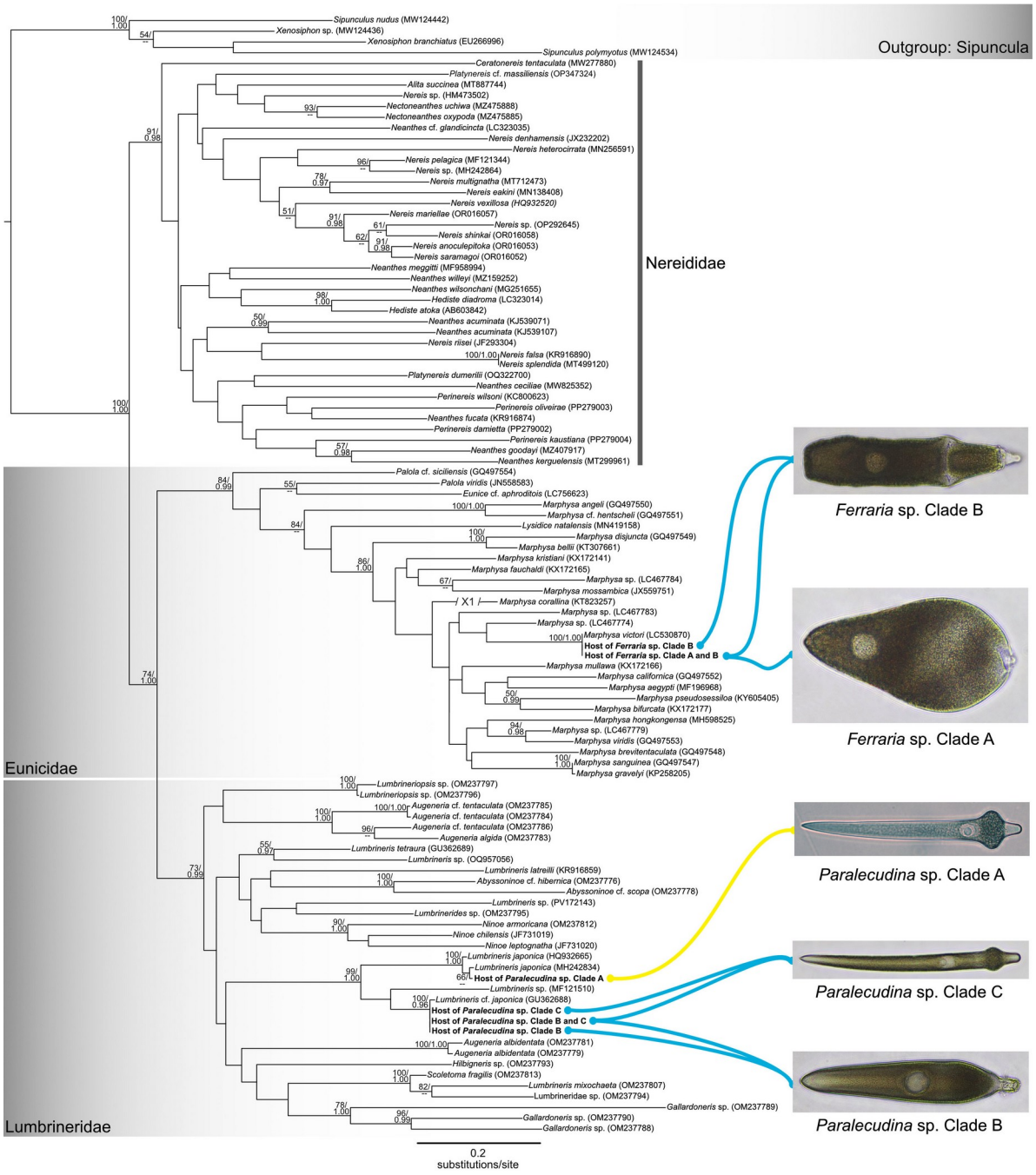

Figure 3.8. Maximum-Likelihood (ML) polychaete host tree inferred from COI gene sequences. Bootstrap values >50 and Bayesian Posterior Probabilities (PP) >0.95 are shown adjacent to nodes (ML/PP). Scale bar represents the inferred evolutionary distance as a rate of base substitutions per site. Host sequences are colored to distinguish locality. Novel sequences presented in this study are written in bold text.

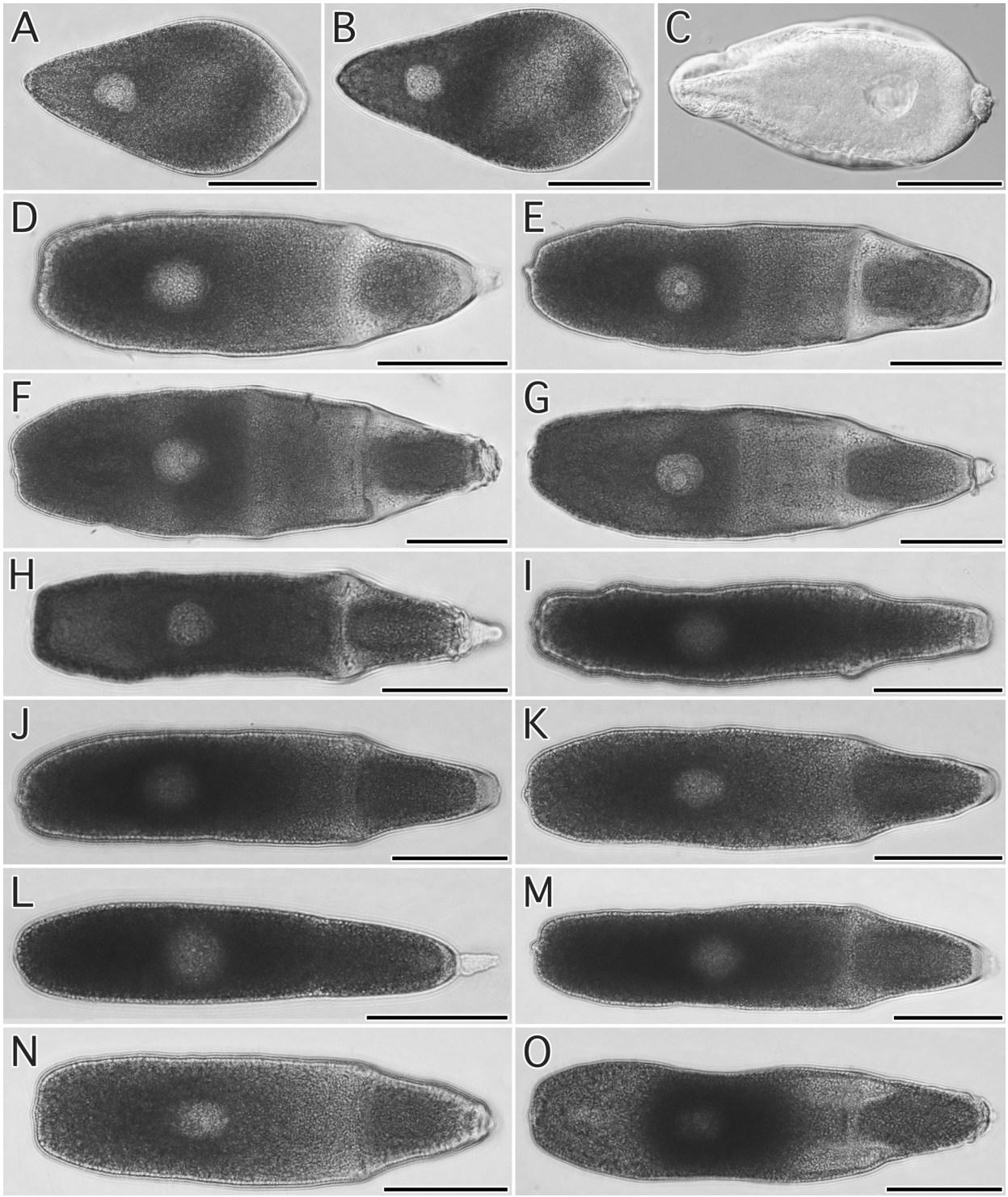

Figure 3.9. Visual comparison of *Ferraria* isolates (scale bars: 100 µm). **(A–C)** *Ferraria* sp. Clade A **(D–O)** *Ferraria* sp. Clade B.

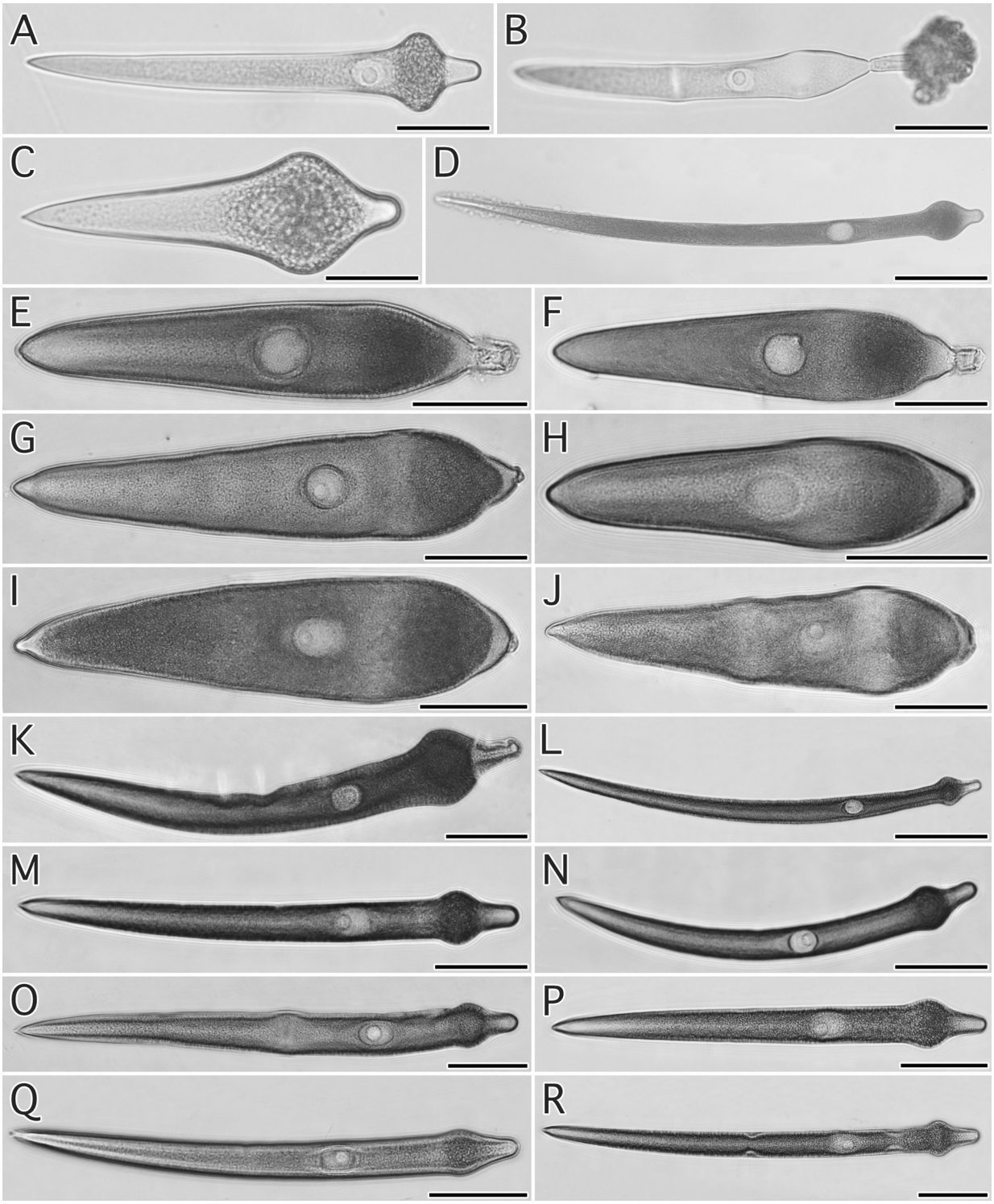

Figure 3.10. Visual comparison of *Paralecudina* isolates (scale bars A–N: 100 µm, scale bars O–R: 100 µm). **(A–D)** *Paralecudina* sp. Clade A **(E–J)** *Paralecudina* sp. Clade B **(K–R)** *Paralecudina* sp. Clade C

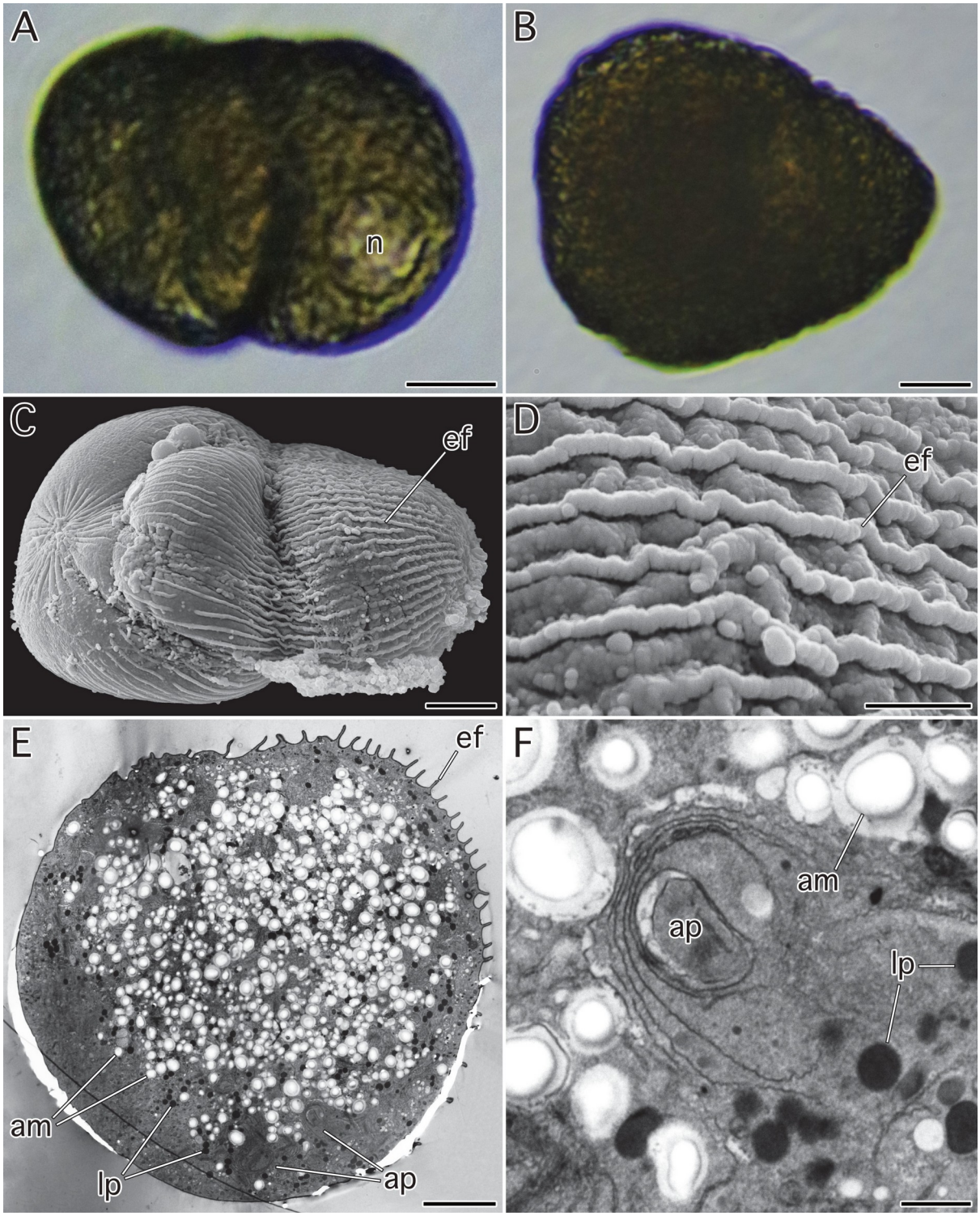

Figure 4.1. Light and electron micrographs of Lecudinidae sp. Clade A. (A–B) Light micrograph showing nucleus (n) and general bean-like morphology. **(C)** Scanning electron microscopy (SEM) image showing general trophozoite morphology and epicytic folds (ef). **(D**) High-magnification SEM image showing epicytic folds (ef) with a density of 1.5 folds/µm. **(E)** Transmision electron microscopy (TEM) image showing round cellular cross-section with visible epicytic fold (ef), amylopectin granules (am), lipid droplets (lp), and putative apicoplast (ap). **(F)** High-magnification TEM cross-section showing amylopectin granules (am), lipid droplets (lp), and putative apicoplast (ap). Scale bars: A–B = 20 µm; C = 10 µm; D = 2 µm; E = 5 µm; F = 1 µm.

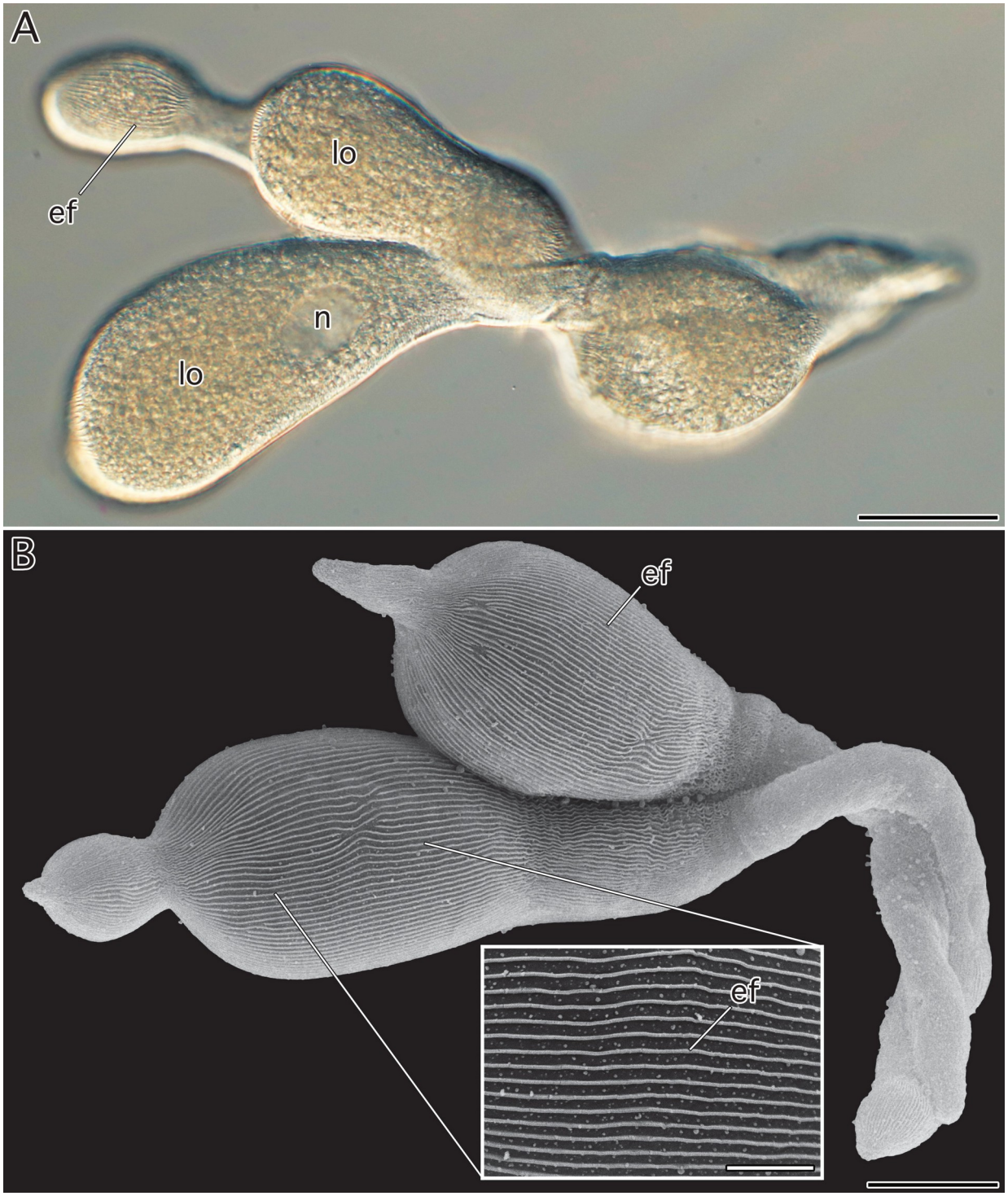

Figure 4.2. Light and electron micrographs of Lecudinidae sp. Clade B (*Undularius glycerae*). (A) Differential interference contrast (DIC) micrograph showing the nucleus (n). Peristaltic movement of the cells appears as bulging lobes (lo). Epicytic folds are also visible (ef). **(B)** Scanning electron micrograph (SEM) shows gamonts in lateral syzygy. Epicytic folds (ef) are also visible running the longitudinal length of the cell. **(B inset)** An SEM showing epicytic folds with a density of 1 fold/µm. Scale bars: A–B = 20 µm; B inset = 10 nm.

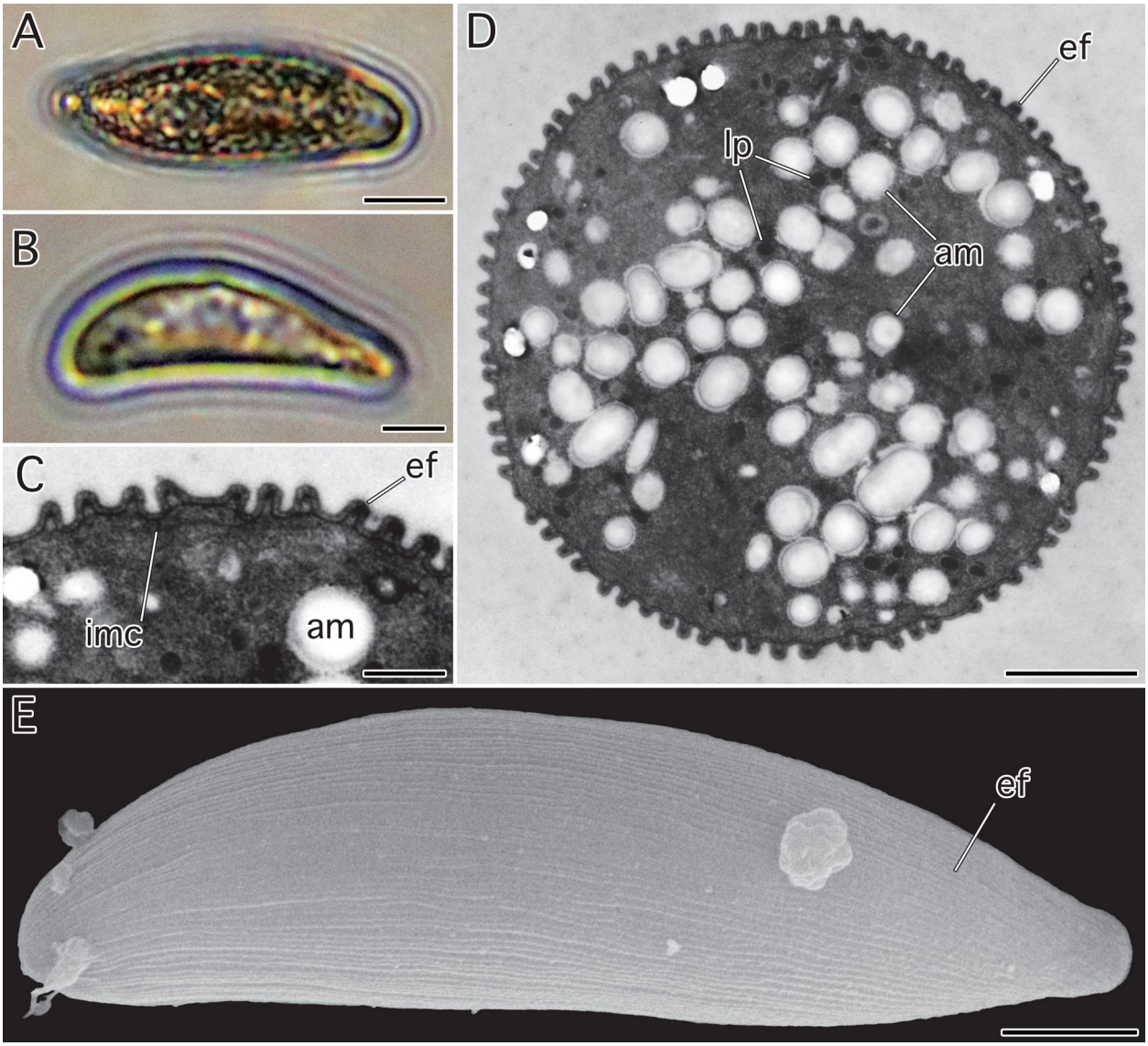

Figure 4.3. Light and electron micrographs of *Difficilina* sp. Clade A (*Difficilina fasoliformis*). (A) Anterior ends (mucrons) are oriented to the right. **(A, B)** Light micrographs of trophozoite isolates. **(C)** Transmission electron micrograph (TEM) showing epicytic folds (ef) with underlying inner membrane complex (imc) and amylopectin granules (am). Fold density is 4 folds/µm. **(D)** A TEM cross-section showing the rounded shape of the trophozoites and epicytic folds (ef). Amylopectin granules (am) and lipid droplets (lp) are also shown. **(E)** Scanning electron micrograph showing general trophozoite morphology and epicytic folds (ef). Scale bars: A–B = 10 µm; C = 500 nm; D = 2 µm; E = 5 µm.

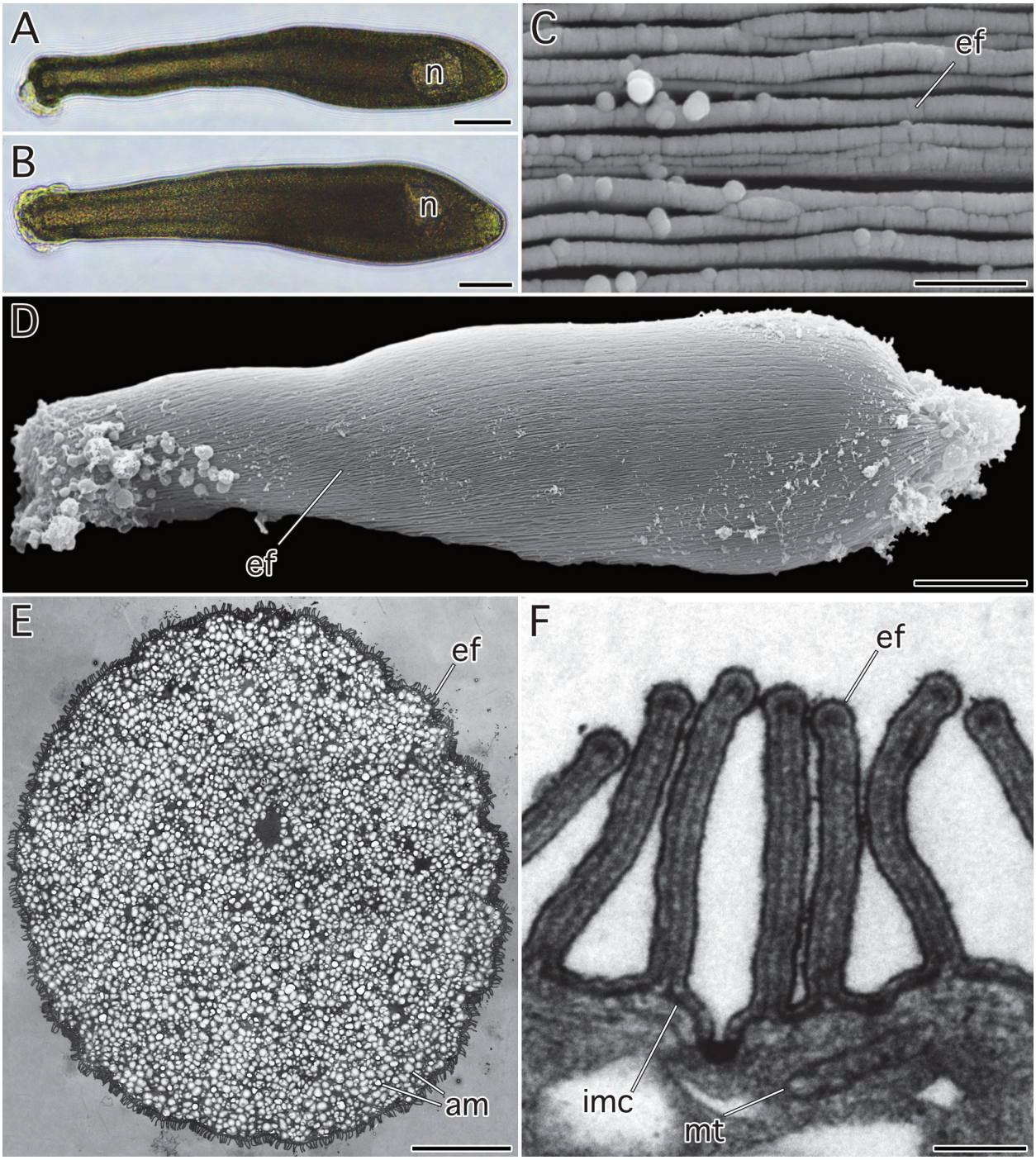

Figure 4.4. Light and electron micrographs of Lecudinidae sp. Clade C. Anterior ends (mucrons) are oriented to the right. **(A–B)** Light micrographs of trophozoite isolates with visible nucleus (n) at anterior of elongate cell. **(C)** Scanning electron microscopy (SEM) image of cell surface showing epicytic folds (ef) with a density of 3.5 folds/µm. **(D)** Whole-cell SEM image showing general trophozoite morphology and epicytic folds (ef). **(E)** Transmission electron micrograph (TEM) showing epicytic folds (ef) and amylopectin granules (am). **(F)** High-magnification TEM image showing epicytic folds (ef) with underlying inner membrane complex (imc) and mitochondrion (mt). Scale bars: A–D = 40 µm; E = 10 µm; F = 250 nm.

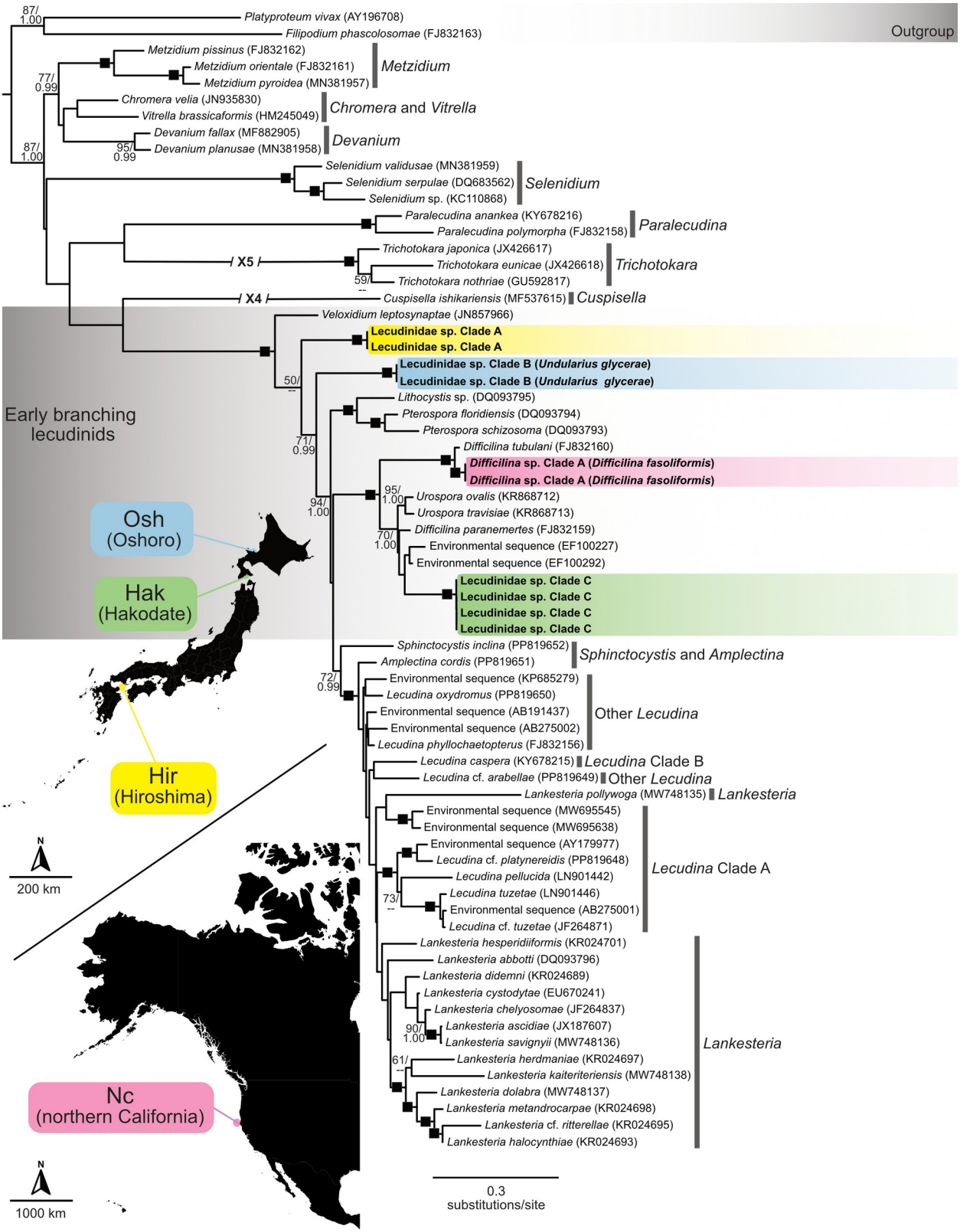

Figure 4.5. Maximum-Likelihood (ML) marine gregarine tree inferred from small subunit 18S rRNA gene sequences. Bootstrap values >50 and Bayesian Posterior Probabilities (PP) >0.95 are shown adjacent to nodes (ML/PP). Black squares indicate statistical support ≥95/0.99. Scale bar represents the inferred evolutionary distance as a rate of base substitutions per site. Clades containing novel molecular data are colored to indicate locality. Novel sequences presented in this study are written in bold text.

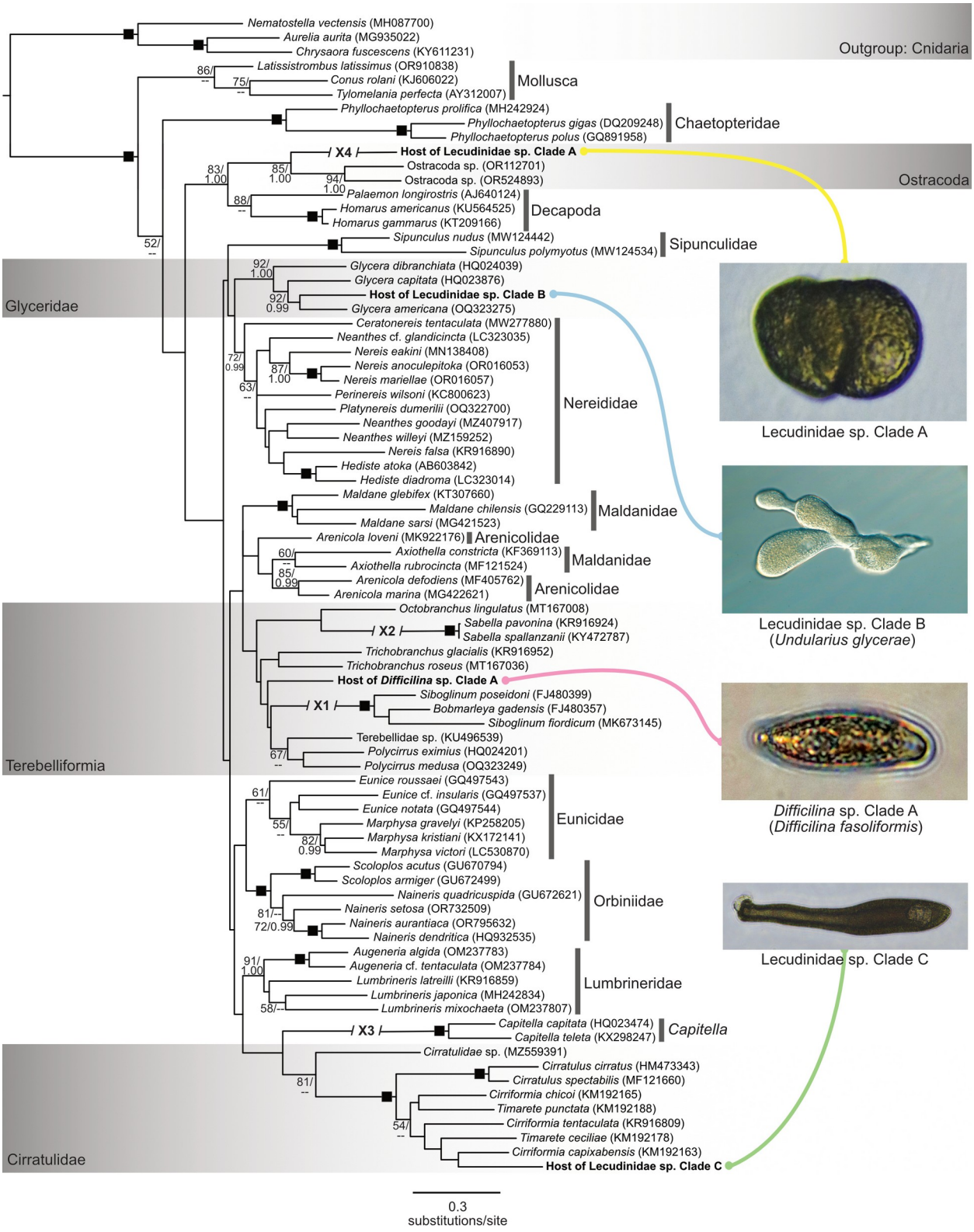

Figure 4.6. Maximum-Likelihood (ML) marine invertebrate host tree inferred from COI gene sequences. Bootstrap values >50 and Bayesian Posterior Probabilities (PP) >0.95 are shown adjacent to nodes (ML/PP). Scale bar represents the inferred evolutionary distance as a rate of base substitutions per site. Host sequences are colored to distinguish locality. Novel sequences presented in this study are written in bold text.

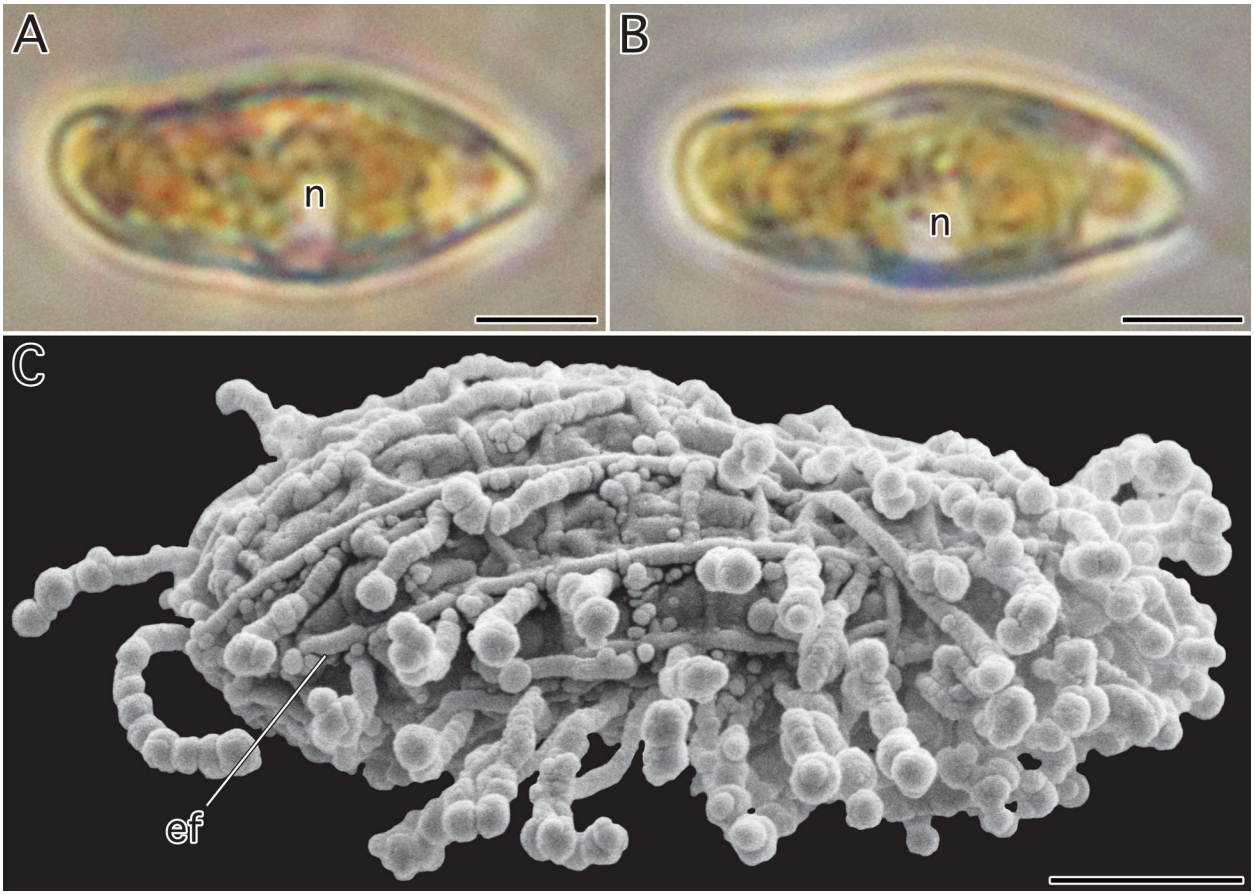

Figure 5.1. Light and electron micrographs of *Lankesteria* sp. Clade A isolates. Anterior ends (mucrons) are oriented to the right. **(A–B)** Light micrographs showing oblong trophozoite and central nucleus (n). **(C)** Whole-body SEM image showing general trophozoite morphology and epicytic folds (ef). Isolates were covered in beaded strands of suspected foreign material. Scale bars: A–C = 5 µm.

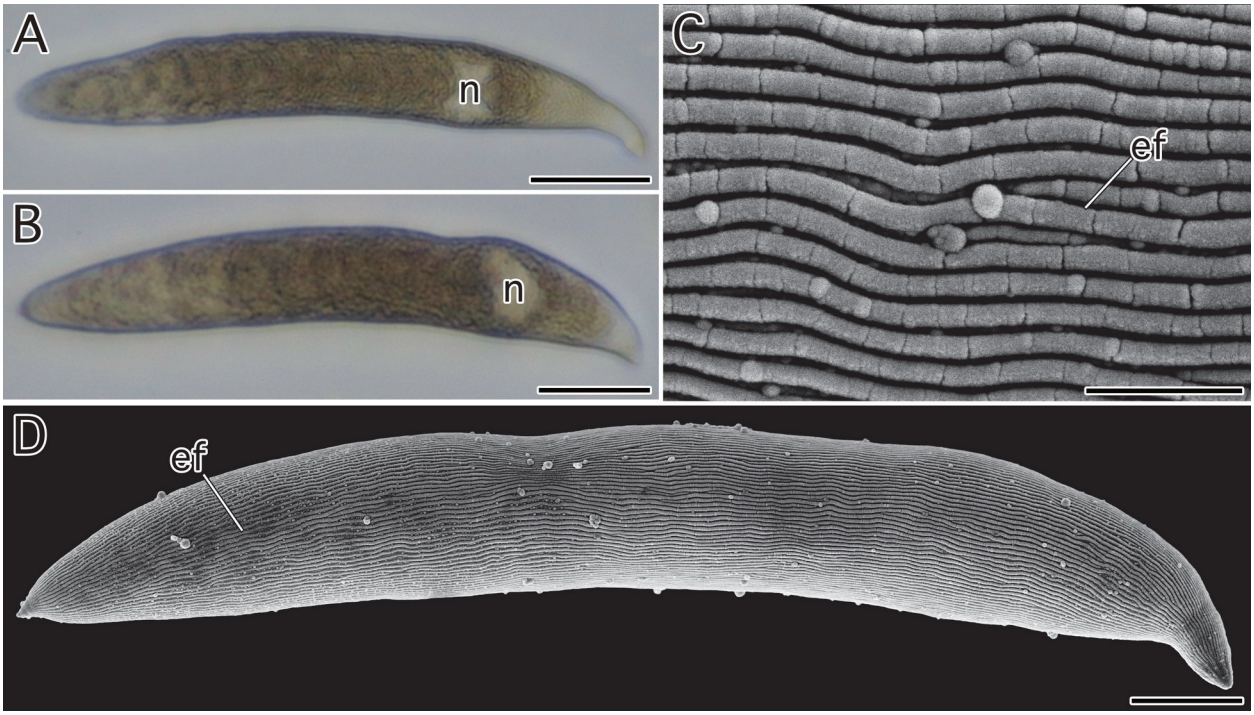

Figure 5.2. Light and electron micrographs of *Lankesteria* sp. Clade B isolates. Anterior ends (mucrons) are oriented to the right. **(A–B)** Light micrographs showing elongate trophozoite and anterior nucleus (n). **(C)** Scanning electron microscopy (SEM) image of cell surface, showing epicytic folds (ef) with a density of 3 folds/µm. **(D)** Whole-body SEM image showing general trophozoite morphology and epicytic folds (ef). Scale bars: A–B = 20 µm; C = 2 µm; D = 10 µm.

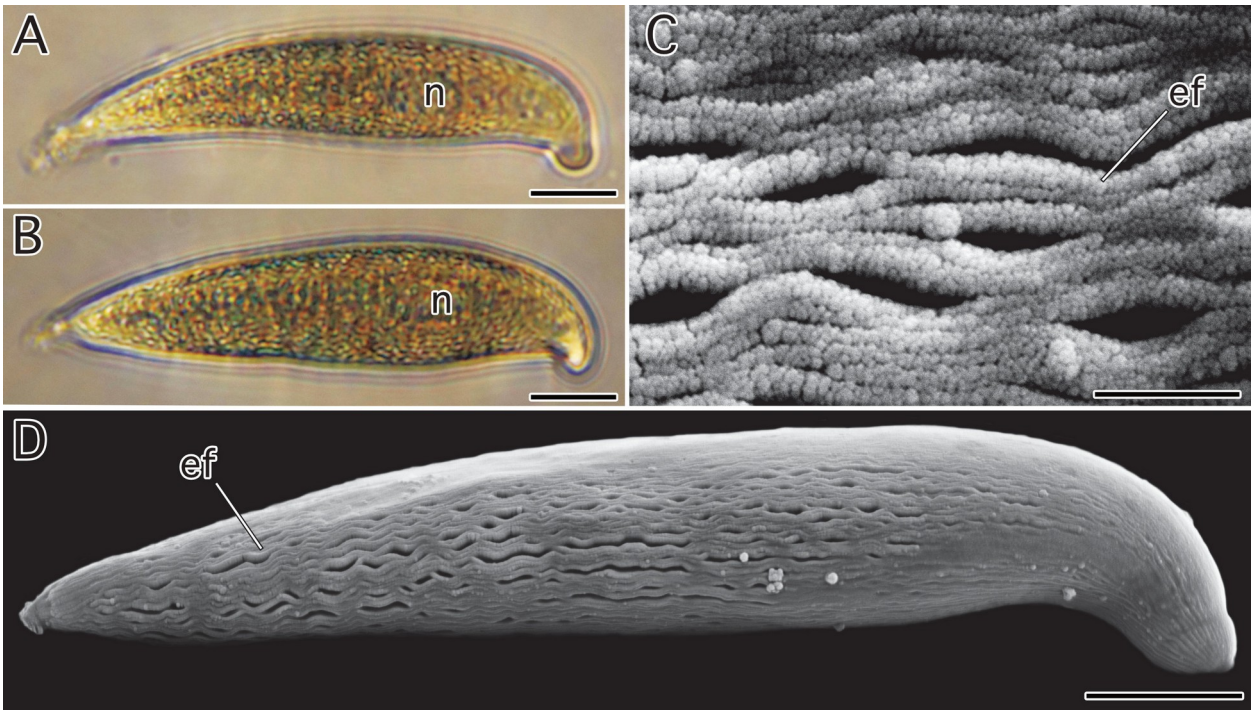

Figure 5.3. Light and electron micrographs of *Lankesteria* sp. Clade C isolates. Anterior ends (mucrons) are oriented to the right. **(A–B)** Light micrographs showing elongate trophozoite with hooked mucron and nucleus (n). **(C)** Scanning electron microscopy (SEM) image of cell surface, showing epicytic folds (ef) with a density of 4 folds/µm. **(D)** Whole-body SEM image showing general trophozoite morphology and epicytic folds (ef). Scale bars: A–B, D = 10 µm; C = 1 µm.

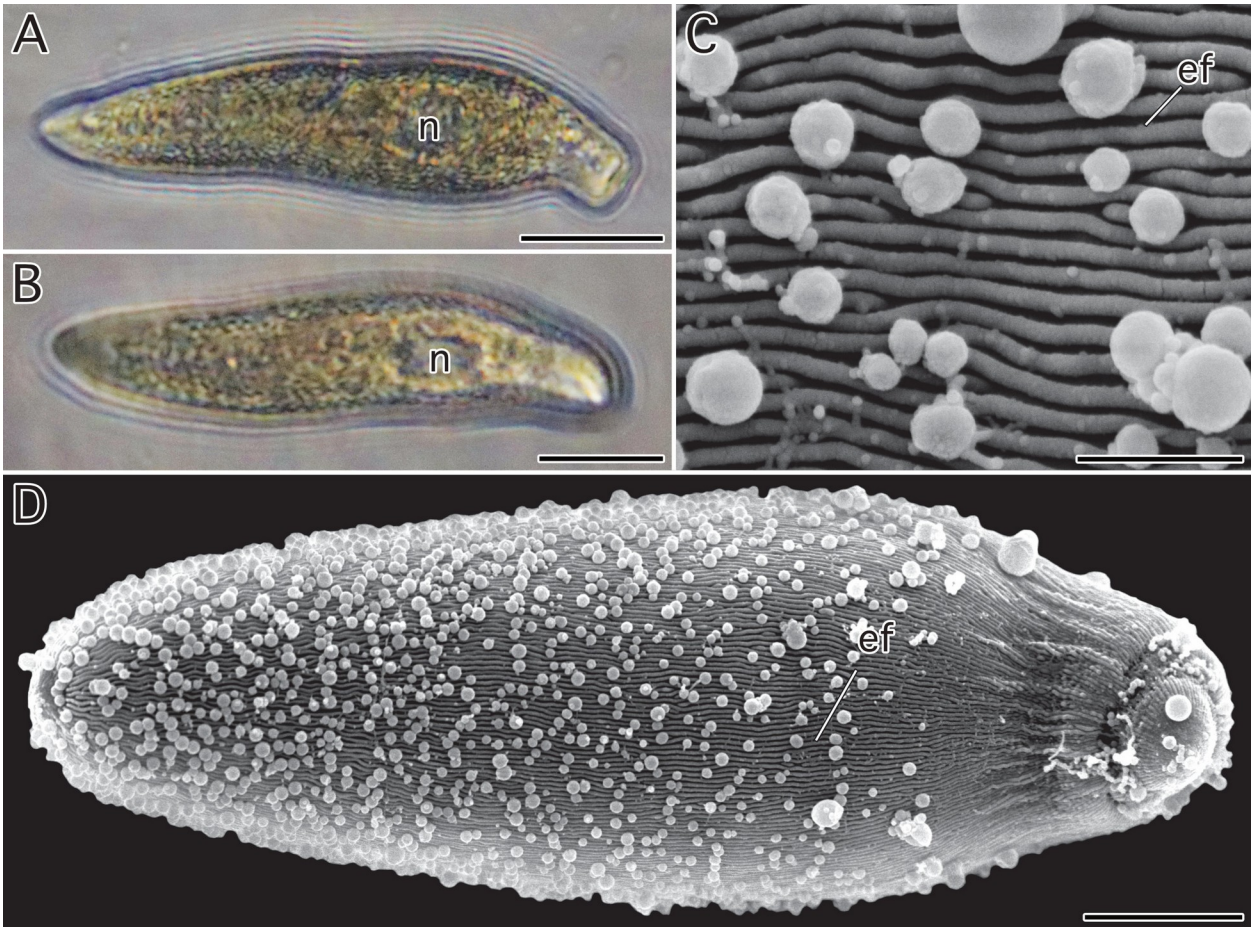

Figure 5.4. Light and electron micrographs of *Lankesteria* sp. Clade D isolates. Anterior ends (mucrons) are oriented to the right. **(A–B)** Light micrographs showing elongate trophozoite with cylindrically protruding mucron and nucleus (n). **(C)** Scanning electron microscopy (SEM) image of cell surface, showing epicytic folds (ef) with a density of 3 folds/µm. **(D)** Whole-body SEM image showing general trophozoite morphology and epicytic folds (ef). Scale bars: A–B = 30 µm; C = 2 µm; D = 10 µm.

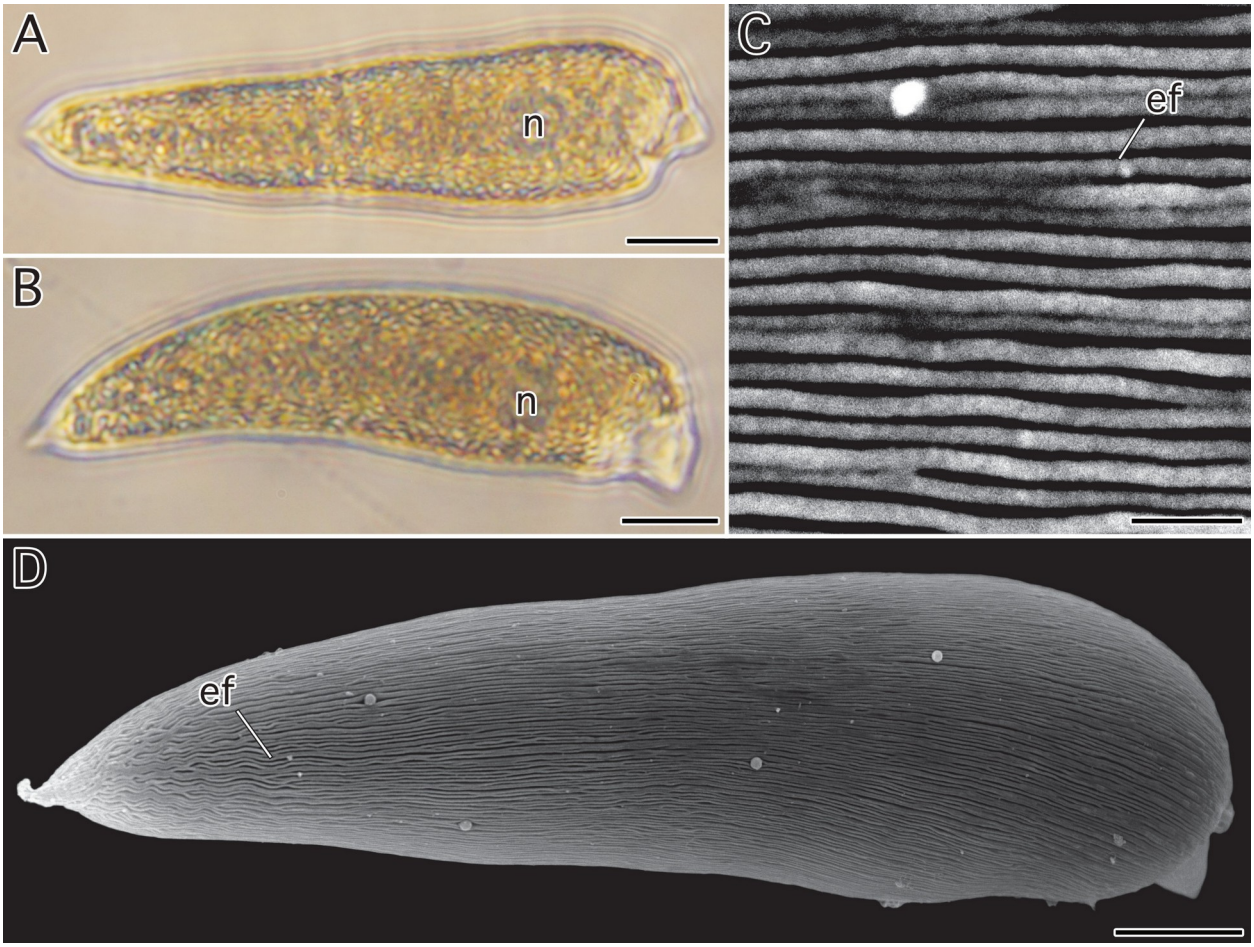

Figure 5.5. Light and electron micrographs of *Lankesteria* sp. Clade E isolates. Anterior ends (mucrons) are oriented to the right. **(A–B)** Light micrographs showing elongate trophozoite with cylindrically protruding mucron and nucleus (n). **(C)** Scanning electron microscopy (SEM) image of cell surface, showing epicytic folds (ef) with a density of 3 folds/µm. **(D)** Whole-body SEM image showing general trophozoite morphology and epicytic folds (ef). Scale bars: A–B, D = 10 µm; C = 1 µm.

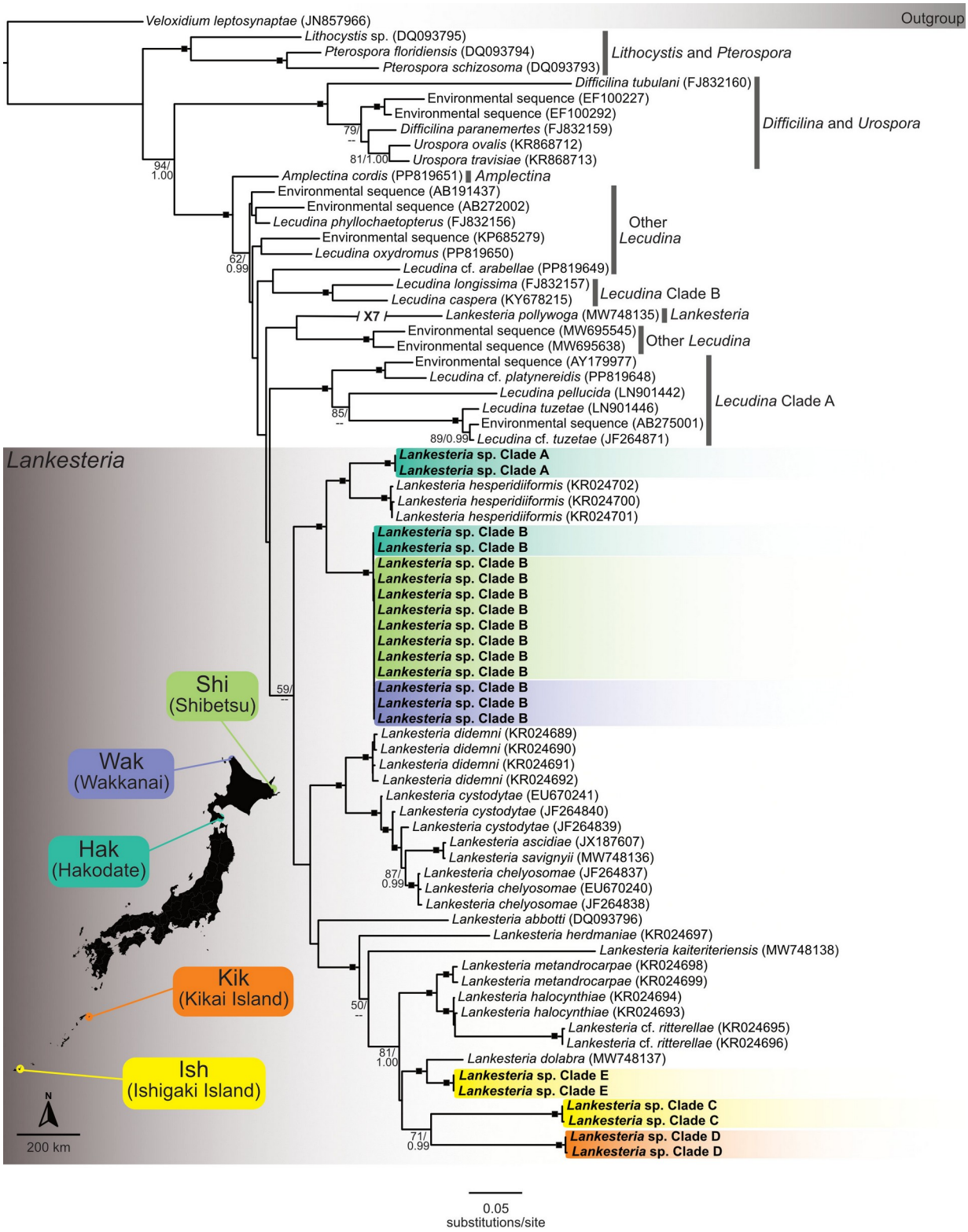

Figure 5.6. Maximum-Likelihood (ML) marine gregarine tree inferred from small subunit 18S rRNA gene sequences. Bootstrap values >50 and Bayesian Posterior Probabilities (PP) >0.95 are shown adjacent to nodes (ML/PP). Black squares indicate statistical support ≥95/0.99. Scale bar represents the inferred evolutionary distance as a rate of base substitutions per site. Clades containing novel molecular data are colored to indicate locality. Novel sequences presented in this study are written in bold text.

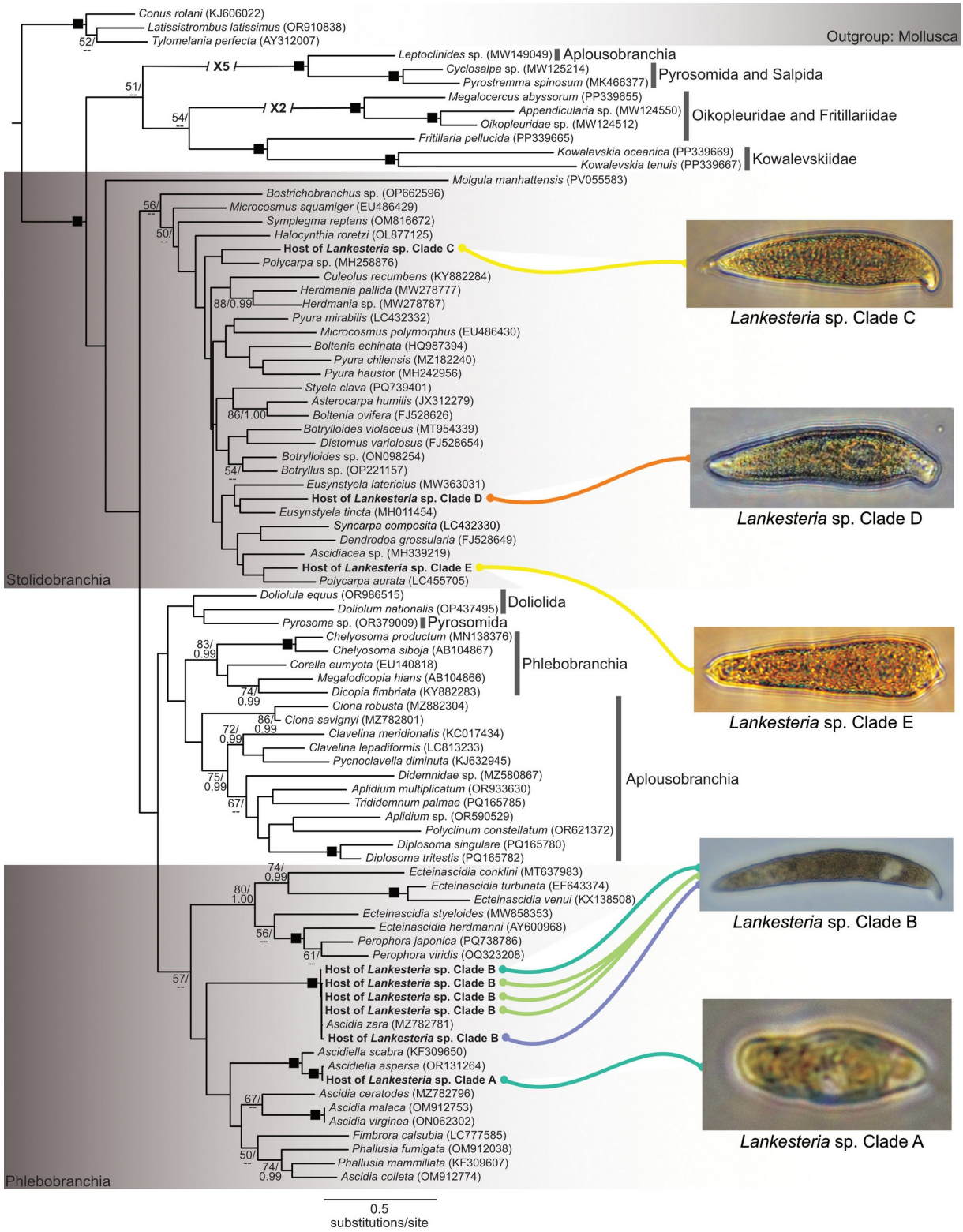

Figure 5.7. Maximum-Likelihood (ML) tunicate host tree inferred from COI gene sequences. Bootstrap values >50 and Bayesian Posterior Probabilities (PP) >0.95 are shown adjacent to nodes (ML/PP). Scale bar represents the inferred evolutionary distance as a rate of base substitutions per site. Host sequences are colored to distinguish locality. Novel sequences presented in this study are written in bold text.

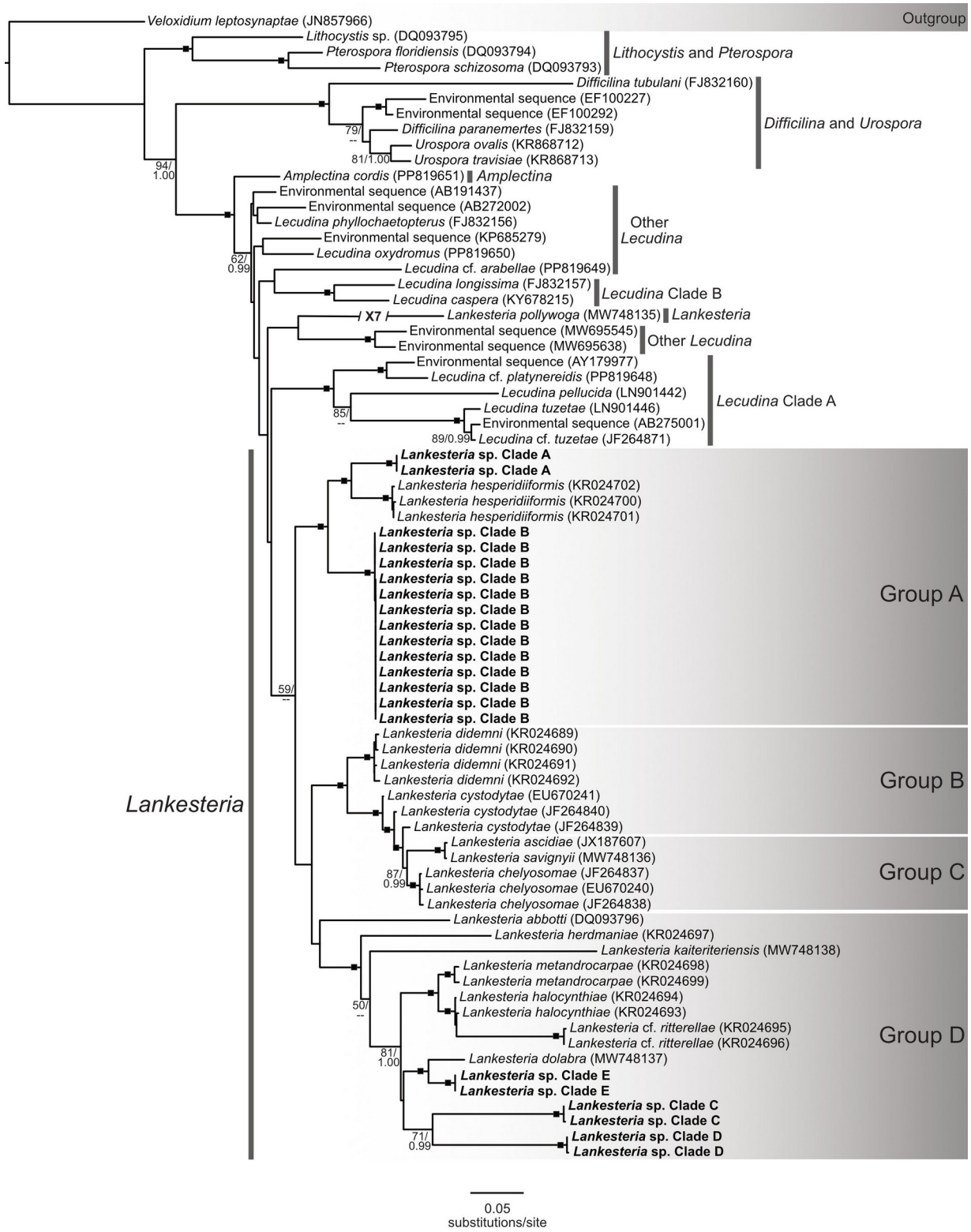

Figure 5.8. Maximum-Likelihood (ML) *Lankesteria* subclade analysis tree inferred from small subunit 18S rRNA gene sequences. Bootstrap values >50 and Bayesian Posterior Probabilities (PP) >0.95 are shown adjacent to nodes (ML/PP). Black squares indicate statistical support ≥95/0.99. Scale bar represents the inferred evolutionary distance as a rate of base substitutions per site. Sequence groups with distinct tunicate host associations are labeled A through D. Novel sequences presented in this study are written in bold text.

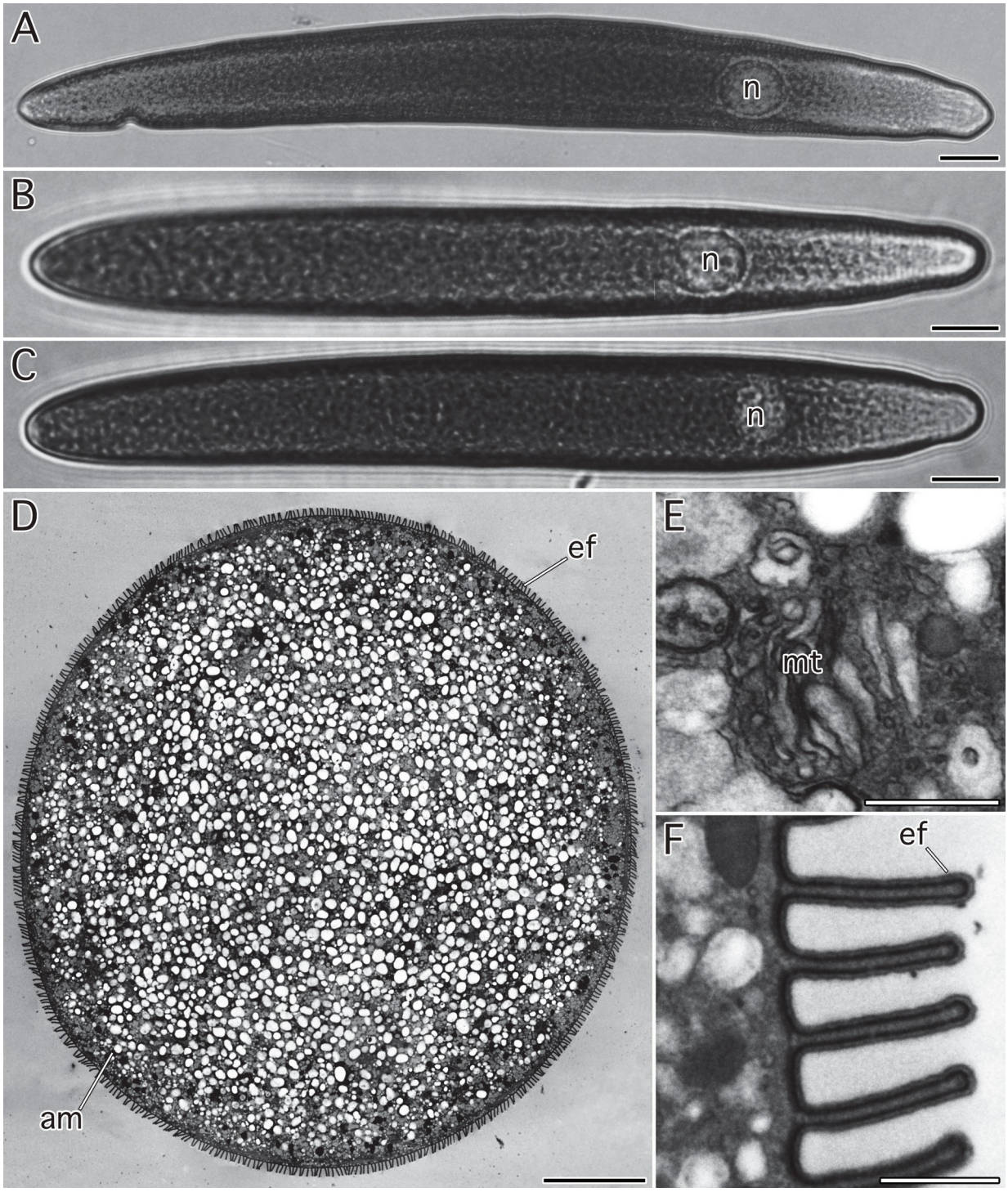

Figure 6.1. Light and electron micrographs of *Lecudina* sp. Clade A isolates. Anterior ends (mucrons) are oriented to the right. **(A–C)** Light micrographs of trophozoite isolates showing nuclei (n). **(D)** Transmission electron microscopy (TEM) cross-section showing the round shape of the trophozoite, numerous amylopectin granules (am), and epicytic folds (ef). **(E)** High-magnification TEM image showing mitochondria (mt). **(F)** High-magnification TEM image showing epicytic folds (ef) with density of 4 folds/µm. Scale bars: A–D = 10 µm; E–F = 500 nm.

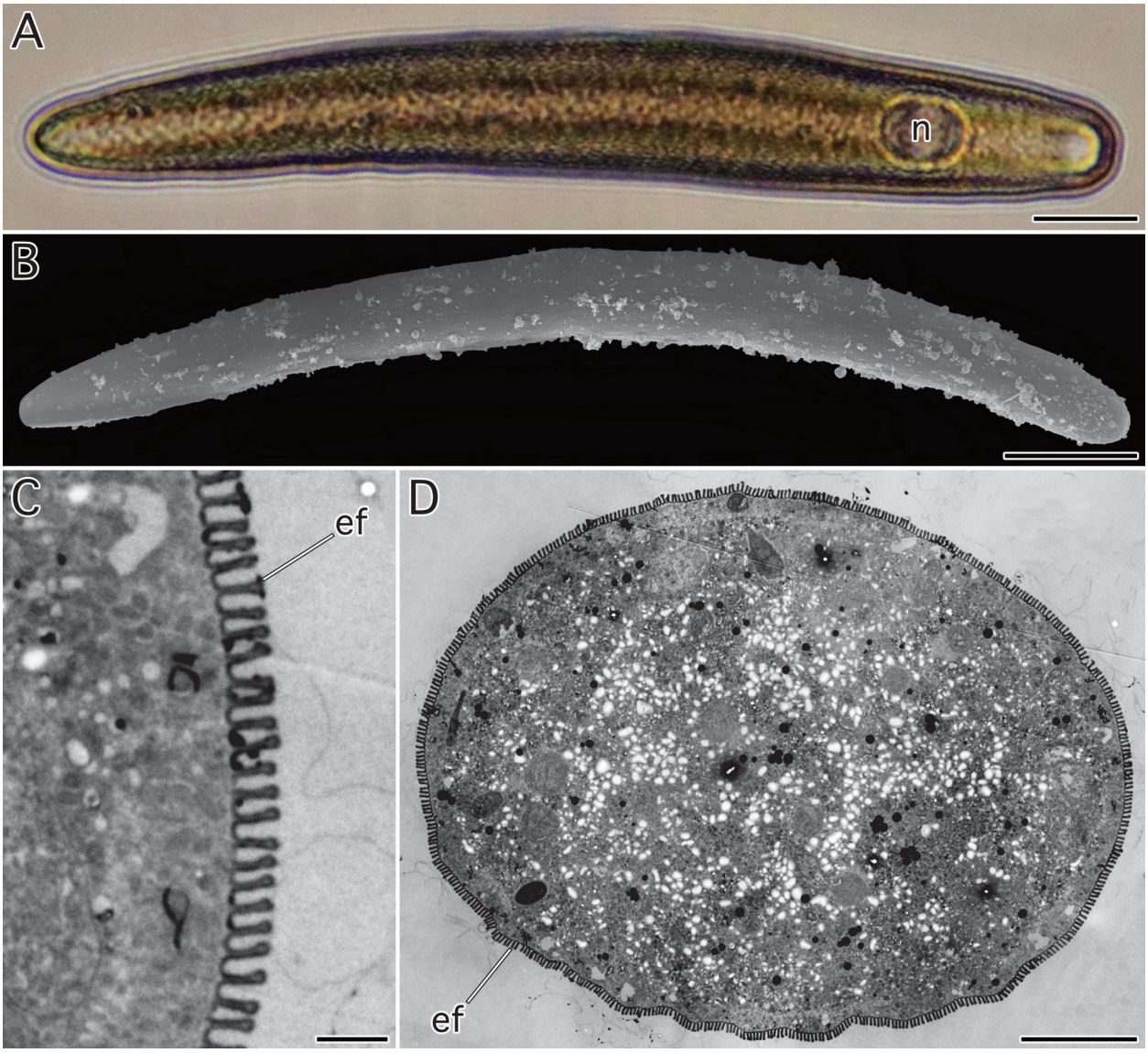

Figure 6.2. Light and electron micrographs of *Lecudina* sp. Clade B (*Lecudina* cf. *longissima*) isolates. Anterior ends (mucrons) are oriented to the right. **(A)** Light micrograph showing the nucleus (n). **(B)** Scanning electron micrograph showing a trophozoite. **(C)** Transmission electron micrograph (TEM) showing epicytic folds (ef) with a density of 4 folds/µm. **(D)** A TEM cross-section of trophozoite with epicytic folds (ef). Scale bars: A = 20 µm; B = 50 µm; C = 1 µm; D = 10 nm.

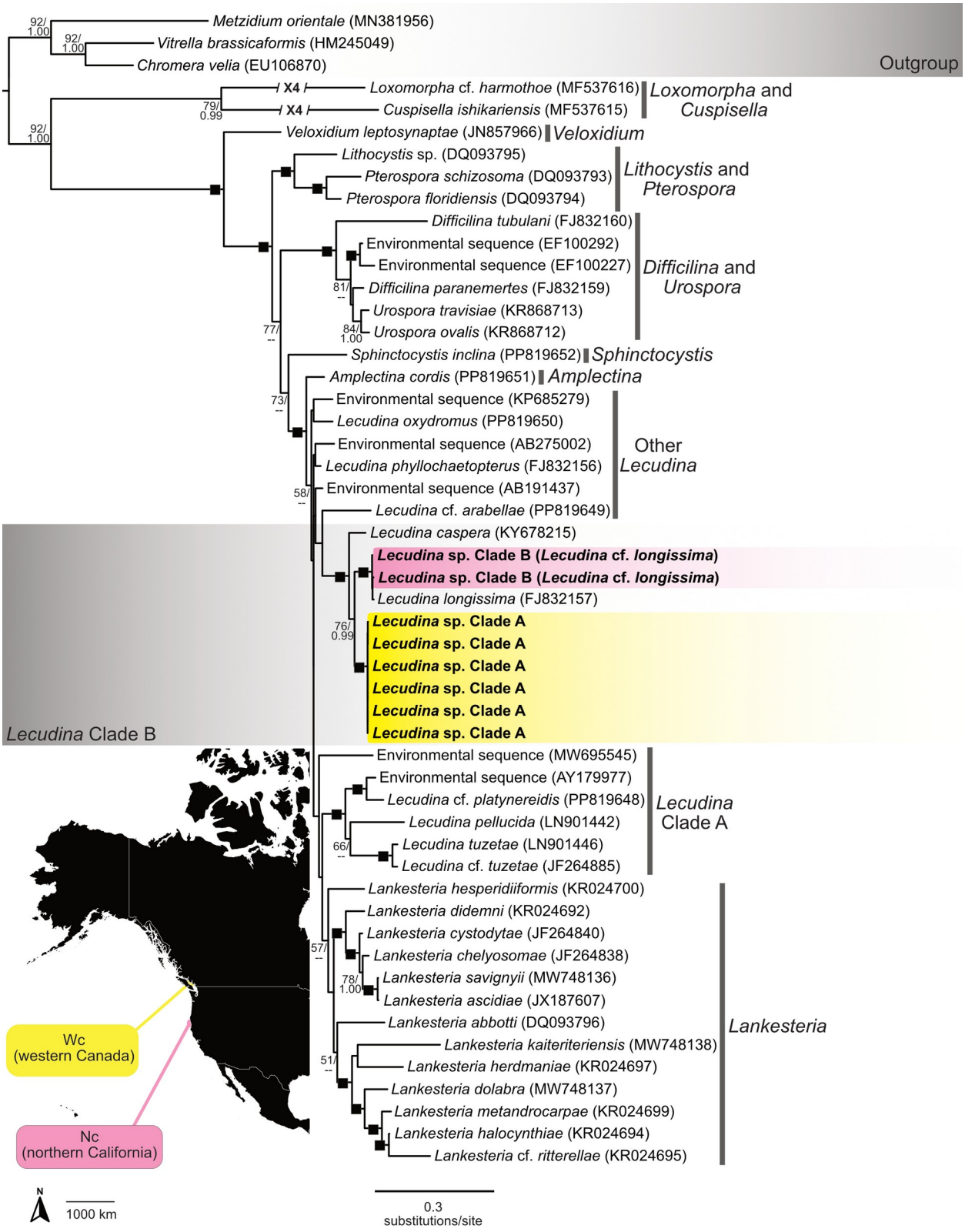

Figure 6.3. Maximum-Likelihood (ML) marine gregarine tree inferred from concatenated 18S and ITS rRNA gene sequences. Bootstrap values >50 and Bayesian Posterior Probabilities (PP) >0.95 are shown adjacent to nodes (ML/PP). Black squares indicate statistical support ≥95/0.99. Scale bar represents the inferred evolutionary distance as a rate of base substitutions per site. Clades containing novel molecular data are colored to indicate locality. Novel sequences presented in this study are written in bold text.

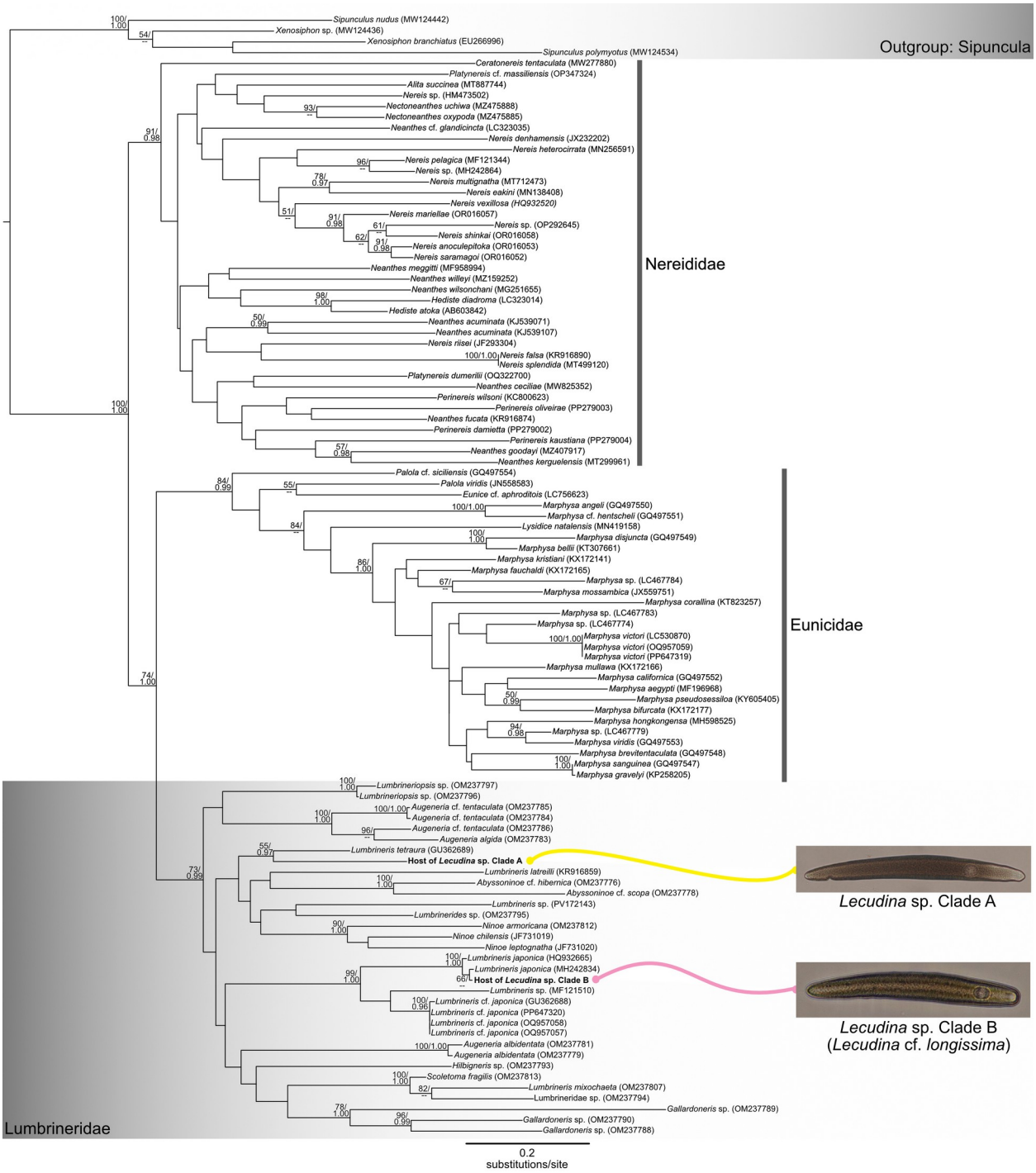

Figure 6.4. Maximum-Likelihood (ML) polychaete host tree inferred from COI gene sequences. Bootstrap values >50 and Bayesian Posterior Probabilities (PP) >0.95 are shown adjacent to nodes (ML/PP). Scale bar represents the inferred evolutionary distance as a rate of base substitutions per site. Host sequences are colored to distinguish locality. Novel sequences presented in this study are written in bold text.

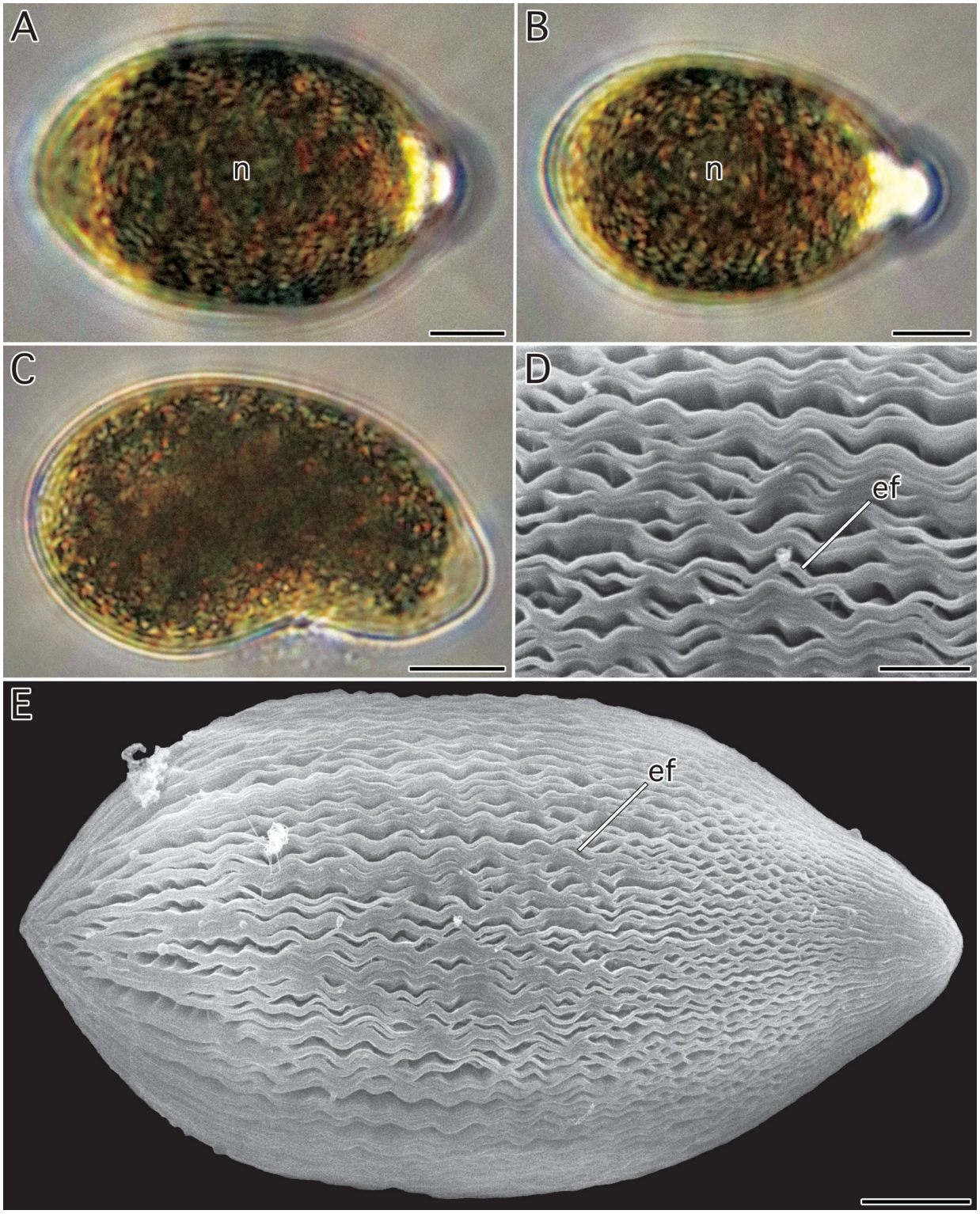

Figure 7.1. Light and electron micrographs of *Lecudina* sp. Clade C (*Lecudina* cf. *tuzetae*) isolates. Anterior ends (mucrons) are oriented to the right. **(A–C)** Light micrographs of trophozoites cells with visible nuclei (n). **(D)** A scanning electron microscopy **(**SEM**)** image showing epicytic folds (ef) with a fold density of 2 folds/µm. **(E)** An SEM image showing trophozoite covered by epicytic folds (ef). Scale bars: A–C = 15 µm; D–E = 10 µm.

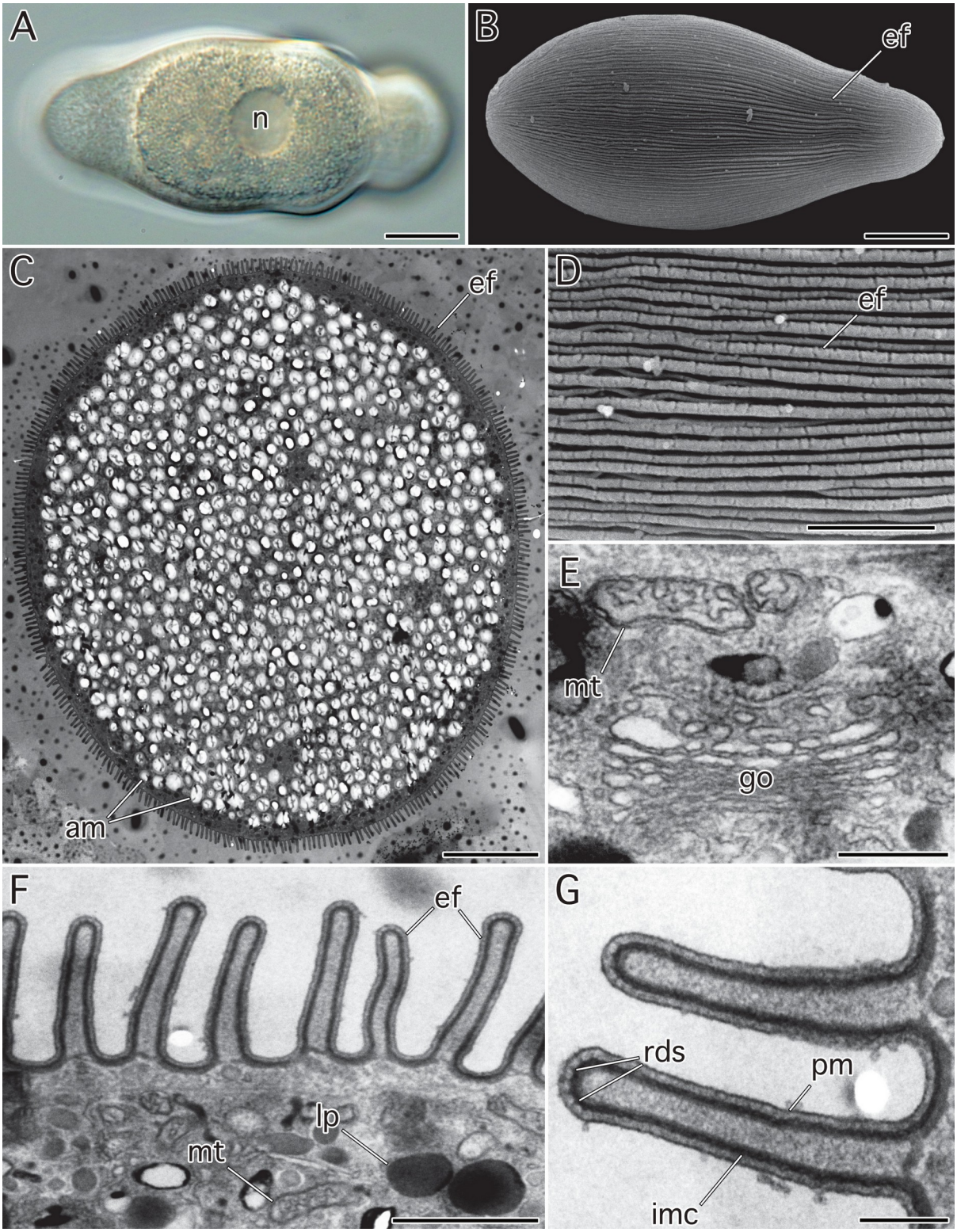

Figure 7.2. Light and electron micrographs of *Lecudina* sp. Clade D (*Lecudina kitase*) isolates. Anterior ends (mucrons) are oriented to the right. **(A)** Differential interference contrast (DIC) micrograph showing the nucleus (n). **(B)** Scanning electron micrograph (SEM) showing epicytic folds (ef). **(C)** Transmission electron micrograph (TEM) cross-section showing epicytic folds (white arrowhead) and amylopectin granules (am). **(D)** An SEM of epicytic folds (ef) and numerous amylopectin granules (am). **(E)** A transmission electron microscopy (TEM) image of a Golgi apparatus (go) and mitochondrion (mt). **(F)** A TEM image of the cell membrane showing mitochondrion (mt), lipid droplets (lp), and epicytic folds at a density of 2 folds/µm. Individual epicytic folds are also indicated **(**ef). **(G)** A TEM image showing rippled dense structures (rds), plasma membrane (pm), and inner membrane complex (imc). Scale bars: A–C = 10 µm; D = 5 µm; E = 500 nm; F = 1 µm; G = 250 nm.

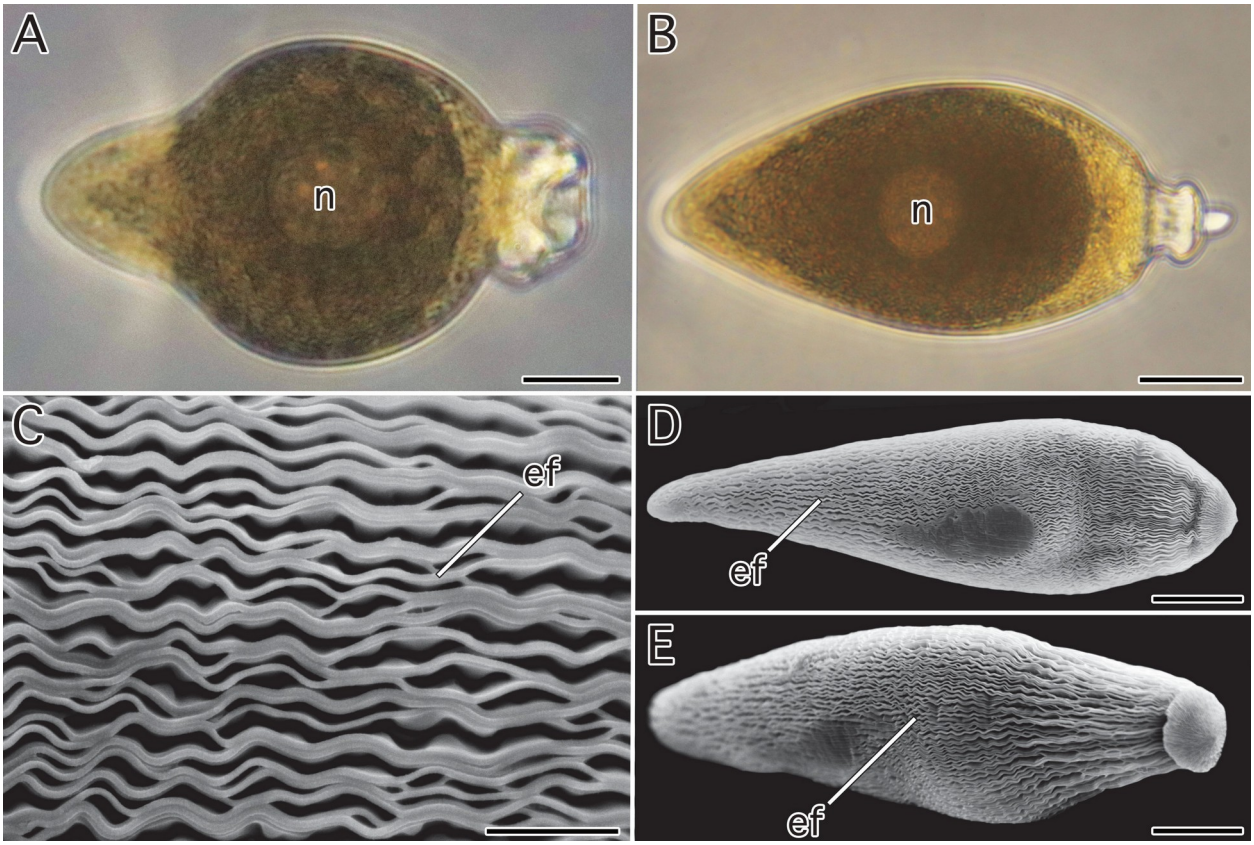

Figure 7.3. Light and electron micrographs of *Lecudina* sp. Clade E isolates. Anterior ends (mucrons) are oriented to the right. **(A–B)** Light micrographs of trophozoite isolates showing nuclei (n) and mucron in button-like configuration. **(C)** Scanning electron microscopy (SEM) image of cell surface showing epicytic folds (ef) with a density of 1.3 folds/µm. **(D–E)** Whole-cell SEM images of isolates showing general morphology of cells covered with epicytic folds (ef). Scale bars: A–B = 20 µm; C = 5 µm; D–E = 40 µm.

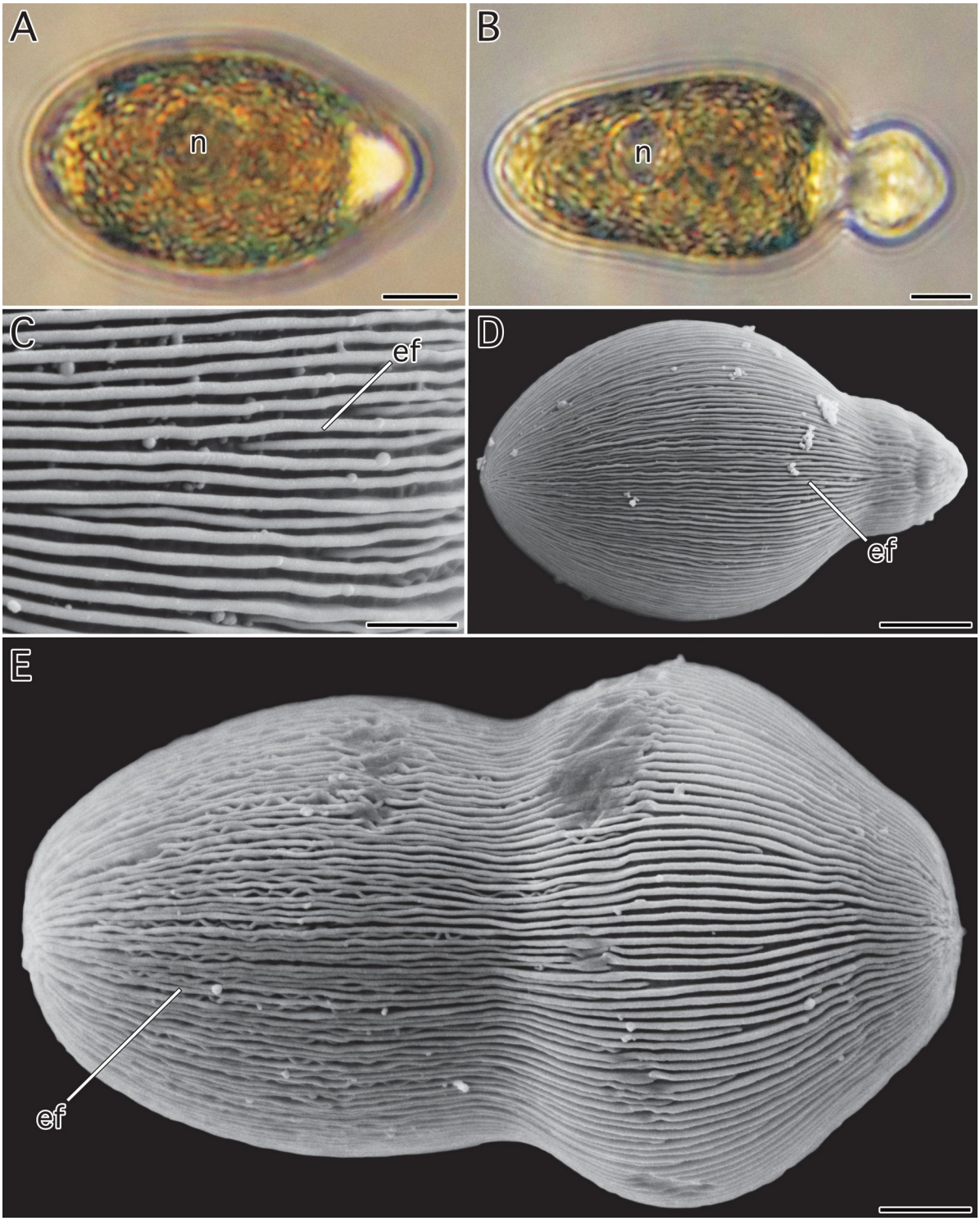

Figure 7.4. Light and electron micrographs of *Lecudina* sp. Clade F isolates. Anterior ends (mucrons) are oriented to the right. **(A–B)** Light micrographs of trophozoite isolates showing nuclei (n) and rounded mucron in contracted **(A)** and extended **(B)** states. **(C)** Scanning electron microscopy (SEM) image of cell surface showing epicytic folds (ef) with a density of 2 folds/µm. **(D–E)** Whole-cell SEM images of isolates showing general morphology of cells covered with epicytic folds (ef). Scale bars: A–B = 10 µm; C = 4 µm; D = 10 µm; E = 5 µm.

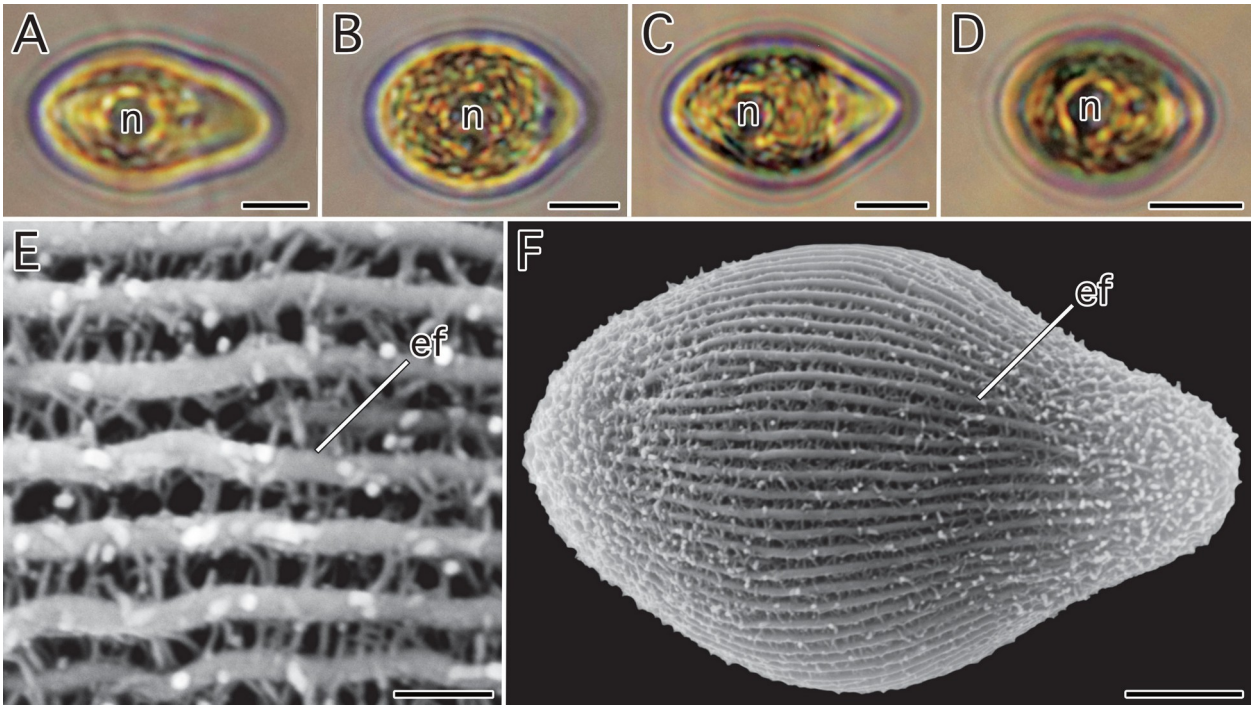

Figure 7.5. Light and electron micrographs of *Lecudina* sp. Clade G isolates. Anterior ends (mucrons) are oriented to the right. **(A–D)** Light micrographs of trophozoite isolates showing nuclei (n). **(E)** Scanning electron microscopy (SEM) image of cell surface showing epicytic folds (ef) with a density of 1.3 folds/µm. **(F)** Whole-cell SEM images of isolates showing general morphology of cells covered with epicytic folds (ef). Scale bars: A–D = 10 µm; E = 1 µm; F = 5 µm.

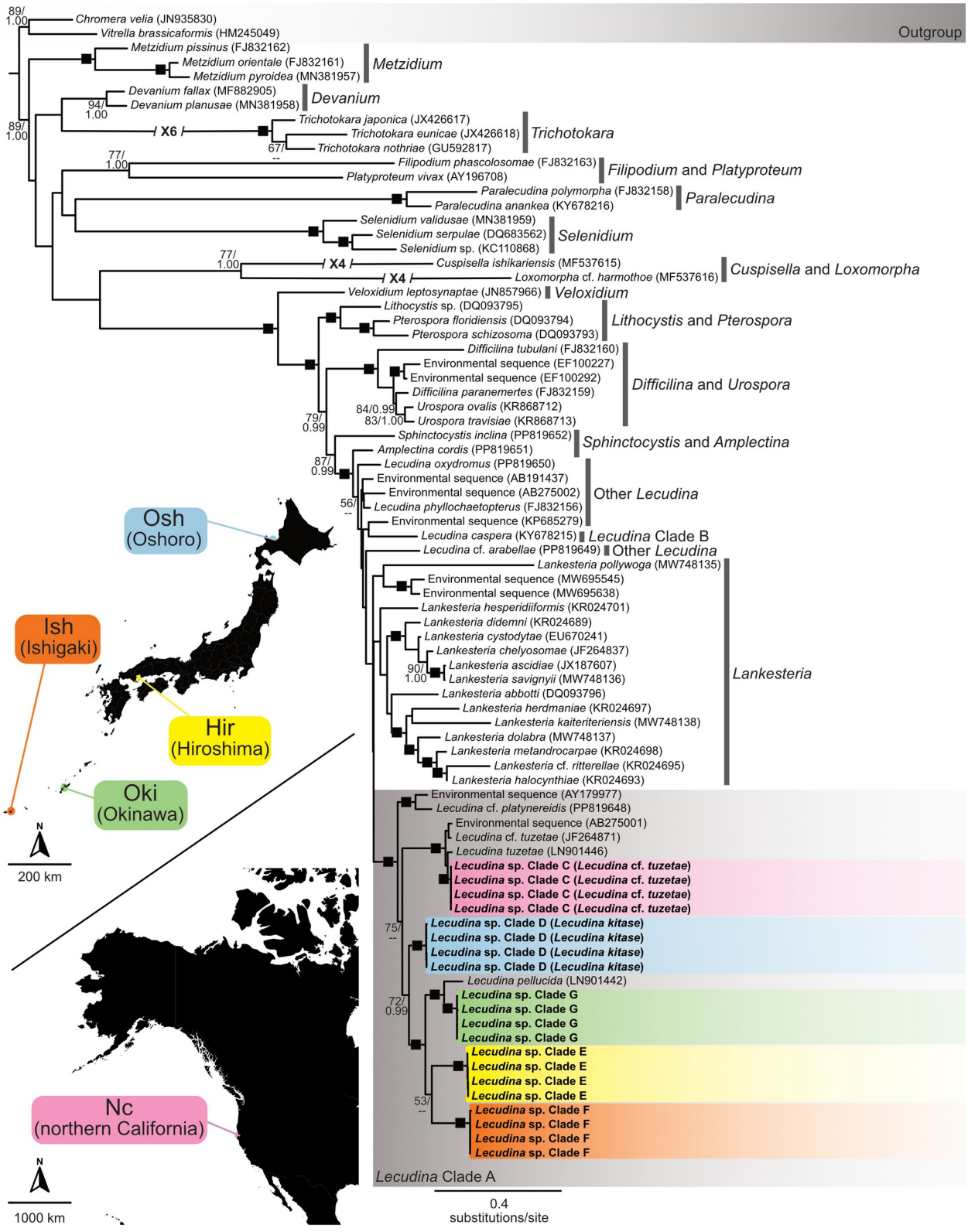

Figure 7.6. Maximum-Likelihood (ML) marine gregarine tree inferred from small subunit 18S rRNA gene sequences. Bootstrap values >50 and Bayesian Posterior Probabilities (PP) >0.95 are shown adjacent to nodes (ML/PP). Black squares indicate statistical support ≥95/0.99. Scale bar represents the inferred evolutionary distance as a rate of base substitutions per site. Clades containing novel molecular data are colored to indicate locality. Novel sequences presented in this study are written in bold text.

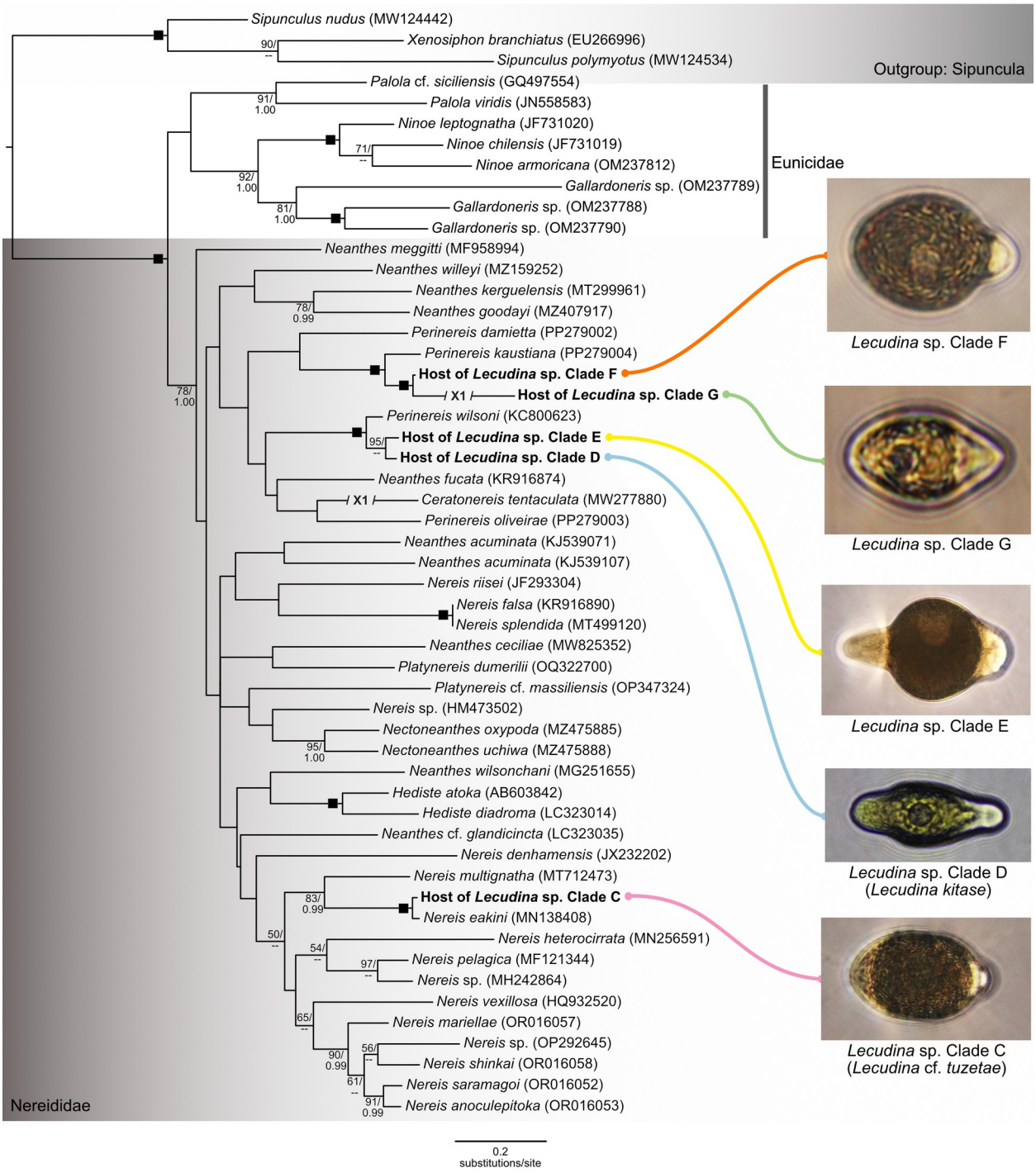

Figure 7.7. Maximum-Likelihood (ML) polychaete host tree inferred from COI gene sequences. Bootstrap values >50 and Bayesian Posterior Probabilities (PP) >0.95 are shown adjacent to nodes (ML/PP). Scale bar represents the inferred evolutionary distance as a rate of base substitutions per site. Host sequences are colored to distinguish locality. Novel sequences presented in this study are written in bold text.

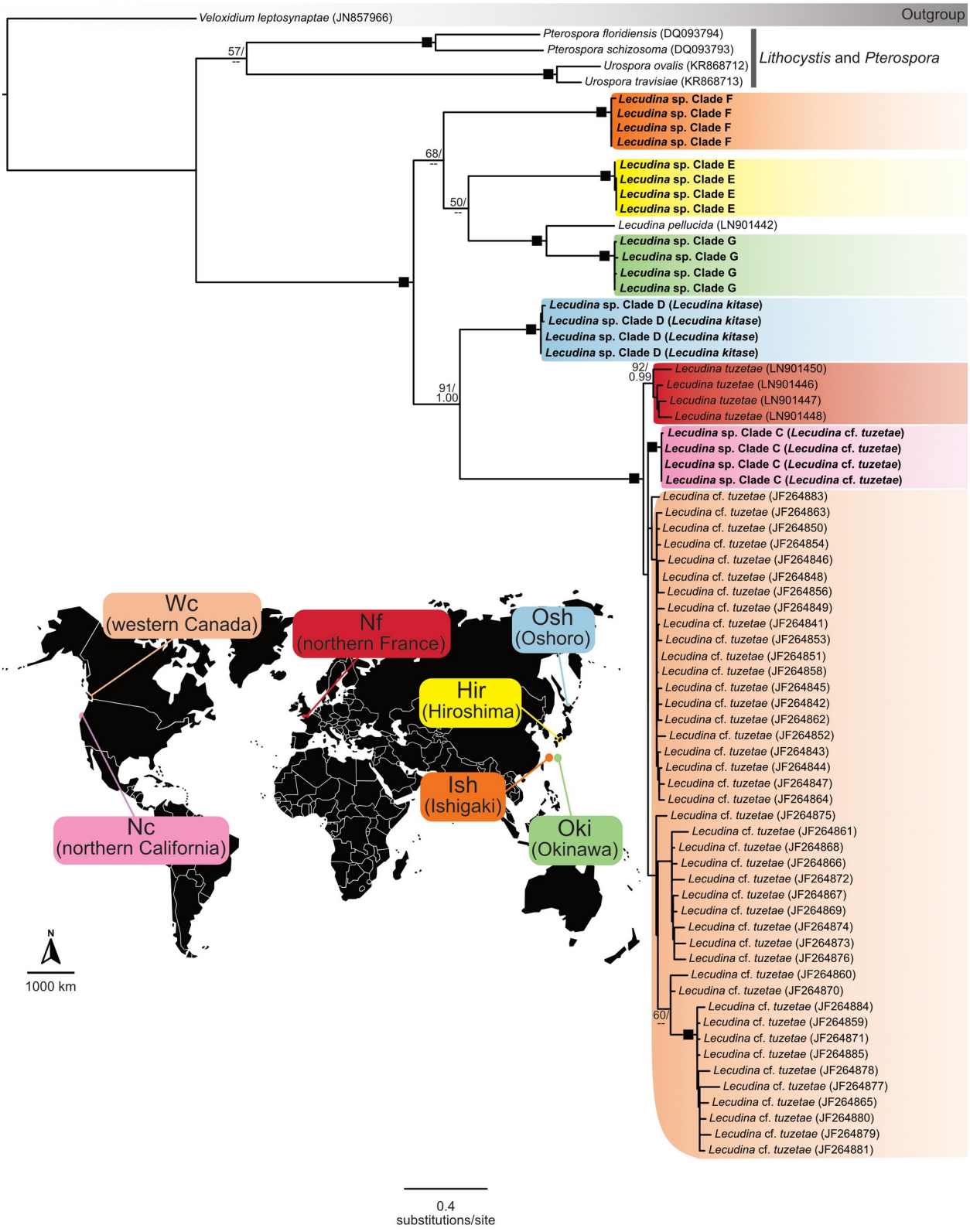

Figure 7.8. Maximum-Likelihood (ML) *Lecudina* Clade A tree inferred from small subunit 18S rRNA gene sequences. Bootstrap values >50 and Bayesian Posterior Probabilities (PP) >0.95 are shown adjacent to nodes (ML/PP). Black squares indicate statistical support ≥95/0.99. Scale bar represents the inferred evolutionary distance as a rate of base substitutions per site. Clades containing novel molecular data are colored to indicate locality. Novel sequences presented in this study are written in bold text.

TABLES

Table 1.1. Summary of marine gregarine genera and host associations for which molecular data exists.

Genus	Host	Type species	Source
Amplecina	Phyllodocidae sp. (polychaete)	*Amplectina cordis*	(Park and Leander, 2024a)
Ancora	*Capitella capitata* (polychaete)	*Ancora sagittata*	(Simdyanov et al., 2017)
Caliculium	*Glossobalanus minutus* (hemichordate)	*Caliculium glossobalani*	(Wakeman et al., 2014b)
Cephaloidophora	*Balanus balanus* (crustacean)	*Cephaloidophora communis*	(Kováčiková et al., 2017)
Cuspisella	*Lepidonotus helotypus* (polychaete)	*Cuspisella ishikariensis*	(Iritani et al., 2018a)
Devanium	Cirratulidae sp. (polychaete)	*Devanium planusae*	(Lax et al., 2024)
Difficilina	*Cerebratulus barentsi* (nemertean)	*Difficilina cerebratuli*	(Simdyanov, 2009)
Ferraria	*Marphysa sanguinea* (polychaete)	*Ferraria cornucephali*	(present work)
Filipodium	*Siphonosoma cumanense* (sipunculid)	*Filipodium ozakii*	(Rueckert and Leander, 2009)
Ganymedes	*Anaspides tasmaniae* (crustacean)	*Ganymedes anaspidis*	(Diakin et al., 2017)
Heliospora	*Gammarus pulex* (crustacean)	*Heliospora longissima*	(Simdyanov et al., 2015)
Lankesteria	*Ciona intestinalis* (ascidian)	*Lankesteria ascidiae*	(Iritani et al., 2021)
Lecudina	*Nereis* sp. (polychaete)	*Lecudina pellucida*	(Odle et al., 2024)
Lithocystis	*Echinocardium cordatum* (echinoderm)	*Lithocystis schneideri*	(Leander et al., 2006)
Loxomorpha	*Harmothoe imbricata* (polychaete)	*Loxomorpha harmothoe*	(Iritani et al., 2018a)
Lunidium	Terebellidae sp. (polychaete)	*Lunidium terebellae*	(Lax et al., 2024)
Metzidium	*Phascolosoma perlucens* (sipunculid)	*Metzidium pissinus*	(Lax et al., 2024)

Paralecudina	*Lumbrineris* sp. (polychaete)	*Paralecudina polymorpha*	(Rueckert et al., 2013)
Polyplicarium	*Notomastus tenuis* (polychaete)	*Polyplicarium lacrimae*	(Wakeman and Leander, 2013)
Polyrhabdina	*Spio fuliginosus* (polychaete)	*Polyrhabdina spionis*	(Paskerova et al., 2021)
Pterospora	*Leiocephalus leiopygos* (polychaete)	*Pterospora maldaneorum*	(Leander et al., 2006)
Selenidium	*Nerine cirratulus* (polychaete)	*Selenidium pendula*	(Lax et al., 2024)
Sphinctocystis	*Phyllodoce citrina* (polychaete)	*Sphinctocystis phyllodoces*	(Park and Leander, 2024a)
Trichotokara	*Nothria conchylega* (polychaete)	*Trichotokara nothriae*	(Rueckert and Leander, 2010)
Trollidium	*Pherusa plumosa* (polychaete)	*Trollidium akkeshiense*	(Wakeman, 2020)
Urospora	polychaetes, mollusks, nemerteans, and echinoderms	*Urospora nemertis*	(Diakin et al., 2016)
Veloxidium	*Leptosynapta clarki* (echinoderm)	*Veloxidium leptosynaptae*	(Wakeman and Leander, 2012)

Table 2.1. Summary of marine gregarine clades, including host identities and collection sites.

Clade name	Published name	Site	Host
Lunidium sp. Clade A	unpublished	Akkeshi Bay[1]	*Nainereis* sp.
Metzidium sp. Clade A	unpublished	Kabira Bay[2]	*Phyllochaetopterus* sp.
Devanium sp. Clade A	unpublished	Oshoro Bay[3]	Cirratulidae sp.
Devanium sp. Clade B	unpublished	Oshoro Bay[3]	Cirratulidae sp.
Devanium sp. Clade C	unpublished	Oshoro Bay[3]	Cirratulidae sp.

[1] 43°1′9″N 144°50′4″E, Hokkaido, Japan, visited on September 7, 2023.

[2] 24°26′4″N 124°8′25″E, Ishigaki Island, Japan, visited on September 15, 2023.

[3] 43°12′37″N 140°51′25"E, Hokkaido, Japan, visited on September 30, 2022.

Table 2.2. List of primers with references.

Primer name	Sequence	Direction	Position[1]	Citation
SR1	5'-TACCTGGTTGATCCTGCCAG-3'	forward	1	Nakayama et al. (1996)
SR1B	5'-GATCCTGCCAGTAGTCATATGCTT-3'	forward	2	Yamaguchi and Horiguchi (2005)
Sel531*	5'-GGTTTGATTCCGGAGAGG-3'	forward	372	present work
Sel804R*	5'-TTCAACTACGAGCTTTTTAACTG-3'	reverse	613	present work
Sel1192*	5'-GATGATTAATAGGGRTAGTTG-3'	forward	852	present work
Sel1353R*	5'-CGACGGTATCTGATCGTC-3'	reverse	991	present work
Sel1717*	5'-CGAACGAGACCTTAACCTG-3'	forward	1318	present work
Sel2070R*	5'-GCATCATTGTAGCGCGC-3'	reverse	1458	present work
GenEukR1	5'-CGGTGTGTACAAACGGCAGGGAC-3'	reverse	1592	Iritani et al. (2021)
SR12B	5'-CGGAAACCTTGTTACGACTTCTCC-3'	reverse	1720	Yamaguchi and Horiguchi (2005)
SR12	5'-CCTTCCGCAGGTTCACCTAC-3'	reverse	1721	Nakayama et al. (1996)
polyLCO	5'-GAYTATWTTCAACAAATCATAAAGATATTGG-3'	forward	n/a	Carr et al. (2011)
polyHCO	5'-TAMACTTCWGGGTGACCAAARAATCA-3'	reverse	n/a	Carr et al. (2011)

[1] Positions for 18S primers are based on the complete *Toxoplasma gondii* 18S sequence (accession number: L37415), measured from the 5' terminus. Positions for primers absent on the *T. gondii* reference sequence are estimated by relative distance from the nearest present primer.

Table 2.3. Comparison between novel archigregarine clades and other close relatives.

	***Lunidium* sp. Clade A**	***Metzidium* sp. Clade A**	***Devanium* sp. Clade A**	***Devanium* sp. Clade B**	***Devanium* sp. Clade C**	***Metzidium pisinnus***	***Metzidium pyroidea***	***Metzidium orientale***	***Metzidium perlucensae***
Host(s)	*Nainereis* sp.	*Phyllochaetopterus* sp.	Cirratulidae sp.	Cirratulidae sp.	Cirratulidae sp.	*Phascolosoma agassizii*	*Themiste pyroides*	*Themiste pyroides*	*Phascolosoma perlucens*
Host tissue	gut	gut	gut	gut	gut	gut	gut	gut	gut
Locality	Akkeshi Bay, Hokkaido, Japan	Kabira Bay, Ishigaki Island, Japan	Oshoro Bay, Hokkaido, Japan	Oshoro Bay, Hokkaido, Japan	Oshoro Bay, Hokkaido, Japan	Bamfield, Vancouver Island, Canada	Oshoro Bay, Hokkaido, Japan	Peter The Great Bay, Sea of Japan	CARMABI research station, Curaçao
Septate	no	no	no	no	no	no	no	no	no
Trophozoite length (µm)	100–228	120–140	70–90	140–220	125–400	64–100	252–402	120–300	117
Nucleus shape	spherical	spherical	spherical	spherical	spherical	ellipsoidal	ovoid	ellipsoidal	ellipsoidal
Nucleus diameter (µm)	6–7	9–11	5–7	5	5	11	22–37	10–25	10
Position of nucleus	central	central	anterior third	anterior third	anterior	anterior	central	central	central
Shape of posterior	pointed	tapered	pointed, tail-like	tapered	pointed	rounded	rounded	pointed	rounded
Epicytic fold density (folds/µm)	0.15	1.2	1.1	1.7	1.4	data absent	data absent	0.3	data absent
Shape of mucron	pointed	rounded	bulbous to broad	rounded	rounded	pointed	rounded	pointed	rounded
Citation	present work	present work	present work	present work	present work	Rueckert and Leander (2009)	Wakeman (2020)	Rueckert and Leander (2009)	Lax et al. (2024)

Table 2.3. Continued.

	Devanium fallax	***Devanium planusae***	***Devanium cincinnus***	***Devanium robustum***	***Lunidium melongena***	***Lunidium antevariabilis***	***Lunidium spiralis***	***Lunidium terebellae***	***Lunidium laculatum***
Host(s)	*Cirriformia tentaculata*	*Cirriformia tentaculata*	*Cirratulidae* sp.	*Cirratulus robustus*	*Thelepus japonicus*	*Amphitritides gracilis*	*Amphitritides gracilis*	*Thelepus japonicas*	*Eupolymnia* sp.
Host tissue	gut	gut	gut	gut	gut	gut	gut	gut	gut
Locality	Roscoff, northern France	Oshoro Bay, Hokkaido, Japan	Hyacinthe Bay, Quadra Island, British Columbia, Canada	Clover Point, Victoria, British Columbia, Canada	Clover Point, Victoria, British Columbia, Canada	Roscoff, northern France	Roscoff, northern France	Clover Point, Victoria, British Columbia, Canada	CARMABI research station, Curaçao
Septate	no	no	no	no	no	no	no	no	no
Trophozoite length (µm)	300-500	115–137	183	104–215	116–136	131–190	105–194	175–430	115–123
Nucleus shape	ellipsoid	ovoid or spherical	spherical	spherical	spherical	ovoid	ovoid	spherical	ovoid
Nucleus diameter (µm)	6–17	10	5	5	15	13–21	13	9–12	10
Position of nucleus	anterior	central	anterior	anterior	central	central	posterior	central	central
Shape of posterior	pointed	pointed	pointed	pointed	rounded	rounded	pointed	pointed	blunt point
Epicytic fold density (folds/µm)	data absent	broad folds	faint	faint	data absent	data absent	data absent	broad folds	data absent (cross-hatched)
Shape of mucron	knob-like for flat-topped	pointed	pointed	knob-like	neck-shaped	plastic	rounded	pointed	blunt point
Citation	Rueckert and Horák (2017)	Wakeman (2020)	Lax et al. (2024)	Lax et al. (2024)	Lax et al. (2024)	Rueckert and Horák (2017)	Rueckert and Horák (2017)	Wakeman et al. (2014)	Lax et al. (2024)

Table 2.3. Continued.

	Lunidium proboscidis	***Lunidium shako***
Host(s)	*Eupolymnia* sp.	*Eupolymnia* sp.
Host tissue	gut	gut
Locality	CARMABI research station, Curaçao	CARMABI research station, Curaçao
Septate	no	no
Trophozoite length (µm)	110–170	108–143
Nucleus shape	spherical	spherical
Nucleus diameter (µm)	10	10
Position of nucleus	central	central
Shape of posterior	rounded point	blunt point
Epicytic fold density (folds/µm)	data absent	data absent
Shape of mucron	blunt, almost square	hat-like
Citation	Lax et al. (2024)	Lax et al. (2024)

Table 3.1. Summary of marine gregarine clades, including host identities and collection sites.

Clade name	Published name	Site	Host
Ferraria sp. Clade A	unpublished	Oshoro Bay[1]	*Marphysa victori*
Ferraria sp. Clade B	unpublished	Oshoro Bay[1]	*Marphysa victori*
Paralecudina sp. Clade A	unpublished	Clover Point[2]	*Lumbrineris* cf. *japonica*
Paralecudina sp. Clade B	unpublished	Oshoro Bay[1]	*Lumbrineris* cf. *japonica*
Paralecudina sp. Clade C	unpublished	Oshoro Bay[1]	*Lumbrineris* cf. *japonica*

[1] 43°12'37"N 140°51'25"E, Hokkaido, Japan, visited between November 2022 and March 2023.

[2] 48°24'14"N 123°21'00"W, British Columbia, visited between November 7 and December 11, 2023.

Table 3.2. List of primers with references.

Primer name	Sequence	Direction	Position[1]	Citation
SR1	5'-TACCTGGTTGATCCTGCCAG-3'	forward	1	Nakayama et al. (1996)
SR1B	5'-GATCCTGCCAGTAGTCATATGCTT-3'	forward	2	Yamaguchi and Horiguchi (2005)
Sel531*	5'-GGTTTGATTCCGGAGAGG-3'	forward	372	present work
Paralecu200F*	5'-GGATAATTGTGCTAATTGTGC-3'	forward	116	present work
Paralecu608F*	5'-GAGGGAGGTAGTGACGAG-3'	forward	433	present work
Tricho499F*	5'-GGTTCTGAGAAACAACTGG-3'	forward	508	present work
Paralecu1077R*	5'-GTATTCCATGCTTGAGCAATC-3'	reverse	764	present work
Paralecu1225F*	5'-GATACGCATTTGRCTGTTAG-3'	forward	856	present work
Tricho1085R*	5'-CTCCACTCCTTGTGGTG-3'	reverse	1130	present work
Paralecu1683R*	5'-GTTAACGGAATCAACCAGAC-3'	reverse	1278	present work
Paralecu1968F*	5'-GGCCGTGAACGAGGAATTC-3'	forward	1539	present work
GenEukR1	5'-CGGTGTGTACAAACGGCAGGGAC-3'	reverse	1592	Iritani et al. (2021)
SR12B	5'-CGGAAACCTTGTTACGACTTCTCC-3'	reverse	1720	Yamaguchi and Horiguchi (2005)
SR12	5'-CCTTCCGCAGGTTCACCTAC-3'	reverse	1721	Nakayama et al. (1996)
25F1R	5'-ATATGCTTAAATTCAGCGG-3'	reverse	n/a	Takano and Horiguchi (2005)
polyLCO	5'-GAYTATWTTCAACAAATCATAAAGATATTGG-3'	forward	n/a	Carr et al. (2011)
polyHCO	5'-TAMACTTCWGGGTGACCAAARAATCA-3'	reverse	n/a	Carr et al. (2011)

[1] Positions for 18S primers are based on the complete *Toxoplasma gondii* 18S sequence (accession number: L37415), measured from the 5' terminus. Positions for primers absent on the *T. gondii* reference sequence are estimated by relative distance from the nearest present primer.

Table 3.3. Comparison between *Ferraria* spp. Clades A, B, and close relatives.

	***Ferraria* sp. Clade A**	***Ferraria* sp. Clade B**	***Ferraria cornucephali***	***Ferraria cornucephali iwamusi***	***Bhatiella marphysae***	***Gopaliella marphysae***	***Viviera marphysae***	***Trichotokara nothriae***	***Trichotokara japonica***
Host(s)	*Marphysa victori*	*Marphysa victori*	Cirratulidae sp.	*Marphysa sanguinea*	*Marphysa sanguinea*	*Marphysa gravelyi*	*Marphysa sanguinea*	*Nothria conchylega*	*Nothria* cf. *otsuchiensis*
Host tissue	gut	gut	gut	gut	gut	gut	gut	gut	gut
Locality	Hokkaido, Japan	Hokkaido Japan	Port Blair, India	Aio Beach, Yamaguchi, Japan	Port Blair, India	Visakhapatnam Harbor, India	Wimereux, France	Wizard Islet, British Columbia, Canada	Sagami-nada Sea, Shizuoka, Japan
Septate	no	undecided: transverse crease present	no	undecided	no	immature unsegmented, mature segmented	no	intermittent	no
Trophozoite length (µm)	294–309	247–564	243–297	350–480	123–300	70–840	300–350	50–155	63–201
Nucleus shape	spherical	spherical	spherical	spherical	ellipsoid or spherical	spherical	spherical	spherical	spherical
Nucleus diameter (µm)	35–38	26–74	23–31	50	17-27	data absent	data absent	8–20	11–20
Position of nucleus	longitudinal axis	posterior half	posterior half	posterior half	posterior half	central	central	central	central
Shape of posterior	tapered	flattened	rounded	flattened	rounded	tapered	tapered	rounded to pointed	rounded to pointed
Epicytic fold density (folds/µm)	6	6	data absent	data absent	data absent	data absent	data absent	5	6–8
Shape of mucron	ball-like or broad	conical	conical	conical	tapered	broad	broad	elongate, hair-like projections	hair-like and antler-like projections
Citation	present work	present work	Setna (1931)	Hoshide (1958), Hoshide (1973), Elbarhoumi and Zghal (2010)	Setna (1931), Elbarhoumi and Zghal (2010)	Ganapati et al. (1974)	Schrével (1963), Elbarhoumi and Zghal (2010)	Rueckert and Leander (2010)	Rueckert et al. (2013)

Table 3.3. Continued.

	Trichotokara eunicae
Host(s)	*Eunice valens*
Host tissue	gut
Locality	Ogden Point, British Columbia, Canada
Septate	no
Trophozoite length (µm)	531–685
Nucleus shape	spherical
Nucleus diameter (µm)	48–53
Position of nucleus	anterior bulb
Shape of posterior	tapered
Epicytic fold density (folds/µm)	3–5
Shape of mucron	bulbous
Citation	Rueckert et al. (2013)

Table 3.4. Comparison between *Paralecudina* sp. Clades A through C, and close relatives.

	***Paralecudina* sp. Clade A**	***Paralecudina* sp. Clade B**	***Paralecudina* sp. Clade C**	***Paralecudina* (*Lecudina*) *polymorpha***	***Paralecudina anankea***
Host(s)	*Lumbrineris* cf. *japonica*	*Lumbrineris japonica*	*Lumbrineris japonica*	*Lumbrineres latreilli*, *Lumbrineris japonica*	*Lumbrineris inflata*
Host tissue	gut	gut	gut	gut	gut
Locality	Clover Point, British Columbia, Canada	Oshoro Bay and Ranshima Beach, Hokkaido, Japan	Ranshima Beach, Hokkaido, Japan	Roscoff, nothern France; Bamfield Marine Station, Vancouver, Canada	Clover Point, British Columbia, Canada
Septate	no	no	no	no	no
Trophozoite length (µm)	105–400	270–615	127–518	200–1120	203–383
Nucleus shape	ellipsoid	ellipsoid to spherical	ellipsoid to spherical	ellipsoid	ellipsoid
Nucleus diameter (µm)	7–20	28–54	14–30	28–60	18–27
Position of nucleus	anterior half	anterior half	anterior half	anterior half	central
Shape of posterior	pointed	rounded	pointed	pointed	pointed
Epicytic fold density (folds/µm)	5	6	5	5	6
Shape of mucron	rounded	rounded	rounded	rounded	tapered
Citation	present work	present work	present work	Schrével (1969), Rueckert et al. (2010), Rueckert et al .(2013)	Iritani et al. (2018b)

Table 4.1. Summary of marine gregarine clades, including host identities and collection sites.

Clade name	Published name	Site	Host
Lecudinidae sp. Clade A	unpublished	Hanaguri[1]	Ostracoda sp.
Lecudinidae sp. Clade B	*Undularius glycerae*	Oshoro Bay[2]	*Glycera* sp.
Difficilina sp. Clade A	*Difficilina fasoliformis*	Crescent City[3]	Terebellidae sp.
Lecudinidae sp. Clade C	unpublished	Mizunashikaihin[4]	Cirratulidae sp.

[1] 34°18'04"N 132°50'20"E, Hiroshima, Japan, visited between October 22 and 29, 2023.

[2] 43°12'37"N 140°51'25"E, Hokkaido, Japan, visited on November 11, 2022.

[3] 41°44'12"N 124°11'40"E, California, USA, visited in January 2023.

[4] 41°48'40"N 141°11'3"E, Hakodate, Hokkaido, Japan, visited on March 24, 2023.

Table 4.2. List of primers with references.

Primer name	Sequence	Direction	Position[1]	Citation
SR1	5'-TACCTGGTTGATCCTGCCAG-3'	forward	1	Nakayama et al. (1996)
SR1B	5'-GATCCTGCCAGTAGTCATATGCTT-3'	forward	2	Yamaguchi and Horiguchi (2005)
Lecu401F*	5'-CAAAGTTTCTGACCCATCAG-3'	forward	275	present work
Sel531*	5'-GGTTTGATTCCGGAGAGG-3'	forward	372	present work
Sel804R*	5'-TTCAACTACGAGCTTTTTAACTG-3'	reverse	613	present work
LecuR*	5'-GAACACGCCGATTCACTC-3'	reverse	724	present work
Sel1192*	5'-GATGATTAATAGGGRTAGTTG-3'	forward	852	present work
Lecu1272F*	5'-GATCAAGAACGAAAGTTAGGGG-3'	forward	942	present work
Sel1353R*	5'-CGACGGTATCTGATCGTC-3'	reverse	991	present work
18SRF	5'-CCCGTGTTGAGTCAAATTAAG-3'	reverse	1154	Mo et al. (2002)
SR9	5'-AACTAAGAACRGCCATGCAC-3'	reverse	1245	Takano and Horiguchi (2005)
Lecu1617R*	5'-CCACGAACTAAGAACGGC-3'	reverse	1252	present work
Sel1717*	5'-CGAACGAGACCTTAACCTG-3'	forward	1318	present work
Sel2070R*	5'-GCATCATTGTAGCGCGC-3'	reverse	1458	present work
GenEukR1	5'-CGGTGTGTACAAACGGCAGGGAC-3'	reverse	1592	Iritani et al. (2021)
SR12B	5'-CGGAAACCTTGTTACGACTTCTCC-3'	reverse	1720	Yamaguchi and Horiguchi (2005)
SR12	5'-CCTTCCGCAGGTTCACCTAC-3'	reverse	1721	Nakayama et al. (1996)
25F1R	5'-ATATGCTTAAATTCAGCGG-3'	reverse	n/a	Takano and Horiguchi (2005)

polyLCO	5'-GAYTATWTTCAACAAATCATAAAGATATTGG-3'	forward	n/a	Carr et al. (2011)
polyHCO	5'-TAMACTTCWGGGTGACCAAARAATCA-3'	reverse	n/a	Carr et al. (2011)

[1] Positions for 18S primers are based on the complete *Toxoplasma gondii* 18S sequence (accession number: L37415), measured from the 5' terminus. Positions for primers absent on the *T. gondii* reference sequence are estimated by relative distance from the nearest present primer.

Table 4.3. Comparison between novel Lecudinidae clades and other close relatives.

	Lecudinidae sp. Clade A	**Lecudinidae sp. Clade B**	**Lecudinidae sp. Clade C**	***Difficilina* sp. Clade A**	***Difficilina cerebratuli***	***Difficilina paranemertis***	***Difficilina tubulani***
Host(s)	Ostracoda sp.	*Glycera* sp.	Cirratulidae sp.	Terebellidae sp.	*Cerebratulus barentsi*	*Paranemertes peregrina*	*Tubulanus polymorphus*
Host tissue	gut	gut	gut	gut	gut	gut	gut
Locality	Hanaguri, Hiroshima, Japan	Oshoro Bay, Hokkaido, Japan	Mizunashikaihin, Hakodate, Hokkaido, Japan	Northern California, United States	Russia: White Sea	Canada: English Bay, Vancouver	Canada: English Bay, Vancouver
Septate	no	no	no	no	no	no	no
Trophozoite length (µm)	60–120	130–270	225–360	45–60	up to 250	240–480	270–350
Nucleus shape	spherical	spherical	spherical	not visible	spherical	spherical	spherical
Nucleus diameter (µm)	20	10–15	30–40	not visible	14–26	20–25	20–25
Position of nucleus	anterior	anterior	central or anterior	not visible	central	central	central or anterior
Shape of posterior	broadly rounded	rounded	rounded	blunt	tapered	tapered	tapered
Epicytic fold density (folds/µm)	1.5	1	3.3	4	4	4	4
Shape of mucron	broadly rounded	papillary	rounded	papillary	papillary	rounded	rounded
Citation	present work	present work	present work	present work	Simdyanov (2009)	Rueckert et al. (2010)	Rueckert et al. (2010)

Table 4.4. Summary of relevant morphological and biogeographical data.

	Pterospora	***Lithocystis***	***Urospora***
Membrane	Pellicular folds forming stellate cross hatch patterns (Landers and Leander, 2005)	*L. foliacae* has crenulated epicytic folds, while *L. schneideri* has epicytic folds with density of 1 fold/µm (Coulon and Jangoux, 1987)	*U. neapolitana* has epicytic folds with density of 2 folds/µm, while *U. ovalis* has epicytic folds with density of 3 folds/µm (Coulon and Jangoux, 1987)
Morphology	Bulbous trunk with bifurcated limbs terminating in finger-like protrusions (Labbé and Racovitza, 1897; Landers and Leander, 2005)	Pear-shaped in the case of *L. foliacae*, or worm-like in the case of *L. schneideri* (Coulon and Jangoux, 1987)	Ovaloid spheres tapered at one end and often joined in syzygy at the other (Coulon and Jangoux, 1987)
Host	Annelida: Maldanidae (Landers and Leander, 2005)	Echinodermata: Spatangidae/Schizasteridae/Cucumariidae/Holothuriidae (Desportes and Schrével, 2013)	Annelida: Tubificidae; Nemertea; Echinodermata: Holothuriidae/Cucumariidae/Spatangidae; Sipunculida; Polychaeta: Cirratulidae (Desportes and Schrével, 2013)
Localities	Murmansk, Russia; Mediterranean Sea; English Channel; North Carolina, USA; Massachusetts, USA; St. Andrews, Canada, Bodega Bay, CA, USA; North Bay, San Juan Island, WA, USA, St. Andrew Bay, FL, USA (Landers and Leander, 2005; Leander et al., 2006; Desportes and Schrével, 2013)	Atlantic Ocean; North Sea; NE Pacific Ocean; NW Pacific Ocean; English Channel; Mediterranean Sea, Bamfield Marine Sciences Centre, Vancouver Island, BC, Canada (Coulon and Jangoux, 1987; Leander et al., 2006; Desportes and Schrével, 2013)	Atlantic Ocean; Mediterranean Sea; Germany; Pacific NW; Greenland; Barents Sea, English Channel, White Sea (Coulon and Jangoux, 1987; Desportes and Schrével, 2013; Diakin et al., 2016; Valigurová et al., 2023)

Table 5.1. Summary of marine gregarine clades, including host identities and collection sites.

Clade name	Published name	Site	Host
Lankesteria sp. Clade A	unpublished	Hakodate Port[1]	*Ascidiella* sp.
Lankesteria sp. Clade B	unpublished	Hakodate Port[1], Shibetsu Port[2], and Wakkanai Port[3]	*Ascidia zara*
Lankesteria sp. Clade C	unpublished	Ishigaki Port[4]	Stolidobranchia sp.
Lankesteria sp. Clade D	unpublished	Hawaii Beach[5]	*Eusynstyela* sp.
Lankesteria sp. Clade E	unpublished	Ishigaki Port[4]	Stolidobranchia sp.

[1] 41°46'29"N 140°42'38"E, Hokkaido, Japan, visited on June 26, 2023.

[2] 43°40'5"N 145°7'51"E, Hokkaido, Japan, visited on September 9, 2023.

[3] 45°24'15"N 141°40'41"E, Hokkaido, Japan, visited on May 1, 2023.

[4] 24°20'41"N 124°8'45"E, Ishigaki Island, Japan, visited on September 19, 2023.

[5] 28°22'47"N 130°0'51"E, Kikai Island, Japan, visited on September 27, 2023.

Table 5.2. List of primers with references.

Primer name	Sequence	Direction	Position[1]	Citation
SR1	5'-TACCTGGTTGATCCTGCCAG-3'	forward	1	Nakayama et al. (1996)
SR1B	5'-GATCCTGCCAGTAGTCATATGCTT-3'	forward	2	Yamaguchi and Horiguchi (2005)
T74F	5'-GTCTCGCAGATTAAGCCATG-3'	forward	34	Iritani et al. (2021)
Lecu401F*	5'-CAAAGTTTCTGACCCATCAG-3'	forward	275	present work
T990F	5'-GAGTGAATCGGCGTGTTC-3'	forward	636	Iritani et al. (2021)
T1140R	5'-GAATACGAATGCCCTCAACC-3'	reverse	755	Iritani et al. (2021)
Lecu1432R*	5'-CTATACTCCCCCCAGAACTC-3'	reverse	1095	present work
T1791R	5'-CTCCGCCTAACTCATGATAC-3'	reverse	1527	Iritani et al. (2021)
GenEukR1	5'-CGGTGTGTACAAACGGCAGGGAC-3'	reverse	1592	Iritani et al. (2021)
SR12B	5'-CGGAAACCTTGTTACGACTTCTCC-3'	reverse	1720	Yamaguchi and Horiguchi (2005)
SR12	5'-CCTTCCGCAGGTTCACCTAC-3'	reverse	1721	Nakayama et al. (1996)
25F1R	5'-ATATGCTTAAATTCAGCGG-3'	reverse	n/a	Takano and Horiguchi (2005)
DinF	5'-CGTTGRTTTATRTCTACWAATCATAARGA-3'	forward	n/a	Salonna et al. (2021)
NuxR1	5'-GCAGTAAAATAWGCTCGRGARTC-3'	reverse	n/a	Salonna et al. (2021)
CatF1	5'-ATRTCTACWAATCATAARGATATTRG-3'	forward	n/a	Salonna et al. (2021)
UxR1	5'-ATAAGCTCGWGAATCHACATC-3'	reverse	n/a	Salonna et al. (2021)

[1] Positions for 18S primers are based on the complete *Toxoplasma gondii* 18S sequence (accession number: L37415), measured from the 5' terminus. Positions for primers absent on the *T. gondii* reference sequence are estimated by relative distance from the nearest present primer.

Table 5.3. Comparison between novel *Lankesteria* clades and other close relatives.

	***Lankesteria* sp. Clade A**	***Lankesteria* sp. Clade B**	***Lankesteria* sp. Clade C**	***Lankesteria* sp. Clade D**	***Lankesteria* sp. Clade E**	***Lankesteria hesperidiiformis***	***Lankesteria dolabra***
Host(s)	*Ascidiella* sp.	*Ascidia zara*	Stolidobranchia sp.	*Eusynstyela* sp.	Stolidobranchia sp.	*Distaplia occidentalis*	*Asterocarpa humilis*
Host tissue	gut	gut	gut	gut	gut	gut	gut
Locality	Hakodate Port, Hokkaido, Japan	Hakodate, Shibetsu, and Wakkanai Ports (Hokkaido, Japan)	Ishigaki Port, Ishigaki Island, Japan	Hawaii Beach, Kikai Island, Japan	Ishigaki Port, Ishigaki Island, Japan	Bamfield, Vancouver Island, Canada	Waikawa Marina, Marlborough, New Zealand
Septate	no	no	no	no	no	no	no
Trophozoite length (µm)	18–24	62–135	95–130	86–125	105–110	35–80	163–207
Nucleus shape	spherical	spherical or ellipsoid	ellipsoid	spherical	spherical	spherical	spherical
Nucleus diameter (µm)	2–3	5–15	14–20	15–25	9–12	14–15	14–22
Position of nucleus	central	anterior	anterior	anterior	anterior	anterior	anterior
Shape of posterior	rounded	rounded	pointed	rounded	tapered	rounded	tapered
Epicytic fold density (folds/µm)	0.4	3	4	3	4	2	3
Shape of mucron	tapered	proboscis-like	bulbous and hooked	cylindrically protruding	beak-like	pointed	triangular
Citation	present work	present work	present work	present work	present work	Rueckert et al. (2015)	Iritani et al. (2021)

Table 5.4. Comparison between *Lankesteria* group and host phylogeny.

	***Lankesteria* sp. Clade A**	***Lankesteria* sp. Clade B**	***Lankesteria hesperidiiformis***	***Lankesteria didemni***	***Lankesteria cystodytae***	***Lankesteria ascidiae***	***Lankesteria savignyii***	***Lankesteria chelyosomae***	***Lankesteria* sp. Clade C**
Host(s)	*Ascidiella* sp.	*Ascidia zara*	*Distaplia occidentalis*	*Didemnum vexillum*	*Cystodytes lobatus*	*Ciona intestinalis*	*Ciona savignyi*	*Chelyosoma columbianum*	Stolidobranchia sp.
Higher host taxon	Phlebobranchia	Phlebobranchia	Aplousobranchia	Aplousobranchia	Aplousobranchia	Phlebobranchia	Phlebobranchia	Phlebobranchia	Stolidobranchia
Lankesteria group	A	A	A	B	B	C	C	C	D
Citation	present work	present work	Mastrototaro and Brunetti (2006), Rueckert et al. (2015)	Rueckert et al. (2015), Granthom-Costa et al. (2023)	Rueckert and Leander (2008), Moreno and Rocha (2008)	Sawada et al. (1998), Mita et al. (2012)	Iritani et al. (2021)	Rueckert et al. (2008), Seo (2025)	present work

Table 5.4. Continued.

	***Lankesteria* sp. Clade D**	***Lankesteria* sp. Clade E**	***Lankesteria abbotti***	***Lankesteria herdmaniae***	***Lankesteria kaiteriteriensis***	***Lankesteria metandrocarpae***	***Lankesteria halocynthiae***	***Lankesteria* cf. *ritterellae***	***Lankesteria dolabra***
Host(s)	*Eusynstyela* sp.	Stolidobranchia sp.	*Cnemidocarpa finmarkiensis*	*Herdmania momus*	*Pyura* sp.	*Metandrocarpa taylori*	*Halocynthia aurantium*	*Ritterella rubra*	*Asterocarpa humilis*
Higher host taxon	Stolidobranchia	Stolidobranchia	Stolidobranchia	Stolidobranchia	Stolidobranchia	Stolidobranchia	Stolidobranchia	Aplousobranchia	Stolidobranchia
Lankesteria group	D	D	D	D	D	D	D	D	D
Citation	present work	present work	Leander et al. (2006), Gaber and Elghazaly (2021)	Rueckert et al. (2015), Gordon et al. (2019)	Iritani et al. (2021)	Zeng et al. (2006), Rueckert et al. (2015)	Zeng et al. (2006), Rueckert et al. (2015)	Koyama et al. (2012), Rueckert et al. (2015)	Alié et al. (2018), Iritani et al. (2021)

Table 6.1. Summary of marine gregarine clades, including host identities and collection sites.

Clade name	Published name	Site	Host
Lecudina sp. Clade A	unpublished	Clover Point[1]	*Lumbrineris* sp.
Lecudina sp. Clade B	*Lecudina* cf. *longissima*	Crescent City[2]	*Lumbrineris japonica*

[1] 48°24'14"N 123°21'00"W, British Columbia, Canada, visited between November 7 and December 11, 2023.

[2] 41°44'12"N 124°11'40"E, California, USA, visited in January 2023.

Table 6.2. List of primers with references.

Primer name	Sequence	Direction	Position[1]	Citation
SR1	5'-TACCTGGTTGATCCTGCCAG-3'	forward	1	Nakayama et al. (1996)
SR1B	5'-GATCCTGCCAGTAGTCATATGCTT-3'	forward	2	Yamaguchi and Horiguchi (2005)
Lecu401F*	5'-CAAAGTTTCTGACCCATCAG-3'	forward	275	present work
Lecu1272F*	5'-GATCAAGAACGAAAGTTAGGGG-3'	forward	942	present work
Lecu1617R*	5'-CCACGAACTAAGAACGGC-3'	reverse	1252	present work
Paralecu1683R*	5'-GTTAACGGAATCAACCAGAC-3'	reverse	1278	present work
Longi1342*	5'-CTGTGATGCCCTTAGATATC-3'	forward	1406	present work
GenEukR1	5'-CGGTGTGTACAAACGGCAGGGAC-3'	reverse	1592	Iritani et al. (2021)
SR12B	5'-CGGAAACCTTGTTACGACTTCTCC-3'	reverse	1720	Yamaguchi and Horiguchi (2005)
SR12	5'-CCTTCCGCAGGTTCACCTAC-3'	reverse	1721	Nakayama et al. (1996)
Vanc1238*	5'-TTACTATCCAAGAATTGGATTGG-3'	forward	n/a	present work
25F1R	5'-ATATGCTTAAATTCAGCGG-3'	reverse	n/a	Takano and Horiguchi (2005)
polyLCO	5'-GAYTATWTTCAACAAATCATAAAGATATTGG-3'	forward	n/a	Carr et al. (2011)
polyHCO	5'-TAMACTTCWGGGTGACCAAARAATCA-3'	reverse	n/a	Carr et al. (2011)

[1] Positions for 18S primers are based on the complete *Toxoplasma gondii* 18S sequence (accession number: L37415), measured from the 5' terminus. Positions for primers absent on the *T. gondii* reference sequence are estimated by relative distance from the nearest present primer.

Table 6.3. Comparison between novel *Lecudina* clades and other close relatives.

	***Lecudina* sp. Clade A**	***Lecudina* sp. Clade B**	***Lecudina longissima***	***Lecudina caspera***	***Lecudina phyllochaetopteri***	***Lecudina brasili***	***Lankesteria dolabra***	***Lecudina laubieri***
Host(s)	*Lumbrineris* sp.	*Lumbrineris japonica*	*Lumbrineris japonica*, *L. zonata*, *L.* sp.	*Lumbrineris inflata*, *Lumbrineris* sp.	*Phyllochaetopterus prolifica*	*Lumbrineris* sp.	*Asterocarpa humilis*	*Lumbrineris* sp., *L. coccinea*
Host tissue	gut	gut	gut	gut	gut	gut	gut	gut
Locality	Clover Point, British Columbia, Canada	Crescent City Jetty, California, USA	Yamaguchi, Japan; western USA; Bamfield, British Columbia, Canada	Clover Point, British Columbia, Canada	English Bay Beach, British Columbia, Canada	Adyar, Chennai, India	Waikawa Marina, Marlborough, New Zealand	Banyuls, France
Septate	no	no	no	no	no	no	no	no
Trophozoite length (µm)	52–150	200–420	200–800	226–420	24–32	150	163–207	400
Nucleus shape	spherical	spherical	spherical or ellipsoidal	spherical	spherical	spherical	spherical	ellipsoidal
Nucleus diameter (µm)	6–10	18–22	10–32	22–25	8–9	data absent	14–22	30
Position of nucleus	anterior	anterior	anterior	anterior third	posterior half	anterior third	anterior	anterior
Shape of posterior	rounded	pointed	pointed	tapered	rounded	rounded	tapered	tapered
Epicytic fold density (folds/µm)	4	4	data absent	4	folds absent	data absent	3	data absent
Shape of mucron	nipple-like	nipple-like	rounded or nipple-like	nipple-like	nipple-like	tapered	triangular	elongate, proboscis-like
Citation	present work	present work	Tsugawa (1944), Hoshide (1958), Levine (1974), Rueckert et al. (2010)	Iritani et al. (2018b), present work	Rueckert et al. (2010)	Ganapati and Aiyar (1937)	Iritani et al. (2021)	Théodoridès (1969)

Table 6.3. Continued.

	Lecudina oxydromus	***Lecudina* cf. *arabellae***
Host(s)	*Oxydromus pugettensis*	Oenonidae sp.
Host tissue	gut	gut
Locality	Bamfield, British Columbia, Canada	Bamfield, British Columbia, Canada
Septate	no	no
Trophozoite length (µm)	70–120	450–600
Nucleus shape	spherical	spherical or ellipsoidal
Nucleus diameter (µm)	10–18	20–35
Position of nucleus	anterior	anterior
Shape of posterior	rounded	pointed
Epicytic fold density (folds/µm)	4–5	3–4
Shape of mucron	rounded	blunt
Citation	Park and Leander (2024a)	Park and Leander (2024a)

Table 7.1. Summary of marine gregarine clades, including host identities and collection sites.

Clade name	Published name	Site	Host
Lecudina sp. Clade C	*Lecudina* cf. *tuzetae*	Crescent City[1]	*Nereis* sp.
Lecudina sp. Clade D	*Lecudina kitase*	Oshoro Bay[2]	*Perinereis* sp.
Lecudina sp. Clade E	unpublished	Hanaguri[3]	*Perinereis* sp.
Lecudina sp. Clade F	unpublished	Kabira Bay[4]	*Perinereis* sp.
Lecudina sp. Clade G	unpublished	Ogamimaru Port[5]	*Perinereis* sp.

[1] 41°44'12"N 124°11'40"E, California, USA, visited in January 2023.

[2] 43°12'37"N 140°51'25"E, Hokkaido, Japan, visited between November 11 and 27, 2022.

[3] 34°18'04"N 132°50'20"E, Hiroshima, Japan, visited on June 9, 2024.

[4] 24°26'46"N 124°8'25"E, Ishigaki Island, Japan, visited on September 16, 2023.

[5] 26°41'28"N 127°59'54"E, Okinawa Island, Japan, visited on January 23, 2024.

Table 7.2. List of primers with references.

Primer name	Sequence	Direction	Position[1]	Citation
SR1	5'-TACCTGGTTGATCCTGCCAG-3'	forward	1	Nakayama et al. (1996)
SR1B	5'-GATCCTGCCAGTAGTCATATGCTT-3'	forward	2	Yamaguchi and Horiguchi (2005)
Lecu401F*	5'-CAAAGTTTCTGACCCATCAG-3'	forward	275	present work
Lecu717MR*	5'-GTGCTGGCACCAGACTTTTCC-3'	reverse	528	present work
Tuz3R*	5'-CGATTCACTCAAAGTACAG-3'	reverse	715	present work
Tuz4*	5'-CTCTCCAGTACTTTCTGAG-3'	forward	1040	present work
Lecu1617R*	5'-CCACGAACTAAGAACGGC-3'	reverse	1252	present work
GenEukR1	5'-CGGTGTGTACAAACGGCAGGGAC-3'	reverse	1592	Iritani et al. (2021)
T1791	5'-CTCCGCCTAACTCATGATAC-3'	reverse	1632	Iritani et al. (2021)
SR12	5'-CCTTCCGCAGGTTCACCTAC-3'	reverse	1721	Nakayama et al. (1996)
Tuz1763*	5'-ATGTATAGAACATGTTTCGCC-3'	forward	n/a	present work
25F1R	5'-ATATGCTTAAATTCAGCGG-3'	reverse	n/a	Takano and Horiguchi (2005)
polyLCO	5'-GAYTATWTTCAACAAATCATAAAGATATTGG-3'	forward	n/a	Carr et al. (2011)
polyHCO	5'-TAMACTTCWGGGTGACCAAARAATCA-3'	reverse	n/a	Carr et al. (2011)

[1] Positions for 18S primers are based on the complete *Toxoplasma gondii* 18S sequence (accession number: L37415), measured from the 5' terminus. Positions for primers absent on the *T. gondii* reference sequence are estimated by relative distance from the nearest present primer.

Table 7.3. Comparison between novel *Lecudina* clades and other close relatives.

	***Lecudina* sp. Clade C**	***Lecudina* sp. Clade D**	***Lecudina* sp. Clade E**	***Lecudina* sp. Clade F**	***Lecudina* sp. Clade G**	***Lecudina tuzetae***	***Lecudina pellucida***
Host(s)	*Nereis* sp.	*Perinereis* sp.	*Perinereis* sp.	*Perinereis* sp.	*Perinereis* sp.	*Nereis diversicolor; N. vexillosa; N. neoneanthes*	*Perinereis cultrifera; Nereis chilkaensis*
Host tissue	gut	gut	gut	gut	gut	gut	gut
Locality	Crescent City, California, USA	Oshoro Bay, Hokkaido, Japan	Hanaguri, Hiroshima, Japan	Kabira Bay, Ishigaki, Japan	Ogamimaru Port, Okinawa, Japan	western Canada; English Channel	English Channel; Madras, India
Septate	no	no	no	no	no	no	no
Trophozoite length (µm)	75–100	60–80	125–190	40–72	25–34	47–182	100–150
Nucleus shape	spherical	spherical	spherical	spherical	spherical	spherical to ovaloid	spherical
Nucleus diameter (µm)	14–20	10–12.5	23–27	9–11	6–8	11–23	10
Position of nucleus	central	central	central	central	central	posterior or central	central
Shape of posterior	rounded	rounded	rounded	rounded	rounded	pointed	rounded
Epicytic fold density (folds/µm)	2	2	1.3	2.1	1.3	3	data absent
Shape of mucron	rounded	rounded	rounded or button-like	rounded	rounded	rounded	cupped
Citation	present work	present work	present work	present work	present work	Schrével (1963), Rueckert et al. (2011b)	Ganapati (1946), Vivier (1968)

Table 7.3. Continued.

	Lecudina caudata	***Lecudina pelmatomorpha***	***Lecudina* cf. *platynereidis***
Host(s)	*Perinereis brevicirris*	*Perinereis marionii*	*Perinereis* sp.
Host tissue	gut	gut	gut
Locality	Aio, Yamaguchi Prefecture, Japan	Cherbourg, northwestern France	Bamfield, British Columbia, Canada
Septate	no	no	no
Trophozoite length (µm)	59–70	150–160	95–110
Nucleus shape	spherical	ovaloid	ovaloid
Nucleus diameter (µm)	10	data absent	20–22
Position of nucleus	central	central	posterior or central
Shape of posterior	rounded	rounded	rounded
Epicytic fold density (folds/µm)	data absent	data absent	2.5
Shape of mucron	papillary	conical	rounded or dome-shaped
Citation	Hoshide (1977)	Schrével (1963)	Park and Leander (2024a)